# MODIFIED ELECTROLESS PLATING TECHNIQUE FOR PREPARATION OF PALLADIUM COMPOSITE MEMBRANES

*by*

**Bo TIAN**
BEng (Chemical)

Thesis presented for the degree

*of*

**MASTER OF SCIENCE IN ENGINEERING**
**(Chemical Engineering)**

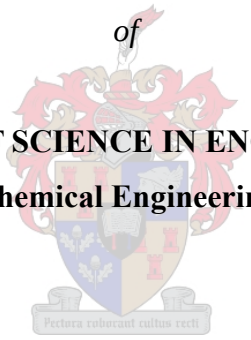


In the Department of Process Engineering
at the University of Stellenbosch

*Promoters:*
**PROF L LORENZEN**
**PROF AJ BURGER**

**STELLENBOSCH**
**December 2005**

# DECLARATION

I, the undersigned, hereby declare that the work contain in this assignment/thesis is my own original work, and that I have not previously in its entirely or in part submitted it at any University for a degree.

…… ……..……..

Signature Date

# ABSTRACT

An increased demand for hydrogen in recent years has led to a revival of interest in methods for hydrogen separation and purification. Palladium (Pd) and palladium composite membranes have therefore received growing attention largely due to their unique permselectivity for hydrogen and good mechanical and thermal stability.

Previous research on Pd composite membranes by Keuler (2000) in the Department of Process Engineering at the University of Stellenbosch has shown that some assumptions which he made during characterisation procedures needed further investigation, such as the assumptions about the influence of support membranes on preparation of Pd composite membranes, method of pre-cleaning before pretreatment, vacuum applied during electroless plating, and heat treatment after electroless plating. In this study, Pd composite membranes (with Pd film thickness of 1.7 μm ~ 4 μm) were prepared on the inside layer (claimed pore diameter of 200 nm) of α-alumina ceramic support membrane tubes, consisting of three layers with varying pore diameters from inside to the outside layer, via a modified electroless plating technique (with a gauge vacuum of 20 kPa applied on the shell side of the plating reactor). Bubble point tests and bubble point screening tests were performed on the support membranes before the electroless plating to investigate the influence of the substrates characteristics on the preparation of the Pd composite membranes. It was found that Pd composite membranes with a better permselectivity can be prepared on a support membrane that contains smaller pore sizes and a smoother surface.

The surface pretreatment step was modified to provide a uniform Pd surface for Pd electroless plating. The membrane was first rinsed in $PdCl_2$ solution for 15 min using a stirrer at a stirring speed of 1300 rpm, and was then dipped into distilled water 10 times (1-2 second each). Subsequently, the membrane was rinsed in $SnCl_2$ solution for 15 min, and was then dipped into distilled water 10 times. These procedures were repeated 4 times. In addition, by using a new method of assessment for heat treatment (i.e. cutting the Pd composite membranes into two pieces and then exposing them to two different heating methods), the most effective heat treatment method could be identified without the influences of the substrates or the plating technique. The preferable procedures was to anneal the Pd composite membrane in $N_2$ for 5 h from 20°C to 320°C, and then oxidize it in air for 2 h at 320°C, followed by annealing it in $N_2$ for 130 min from 320°C to 450°C and then in $H_2$ for 3 h at 450°C. Finally the membrane was cooled down in $N_2$ to 350°C and held at this temperature for 30 min. Additional oxidation in air for more than 10 hours changes the

structure of the Pd films. PdO then forms and decreases the $H_2$ permeation through the Pd composite membrane. More detailed characterisations of the Pd composite membranes were performed by membrane permselectivity tests (from 350°C to 550 °C) using either $H_2$ or $N_2$ in single gas test, membrane morphology and structure analysis using scanning electron microscopy (SEM), energy dispersive detectors (EDS), atomic force microscopy (AFM), Brunauer-Emmett-Teller (BET) and X-ray diffraction (XRD) analysis.

Hydrogen permeability between 4.5-12 μmol/($m^2$.Pa.s) and an average hydrogen/nitrogen permselectivity of ≥ 150 were achieved in this study. The permselectivities of the heat treated membranes were superior to Keuler's membranes, which had an average permselectivity of ≥ 100. AFM and BET analysis showed that dense and smooth Pd films with smaller Pd crystals sizes and compact Pd layers were obtained.

# OPSOMMING

‘n Verhoogde aanvraag na waterstof die afgelope aantal jare het gelei tot ‘n hernude belangstelling in metodes vir die skeiding en suiwering van waterstof. Palladium (Pd) en palladium saamgestelde membrane het dus weer hernude aandag gekry weens hulle unieke permeselektiwiteit vir watrestof, en goeie meganiese en termiese stabiliteit.

Vorige navorsing oor Pd saamgestelde membrane in die Departement Prosesingenierswese by die Universiteit van Stellenbosch deur Keuler (2000) het aangedui dat sekere aannames gemaak is tydens die karakteriserings prosedures en dat dit verder ondersoek moet word. In hierdie studie, is Pd saamgestelde membrane (1.7 μm ~ 4 μm) op ∝-alumina basis keramiek membraan via ‘n gewysigde elektrolitiese plateringsproses voorberei (absolute vakuum van 20 kPa is op die mantel kant van die reaktor aangewend). Borrelpunt toetse en borrelpunt siftingstoetse is op die membrane voor Pd bedekking uitgevoer om die invloed van die substraat eienskappe op die voorbereiding van die Pd membrane te bepaal. Daar is gevind dat Pd saamgestelde membrane met ‘n verhoogde permeselektiwiteit op basis membrane met kleiner porieë en ‘n gladder oppervlak voorberei kan word.

Die oppervlak behandelings prosedure is gewysig om ‘n meer uniforme Pd oppervlak vir Pd platering daar te stel. Die membrane is eers vir 15 min in ‘n $PdCl_2$ oplossing teen 1300 opm afgespoel, en daarna 10 keer in gedistileerde water afgespoel (1-2 sekondes elk). Die membrane is toe vir 15 minute in $SnCl_2$ oplossing afgespoel, gevolg deur 10 keer se indoping in gedistileerde water. Hierdie prosedures is vier keer herhaal. ‘n Nuwe metode om die doeltreffendheid van die hitte-behandelings prosedure te bepaal (dws, deur die membraan te deel in twee ewe groot gedeeltes en dan aan verskillende verhittings metodes bloot te stel), sonder die invloed van die basis-substraat of dekkings tegniek, is ook ontwikkel. Die voorgestelde prosedure is om die Pd mebraan te temper in $N_2$ vir 5 uur van 20 $^oC$ tot 320 $^oC$, dan in lug te oksideer by 320 $^oC$ vir 2 uur gevolg deur weer te temper in $N_2$ vir 130 min van 320 $^oC$ tot 450 $^oC$ en in $H_2$ by 450 $^oC$ vir 3 uur. Die membraan is toe in $N_2$ tot 350 $^oC$ afgekoel en vir 30 minute by hierdie temperatuur gehou. Addisionele lug oksidasie vir langer as 10 uur verander die struktuur van die Pd film. PdO word dan gevorm, en verminder die $H_2$ deurdringingsvermoë op die Pd membraan. ‘n Beter karakterisering van die Pd saamgestelde membrane is met behulp van permeselektiwiteits toetse (van 350 $^oC$ tot 450 $^oC$ in $H_2$ of $N_2$ as enkele gas toets), en membraan morfologie en struktuur analiese is met behulp van SEM, EDS, AFM, BET en XRD uitgevoer.

Waterstof deurdringingsvermoë van tussen 4.5–12 μmol/($m^2$.Pa.s) en ’n gemiddelde waterstof/stikstof selektiwiteit van $\geq$ 150 is bereik gedurende die studie. Die selektiwiteit van die hittebehandelde memb`rane was beduidend beter as Keuler se membrane wat ’n gemiddelde selektiwiteit van $\geq$ 100 het. AFM en BET analises toon dat meer digte en gladde Pd lagies met kleiner Pd kristalgroottes en kompakte Pd lae gevorm is.

# TABLE OF CONTENTS

# ACKNOWLEDGEMENTS

I would like to give great thanks to **Prof L Lorenzen** and **Prof AJ Burger** for their leadership, wisdom and encouragement though my work.

I would like to thank **Mrs H Botha, Dr M Meincken** and **Mrs E Spicer** for assisting me with analyses.

I would like to thank **Dr LV Dyk** and **Mr. W Mwase** for their friendship, support and advice.

I would like to thank **Mr. J Barnard, Mr. A Cordier,** and **Mr. H Koopman** for their assistance with the construction of the experimental setup, and all the other staff members in Department of Process Engineering at the University of Stellenbosch.

I would like to thank **Mr. RM Burton, Ms Enid Thom and Ms Thanja Allison** for helping me edit my thesis.

I would like to thank the Department of Process Engineering at the University of Stellenbosch for financial support.

I also would like to give special thanks to the following people:
**ZengHua Tian and Ling Li** (my parents),
**XueYe Li, and GuoYu Zhao** (my grandparents),
**Lin Shi** (my fiancé),
All the other members of my family,
All my friends in my church cell group and Chinese bible study fellowship,
For every friend that support, listened and/or gave advice.

**Most of all, I want to thank the LORD for His love and grace, and every gift of life.**

# CHAPTER 1: INTRODUCTION

There is an increased demand for hydrogen in petroleum refining, petrochemical production and in semi-conductor processing, as well as in new energy-related applications, such as clean fuel for vehicles and fuel cells. This motivates research into various methods for hydrogen generation, separation from gas mixtures and purification of any separated hydrogen streams. Palladium (Pd) and palladium composite membranes have therefore received growing attention for the separation and purification of hydrogen, largely due to their unique permselectivity for hydrogen and good mechanical and thermal stability (Hou, 2003).

Alloying palladium membranes, with other precious metals such as silver or copper, not only prevents the hydrogen embrittlement, which happens when palladium-based membranes are used under 290 °C, but also increases the hydrogen permeability to a better level (Cheng, 1999; Nam, 2001). Originally used in the form of relatively thick dense metal membranes, recent developments look at the employment of composite membranes in which the palladium or palladium alloy is deposited as a thin film onto a porous substrate. The porous substrates include symmetric and asymmetric disks or tubes composed of alumina, alumina-zirconia, glass, or stainless steel. Because of the relatively smooth surface, the porous ceramic substrates have been applied extensively to the preparation of Pd composite membranes, and some successful experimental results have been reported (Tong, 2005). Such composite membranes have good stability and reduce material costs, but their main attribute is providing a structure possessing both higher hydrogen fluxes as well as better mechanical properties than the relatively thick pure palladium membranes (Hou, 2003).

Several methods have been proposed and developed to prepare palladium composite membranes including magnetron sputtering, spray pyrolysis, and chemical vapour deposition. However, a generally simpler and often more effective method of preparation is the so-called electroless plating technique with an autocatalyzed reaction, which has a number of advantages over other preparation methods. These include uniformity of deposits on complex shapes, hardness of the deposits, low cost and very simple equipment. Conventionally, three main steps were performed in preparing the membranes, namely pretreatment (or pre-seeding, surface sensitisation and activation), palladium electroless plating, and heat treatment (or calcinations, thermal treatment).

As indicated in the literature, several parameters, which mainly affect the preparation of thin palladium composite membranes, have been extensively investigated (Souleimanova, 1999; Li, 2000; Cao, 2004). However, there were still some factors needing further exploration. An important consideration is the selectivity of the produced palladium-based membranes, relatively high selectivity is preferred for the reason that the demands for exceptionally pure hydrogen are increasing. On the other hand, the flux of permeated hydrogen is expected to be inversely proportional to the membrane thickness. The preparation of thinner membranes is thus preferred to increase the flux as well as to reduce the cost of preparation. Furthermore, accompanying uncertainties are the influence of the pore size and morphology of the support membrane to palladium membrane preparation and permeation performance, the effect of the vacuum that was applied on the shell side of the reactor during the electroless plating, and the influence of heat treatment of palladium membranes after plating. Nonetheless, another perceived problem in the adoption of palladium composite membranes for commercial use is the lifetime of the membranes under high temperatures and pressures. This is an important consideration, bearing in mind not only the cost of the palladium, but also the crucial cost of the porous substrates on which the palladium film is deposited.

Previous research on Pd composite membranes by Keuler (2000) in the Department of Process Engineering at the University of Stellenbosch showed that some assumptions which he made during characterisation procedures still needed further investigation, such as the assumptions about the influence of support membranes on preparation of Pd composite membranes, method of pre-cleaning before pretreatment, vacuum applied during electroless plating, and heat treatment after electroless plating. Therefore, the objectives of this study are listed as the following:

- To improve upon the existing electroless plating technique developed by Keuler (2000) and to reproduce the Pd composite membrane (Pd films deposited on the inside of α-alumina support membranes with a length of 15 cm).
- To investigate the influence of support membranes on the permselectivity of Pd composite membranes.
- To modify the preparation procedures of Pd composite membranes, including membrane pre-cleaning method, membrane surface pretreatment method, Pd electroless plating with vacuum, and heat treatment method.
- To further characterise the Pd composite membrane by membrane permselectivity tests (from 350°C to 550 °C) using either $H_2$ or $N_2$ in single-gas-testing), membrane morphology and structure analysis using scanning electron microscopy (SEM), energy dispersive detectors

(EDS), atomic force microscopy (AFM), Brunauer-Emmett-Teller (BET) and X-ray diffraction (XRD) analysis.

This research provides some contributions to the present knowledge of palladium membranes. Firstly, the influence of support membranes has been researched. Secondly, the palladium electroless plating technique was improved, and thirdly, improved characterisation studies of palladium composite membranes have been performed.

A literature review and background study in relation to the industrial uses of hydrogen, membrane processes, inorganic membranes, palladium and palladium membranes, various preparation and characterisation techniques of palladium membranes, as well as the development of Pd membrane reactors are presented in Chapter 2. In Chapter 3, a series of detailed experimental procedures, including bubble point tests, a modified electroless plating technique, heat treatment, and a range of analytical methods for membrane characterisation, are discussed. Chapter 4 focuses on discussions and investigations of the different steps for the modified palladium electroless plating method. Thereafter, the results of membrane permeability and selectivity tests for the palladium composite membrane are discussed in Chapter 5. Finally, surface morphology, crystal structure, and composition of Pd composite membrane are discussed in Chapter 6. To sum up, Chapter 7 provides the conclusions obtained from the experiments, followed by recommendations and future work.

# CHAPTER 2: BACKGROUND AND LITERATURE REVIEW

## 2.1 HYDROGEN

Hydrogen is a very important molecule with an enormous breadth and extent of application and use. It is currently used in many industries, from chemical and refining to metallurgical, glass and electronics. Hydrogen is used primarily as a reactant. Hydrogen is one of the oldest known molecules and is used extensively by many industries for a variety of applications. There has been an increasing demand for hydrogen in recent years in both the petroleum refining and petrochemical industries and in semi-conductor processing and fuel cell applications. Its use in petroleum refining has recently seen rapid grow due to a combination of factors relating to changes in crude; environmental regulations such as limits of sulphur in diesel, allowable limits of NO, and SO in off-gas emissions into the atmosphere, aromatic and light hydrocarbon concentrations in gasoline, etc. Moreover, it is also being used as a fuel in space applications, as an "$O_2$ scavenger" in heat treating of metals, and for its low viscosity and density.

Therefore, a number of hydrogen applications have led to a revival of interest in methods for separation of hydrogen from gas mixtures and in purification of any separation hydrogen streams. Palladium and palladium membranes have consequently received growing attention for separation and purification of hydrogen, largely due to the unique permselectivity of palladium to hydrogen and good mechanical stability.

## 2.2 MEMBRANE

What is a membrane? According to Scott and Hughes (1996), a membrane is a semi-permeable phase, often a thin polymeric solid, which restricts the motion of certain species. This added phase is essentially a barrier between the feed stream for separation and the one product stream. This membrane or barrier controls the relative rates of transport of various species through itself and thus, as with all separations, gives one product depleted in certain components and a second product concentrated in these components. The performance of a membrane is defined in terms of two simple factors, flux and selectivity, defined as:

Flux or permeation rate: the volumetric (mass or molar) flow rate of fluid passing through the membrane per unit area of membrane per unit time.

Permselectivity: (for inorganic membranes) a ratio of permeance, a term used to define the preferential permeation of certain gas or fluid species through the inorganic membranes.

In this literature study, the following definitions will be used:

- Permeability [mol. m/($m^2$.Pa.s)]
- Permeance [mol/($m^2$.Pa.s)]
- Flux, permeation rate or permeation [mol/($m^2$.s)]
- Flow rate [mol/s]
- Permselectivity ( ratio of permeance) [no unit]

In this project, permeability is determined by the volumetric (mass or molar) flow rate of fluid passing through the membrane, per unit of membrane thickness, per unit of membrane surface area per unit time.

### 2.2.1 MEMBRANE CLASSIFICATION

Generally membranes can be classified into three types (Scott and Hughes, 1996) as follows:

- Synthetic polymers; a vast source in theory although perfluoropolymers, silicone rubbers, polyamides and polysulphones are prominent.
- Modified natural procedures; cellulose-based.
- Miscellaneous; include inorganic, ceramic, metals, dynamic and liquid membranes.

**Symmetric and asymmetric (Scott and Hughes, 1996)**

Two types of structures are generally found in membranes (solid material), namely symmetric and asymmetric. Membranes with a uniform pore structure across the thickness of the membrane and made in a single step, are called symmetric membranes. Symmetric membranes by definition of a uniform structure are of three general types: with approximate cylindrical pores, porous and non-porous (homogenous). Single step membranes with a changing structure throughout the thickness are asymmetric. Asymmetric membranes are characterised by a non-uniform structure comprising an active top layer or skin supported by a porous support or sublayer. There are three types: porous, porous with a top layer and composites. When a membrane consists of two or more layers, prepared in consecutive steps, it is called a composite membrane. For composite membranes, the initial layer usually provides mechanical strength and acts as a support on which further layers are deposited. The second and subsequent layers determine the membrane's separation properties.

Membranes can be classified based on their morphology or separation process. Current gas separation membranes are thin dense films, integrally skinned asymmetric membranes or composites mainly prepared from glassy polymers. Asymmetric membranes have a dense top layer and a porous substructure, and are formed by a phase inversion process. Composites have a dense top layer and a porous substructure. The top layer is created in a separate step, for example by coating. In both cases, the permselective top layer should be as thin as possible (<1 μm) to achieve a high flux. The substructure should have good mechanical strength with negligible gas transport resistance. Thin polymeric films by themselves are too weak to withstand the high differential gas pressures required in gas separation operations. Membranes with a support layer are therefore the most common. The advantage of a composite membrane is that the top layer and the support can be optimised separately.

### 2.2.2 MEMBRANE PROCESS

Membrane separations are in competition with physical methods of separation such as selective adsorption, absorption, solvent extraction, distillation, crystallisation, cryogenic gas separation, etc. The feature which distinguishes membrane separation from other separation techniques is the provision of another phase, the membrane. This phase, such as solid, liquid or gaseous, introduces an interface between the bulk phases involved in the separation and can give advantages of efficiency and selectivity. The membrane can be neutral or charged, porous or non-porous, and act as a permselectivity barrier (Scott and Hughes, 1996).



The main uses of membranes in industry are the following:

- The filtration of micron and submicron size suspended solids from liquid or gases containing dissolved solids.
- The removal of macromolecules and colloid from liquids containing ionic species.
- The separation of mixtures of miscible liquids.
- The selective separation of gases and vapours from gas and vapour streams.
- The selective transport of ionic species only.
- The virtually complete removal of all material suspended and dissolved in water.

Throughout a certain membrane process, transport of selected species through the membrane is achieved by applying a driving force across the membrane. The flow of material across a membrane has to be kinetically driven by the application of mechanical, chemical or electrical forces. Table 2.1 shows the different membrane processes.

**Table 2.1 Membrane separation processes and materials (Scott and Hughes, 1996)**

| Membrane separation Process | Membrane type | Driving force | Application |
|---|---|---|---|
| Microfiltration | Symmetric microporous | Hydrostatic pressure | Clarification, sterile filtration |
| Ultrafiltration | Asymmetric microporous | Hydrostatic pressure | Separation of macromolecular solutions |
| Nanofiltration | Asymmetric microporous | Hydrostatic pressure | Separation of small organic compounds and selected salts from solutions |
| Hyperfiltration (Reverse Osmosis) | Asymmetric, composite with homogeneous skin | Hydrostatic pressure | Separation of microsolutes and salts from solutions |
| Gas separation | Asymmetric or composite, homogeneous or porous polymer | Hydrostatic pressure, concentration gradient | Separation of gas mixtures |
| Dialysis | Symmetric microporous | Concentration gradient | Separation of microsolutes and salts from macromolecular solutions |
| Pervaporation | Asymmetric, composite | Concentration gradient, vapour pressure | Separation of mixtures of volatile liquids |
| Vapour permeation | Composite | Concentration gradient | Separation of volatile vapours and gases |
| Membrane Distillation | Microporous | Temperature | Separation of water from non-volatile solutes |
| Electrodialysis | Ion-exchange, homogeneous or microporous polymer | Electrical potential | Separation of ions from water and non-ionic solutes |
| Electro-osmosis | Microporous charged membrane | Electrical potential | Dewatering of solutions of suspended solids |
| Electrophoresis | Microfiltration membranes | Electrical potential, hydrostatic pressure | Separation of water and ions from colloidal solutions |
| Liquid Membranes | Microporous, liquid carrier | Concentration, reaction | Separation of ions and solutes from aqueous solutions |

To be effective for separation, membrane materials should ideally contain the following properties:

- Chemical resistance (to both feed and cleaning fluids).
- Mechanical stability.
- Thermal stability.
- High permeability.
- High selectivity.

- Stable operation.

The membrane process related to this study is gas separation by means of palladium composite membranes.

### 2.2.3 MEMBRANE SHAPE

Scott and Hughes (1996) proposed that membranes be made in a number of different formats. The main categories of membrane shapes are listed below:

- Spiral wrap

The spiral wrap format utilises flat sheet membranes, but assembles it in a cartridge, usually referred to as an element that generally has a high packing density.

- Tubular

Tubular membranes are usually made by casting a membrane onto the inside of a pre-formatted tube, which is referred to as the substrate. The diameters of tubes range from 5-25 mm, with 12.5 mm being the most frequently used.

- Hollow fibre

The hollow fibres that make up these membranes are usually less than 1 mm in diameter, and unlike all other formats, there is no additional supporting layer. The membrane skin may be on the outside of the fibre, the inside or on both surfaces.

- Flat sheet

The membrane layer is cast onto a sheet of a non-woven backing which is then cut to size to match the modules. This may be processed further to form a cassette or envelope that contains an integral permeable space.

The membrane supports used in this study are tubular α-alumina ceramic membranes.

## 2.3 INORGANIC MEMBRANES

All membranes are either organic (polymeric) or inorganic. There are two types of inorganic membranes: dense and porous. From a material science and catalysis point of view, the terminology for inorganic membranes is standardised by the IUPAC definitions (Noble and Stern, 1995). Table

2.2 is modified referring to the IUPAC definitions.

**Table 2.2: Terminology of inorganic membranes (Noble and Stern, 1995)**

| Terminology | Pore diameter (nm) | Main types of separation mechanism | types of filtration/separation |
|---|---|---|---|
| Macroporous | $d_p > 50$ | Knudsen diffusion | Microfiltration |
| Mesoporous | $2 < d_p < 50$ | Surface diffusion and Capillary condensation | Ultrafiltration |
| Microporous | $d_p < 2$ | Molecular sieve separation | Nanofiltration/gas separation |
| Non-porous, (Dense) | $d_p = 0$ | Solution diffusion mechanism | Solution/Diffusion |

As palladium membranes belong to dense inorganic membranes, the subsequent information concerns dense inorganic membranes. They can be classified into either metal membranes or solid electrolyte membranes, which are prepared by different methods and from different materials. The preparation method consequently has a definite effect on the pore structure.

### 2.3.1 DENSE INORGANIC MEMBRANES

There are several classes of dense inorganic membranes. They are mainly classified into the following categories (Keuler 2000):

#### 2.3.1.1 Dense metal membranes

Dense metal membranes are principally made from palladium and its alloys. Atomic hydrogen can easily dissolve in palladium and its alloys. Pd can be alloyed with Ag, Ru, Rh, Ni or Au and other precious metal. Ag is, however, most commonly metal alloyed to Pd to prevent hydrogen embrittlement of pure Pd that occurs below 300 °C. Sheets and sheets in tubular form with a thickness of 20 μm or less can be prepared easily. Johnson Matthew has used palladium-silver (77 wt %, 23 wt %) alloy membranes for hydrogen purification since the early 1960s. However, there were still several problems, i.e. membrane cost, durability, poisoning by carbon and sulphur compounds, and selectivity have restricted large scale progress in industry. Permeance of alloyed membrane tends to be lower than that of pure palladium membrane due to thick alloy film layers. Optional metals like niobium, tantalum and vanadium have also been investigated for hydrogen

separation.

#### 2.3.1.2 Nonporous electrolyte membranes

Solid electrolytes are impervious to gases and liquids, except allowing some ions to pass through their lattices under an applied voltage difference or a chemical potential difference. Calcium-stabilised zirconia allows for oxygen transport, while other gases cannot pass through (Itoh, 1990). PbO selectively separates oxygen from other gases. Other electrolytes investigated include simple or complex halides ($RbAg_4I_5$), simple or complex oxides (β-aluminas) and oxide solid solutions ($ZrO_2$-$Y_2O_3$, $ZrO_2$-CaO, $ThO_2$-$Y_2O_3$) (Hsieh, 1996).

#### 2.3.1.3 Dense inorganic polymer membranes

These types of membranes have been developed for separation and reaction at intermediate temperatures (up to 200 °C for long periods of time). Organic membranes cannot withstand such high temperatures. Polyphosphazenes (Hsieh, 1996) are amorphous rubbery polymers which exhibit a higher permeance but lower selectivity than glassy polymer membranes. They are very selective in separating acidic (carbon dioxide and hydrogen sulphide) and non-acidic gases (methane). They consist of alternating phosphorous and nitrogen double and single bonds in a polymer network. Polysilazanes, containing silicon and nitrogen bonds, are another class of organometallic polymers that can be used as membranes.

#### 2.3.1.4 Dense metal composite membranes

This category of membranes have a dense metal substrate as support with some sort of palladium modification. Dense Pd-porous stainless steel membranes thus fall outside this group and are discussed separately. Refractory metals like vanadium, tantalum and niobium have a very high hydrogen permeance, they are cheap compared to palladium, easy to fabricate in tubes and they are stronger than palladium. They are, however, much more prone to hydrogen embrittlement. Niobium must operate above 420 °C and tantalum above 350 °C in hydrogen. Buxbaum et al. (1993) have done extensive research on refractory metals coated with palladium for hydrogen separation. A palladium coating is necessary to reduce surface poisoning. They used commercial niobium (150 μm thickness) and tantalum (75 μm thickness) tubes coated with palladium by electroless plating. These membranes were very stable.

Edlund (1995) made many multi-layered membranes based on vanadium as substrate. A typical example was Pd-$SiO_2$-V-$SiO_2$-Pd (25-25-30-25-25 μm). The $SiO_2$ was compared to many other oxides in the 5-layer membrane, but gave the best hydrogen permeance results.

### 2.3.2 POROUS INORGANIC MEMBRANES

Advances and research in the field of porous inorganic membranes have been dramatic in recent years (Soria, 1995). Industrial application of inorganic membranes started during the post World War II period in the field of nuclear power. The uranium isotope, $^{235}U$, was enriched from 1% to between 3 and 5% for fuel in nuclear reactors, or up to 90% for nuclear weapons. Since the 1940s, membranes have played an important role in gaseous diffusion with France, the United States and the Soviet Union leading the way. Composite membranes have been in very high demand. Thin separation layers allow for high fluxes, while the support gives mechanical strength. The pores in porous membranes can be divided into three classes:

- Macroporous > 50 nm,
- Mesoporous 2 nm < pore size < 50 nm, and
- Microporous < 2 nm.

#### 2.3.2.1 Porous glass

Macroporous Vycor glass membranes became available in the 1940s. They are made by acid leaching one of the phases in the glass. Currently these membranes can be prepared with pores as small as 4 nm. However, the brittleness and loss of microstructure when heated for long periods at elevated temperatures (> 300 °C) limit their application.



#### 2.3.2.2 Porous metal

Porous silver membranes were commercialised in the 1960s, but their use has been limited. Porous stainless steel membranes have been employed as high quality filters for many years. Porous stainless steel membranes can be used as supports for preparing composite membranes. The large pore size of these membranes and the possibility of inter metal diffusion at higher temperatures require some substrate modification.

#### 2.3.2.3 Molecular sieving membranes

Molecular sieving membranes have pore sizes ranging from 0.2 to 1 nm. Carbon molecular sieves, silica molecular sieves and zeolites are the most widely known. Carbon molecular sieves can separate molecules differing by as little as 0.02 nm in critical dimensions (Hsieh, 1996). They are prepared by pyrolysis of the membrane material between 500 °C and 750 °C. The pyrolysis temperature and conditions determine the pore size. These membranes are usually formed as hollow fibres (outer diameter between 5 microns and 1mm).

#### 2.3.2.4 Porous ceramic and composite membranes

Ceramics have several properties that make them the superior choice for inorganic membranes. $Al_2O_3$ remains stable up to 800 °C without degradation of the pore structure, it is resistant to corrosive environments, it is mechanically stable and can withstand pressure drops of up to 1.5 MPa. Metals and oxides can easily be dispersed on the membrane surface and into the pores to add catalytic properties. The acidity of the support must be taken into account and modified if it catalyses undesirable reactions.

Ceramics are mainly used as composite membranes, where several layers with decreasing pore sizes are deposited on one another. The final or permselective layer is typically a few microns thick and allows for high fluxes. A common example is one or more α-alumina support layers with a final γ-alumina separation layer, yielding a membrane with 4 to 5 nm pores. The top layer determines the characteristics (permeance and selectivity) and the pore size of the membrane. Top layers that have been deposited and studied include γ-alumina, zirconia, titania, oxide mixtures, zeolites, silica, metals and metal alloys. Each of these top layers will result in different pore sizes, with the aim making the membrane very selective (very small pore sizes in the Angstrom range) and allowing for a high flux to pass through the membrane (very thin selective layers in the nanometer range).

#### 2.3.2.5 Zeolite membranes

Zeolite membranes are composite membranes, where a thin zeolite layer is deposited on a support (usually α-alumina with or without γ-alumina modification). Jansen et al. (1998) prepared a specific zeolite structure (called a MFI-type zeolite) on steel, silicon and quartz. This type of membrane has received much attention in the last decade because zeolites can separate molecules in the Angstrom range. Possible applications are for use in isomerisation processes, hydrogen separation, water-alcohol separation and separation of organic compounds.

## 2.4 GAS SEPARATION MECHANISM

Separation of mixtures of gases is possible using either porous or non-porous membranes although they are quite different mechanisms of transport. Gas permeance is the only means by which membranes can be used to separate gas mixtures without change in phase. Separation of different gases is achieved by virtue of differences in molecular size and gas solubility in the membrane. Gases of smaller size have a larger coefficient, and in the convection-free environment in the pores of a membrane can be suitably separated by virtue of the different mobilities. The solubility of gas components in the membrane will be combined with diffusion to determine the permeability and

selectivity of separation. This is particularly true of asymmetric membranes which have a dense skin layer which controls performance.

### 2.4.1 KNUDSEN DIFFUSION

When viscous flow dominates, (Noble and Stern, 1995) molecules collide more with one another than with the pore walls of the membrane (see Figure 2.1). The pore diameter is large compared to the mean free path of the molecule and no separation can take place. By decreasing the pore size, separation can occur when molecules collide more with the pore walls than with one another. The flux (J) through a membrane of thickness *l* is:

$$J_i = \frac{G_f S_c}{\sqrt{2\pi M_i R_0 T}} \frac{\Delta P_i}{l} \qquad (2.1)$$

with $G_f$ the geometric factor accounting for porosity and tortuosity, $\Delta P$ the pressure difference across the membrane, M the molecular weight and $S_c$ the Sievert's constant. The separation factor for an equimolar gas mixture diffusing by Knudsen diffusion is the square root of the ratio of the molar masses:

$$\alpha_{ij} = \sqrt{\frac{M_i}{M_j}} \qquad (2.2)$$

Separation by Knudsen diffusion is limited in membrane reactors, since most of the feed is lost through the membrane's pores, which reduces the product yield. The best separation is obtained for light components like hydrogen.

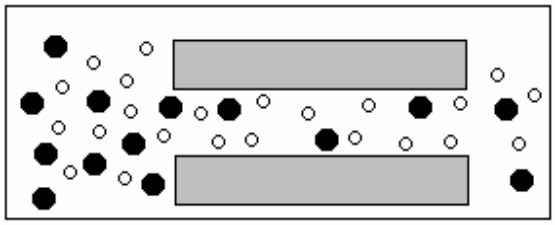

**Figure 2.1: Knudsen diffusion (Keuler, 2000)**

### 2.4.2 SURFACE DIFFUSION

Surface diffusion is an adsorption-dependent process (see Figure 2.2). It can occur in parallel with Knudsen diffusion, but at higher temperatures Knudsen diffusion dominates, as molecules desorb from the surface. Molecules adsorb onto the pore wall and migrate along the surface of the membrane pore. The permeability of the more strongly adsorbed molecule is increased (Noble and

Stern, 1995).

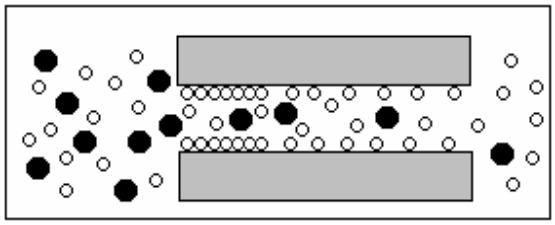

**Figure 2.2: Surface diffusion (Keuler, 2000)**

### 2.4.3 CAPILLARY CONDENSATION

Condensable vapour components in a mixture can condense in pores and block gas-phase diffusion through it if the pores are small enough (see Figure 2.3). The condensate will evaporate on the low pressure side of the membrane. The result is that the permeance of other components will be slow and limited by their solubility in the condensable component (Noble and Stern, 1995).

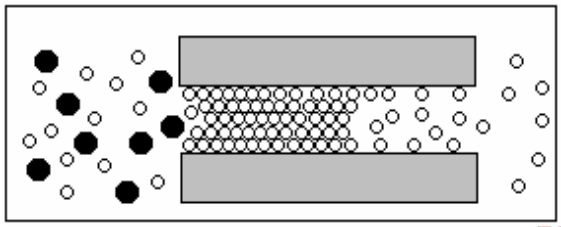

**Figure 2.3: Capillary condensation (Keuler, 2000)**

### 2.4.4 MOLECULAR SIEVE SEPARATION

Molecular sieve membranes allow for molecular sieve separation (see Figure 2.4). Pore sizes are less than 1 nm and allow for diffusion of only very small molecules (Noble and Stern, 1995).

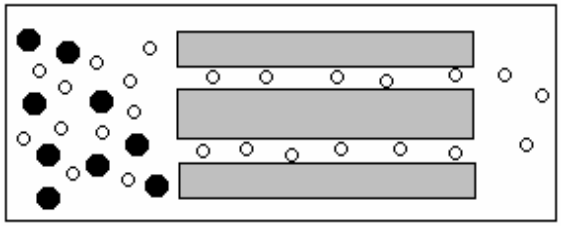

**Figure 2.4: Molecular sieve separation (Keuler, 2000)**

### 2.4.5 FLOW THROUGH NON-POROUS MEMBRANES

Hydrogen and oxygen transport through a non-porous membrane is illustrated in Figure 2.5. For hydrogen permeance there are several transport steps (Ward and Dao, 1999). A mathematical description of each process has been described by Ward and Dao (1999). These processes include:

- Molecular transport from the bulk to the surface film layer.
- Dissociative adsorption on the membrane surface.
- Atomic hydrogen dissolves in the membrane.
- Diffusion of hydrogen through the bulk membrane.
- Transition from the bulk to the surface on the low pressure side.
- Hydrogen atoms recombine to form molecules and desorb on the other side of the membrane.
- Gas transport from the membrane surface into the bulk gas.

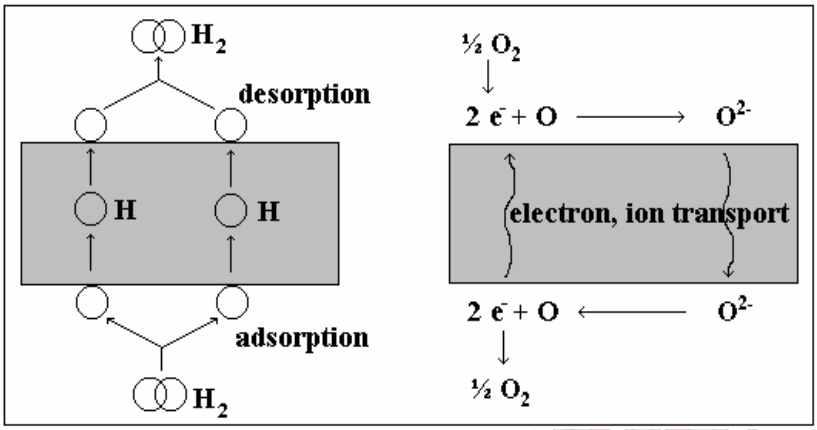


**Figure 2.5: Hydrogen and oxygen flow through a non-porous membrane (Keuler, 2000)**

The permeation flux (J) can be expressed using Fick's law (Buxbaum and Kinney, 1996):

$$J = \frac{D\ (C_{i,1} - C_{i,2})}{l} \qquad (2.3)$$

The diffusivity (D) is an Arrhenius function:

$$D = D_0 e^{-E_D / R_0 T} \qquad (2.4)$$

The hydrogen surface concentration (C) is the product of the Sievert's constant ($S_c$) and the hydrogen pressure ($P_{H_2}$):

$$C = S_c P_{H_2}^n \qquad (2.5)$$

When Sievert's law applies, n = ½. The conditions for Sievert's law have been discussed by Shu et

al. (1991) and Ward and Dao (1999). In general, as films get thicker (above10 μm) they approach Sievert's law and n = ½. Diffusion becomes the rate limiting step in hydrogen permeation. For very thin films, in the order of a few microns, the value of n approaches one. Hydrogen chemisorption on the palladium surface becomes the rate limiting step. Surface poisoning, grain boundaries and external mass transfer will cause further deviations from Sievert's law. The limiting transport mechanism is very temperature dependent. Ward and Dao (1999) concluded the following after an intensive investigation into hydrogen transport:

- Diffusion is likely to be rate limiting above 300 °C, even for thin membranes (approaching 1 μm).
- Desorption is likely to be rate limiting at lower temperatures.
- Adsorption is likely to be rate limiting for low hydrogen partial pressure and high surface contamination.
- For thin films (much less than 10 μm), external mass transfer becomes important, especially on the low pressure side.
- The membrane fabrication technique plays a significant role in permeation, which is probably related to the microstructure.


Furthermore, the permeability ($P_{er}$) expressed in mol.m/($m^2$.Pa.s) is defined as:

$$P_{er} = S_c D_0 e^{-E_D/R_0T} = P_0 e^{-E_D/R_0T} \qquad (2.6)$$

The flux equation can now be expressed in terms of pressure difference and permeability. Substituting equations (2.4) and (2.5) into (2.3), and then (2.6) into the result gives:

$$J = \frac{S_c D_0 e^{-E_D/R_0T}}{l}\left(P_{H_{2x}}^n - P_{H_{2y}}^n\right) = \frac{P_{er}}{l}\left(P_{H_{2x}}^n - P_{H_{2y}}^n\right) \qquad (2.7)$$

And the permeance ($P_m$) in mol/ ($m^2$.Pa.s) is:

$$P_m = \frac{P_{er}}{l} \qquad (2.8)$$

The hydrogen flux is very high through palladium and palladium alloys, mainly because palladium has a high hydrogen solubility. $D_o$ and $E_D$ values for the different palladium phases and at different temperatures have been given by Shu et al. (1991).

Oxygen permeance through silver is similar to that of hydrogen through palladium. The value of n can be taken as ½. Competitive adsorption by other gases in a gas mixture on silver reduces the oxygen permeability. For nonporous silica glass, the activation energy for hydrogen permeance is significantly higher than for palladium. For palladium it is in the order of 20 to 25 kJ/mol (Shu et al., 1991) and for silica about 35 kJ/mol (Gavalas et al., 1989).

## 2.5 PALLADIUM

Palladium was named after the asteroid Pallas, which was discovered at about the same time. Pallas was the Greek goddess of wisdom. Discovered in 1803 by Wollaston, Palladium is found with platinum and other metals of the platinum group in placer deposits of Russia, South America, North America, Ethiopia, and Australia. It is also found associated with the nickel-copper deposits of South Africa and Ontario. Palladium's separation from the platinum metals depends upon the type of ore in which it is found (Li, 1997).

### 2.5.1 THE CHARACTERISTICS

See basic characteristics of palladium in Table 2.3.

**Table 2.3 The characteristics of Pd (Li, 1997)**

| **Name** | **Symbol** | **Group number** | **Group name** |
|---|---|---|---|
| Palladium | Pd | 10 | Precious metal, or Platinum group |
| **Atomic number** | **Atomic weight** | **Period number** | **Block** |
| 46 | 106.42 (1) g | 5 | d-block |

### 2.5.2 BRIEF DESCRIPTION

A brief description is presented in Table 2.4.

**Table 2.4 Brief description of Pd (Li, 1997)**

| **Colour** | **Standard state** | **Classification** | **Density of solid** | **Molar volume** |
|---|---|---|---|---|
| silvery white metallic | solid at 298 K | Metallic | 12023 [kg/ $m^3$] | 8.56 [$cm^3$/mol] |
| **Melting Point** | **Boiling Point** | **Oxidation States** | **Liquid range** | |
| 1828.05 K or 1554.9 ºC | 3236 K or 2963 ºC | 3 or 2 | 1407.95 K | |

### 2.5.3 AVAILABILITY

Palladium is available in many forms including wire, foil, "evaporation slugs", granule, powder, rod, shot, sheet, and sponge. Palladium is a steel-white metal, does not tarnish in air, and is the least dense and lowest melting of the platinum group metals. When annealed, it is soft and ductile. Cold working increases its strength and hardness (Li, 1997).

### 2.5.4 ISOLATION

It would not normally be necessary to make a sample of palladium in the laboratory as the metal is available commercially. The industrial extraction of palladium is complex as the metal occurs in ores mixed with other metals such as platinum. Sometimes extraction of the precious metals such as platinum and palladium is the main focus of a particular industrial operation while in other cases it is a byproduct. The extraction is complex and expensive and only worthwhile since palladium is the basis of important catalysts in industry. Therefore, it is very necessary to prepare Pd-based membranes in economical and efficient methods so that they could be used in industry for Hydrogen separations and purifications (Li, 1997).

### 2.5.5 USES

The following uses for palladium are gathered from a number of sources as well as from anecdotal comments (Li, 1997).

- good catalyst for hydrogenation and dehydrogenation reactions,
- alloyed for use in jewellery,
- can be beaten into leaves as thin as 1/250000 inch,
- used in dentistry (crowns),
- used in fine instruments such as watches and some surgical instruments,
- used to make electrical contacts, and
- used to separate and purify hydrogen gas.

At room temperatures, when hydrogen is forced through Pd, the metal has the unusual property of absorbing up to 900 times its own volume of hydrogen. Hydrogen readily diffuses through heated palladium and this provides a means of purifying the gas.

### 2.5.6 PALLADIUM-HYDROGEN SYSTEM

The solubility characteristics of hydrogen in small palladium crystallites (nm range) are different to those in bulk palladium (Boudart and Hwang, 1975). Structural changes for palladium in hydrogen

presented in this study are for bulk palladium or palladium films and not palladium crystallites. At temperatures below 298 °C and pressures below 2.0 MPa, the β phase of palladium will co-exist with the α phase in a hydrogen atmosphere (see Figure 2.6 from Shu et al., 1991). There is a considerable difference in lattice expansion of the two phases, for example, a hydrogen to palladium ratio of 0.5 results in an expansion of about 10% in volume. Severe strains are induced by the nucleation and growth of the β phase in the α phase matrix (Keuler, 2000).

De Ninno et al. (1997) discussed the stress fields that are created when hydrogen dissolves in palladium under 300 °C. The results were hardening, embrittlement and distortion of the film, which led to cracks in the membrane after a few hydrogenation-dehydrogenation cycles. To avoid these negative effects, the palladium must be kept in the α phase above 300 °C at all times.

Alternatively, the palladium can be alloyed to suppress α to β phase transitions and avoid distortion. The permeability of the alloy should be comparable to or better than that of the pure palladium, have high mechanical strength, and be resistant to poisoning.

Aoki et al. (1996) performed temperature cycling tests on palladium. Thin Pd films (< 1 μm) prepared by chemical vapour deposition remained stable for many temperature cycles between 100 °C and 300 °C.

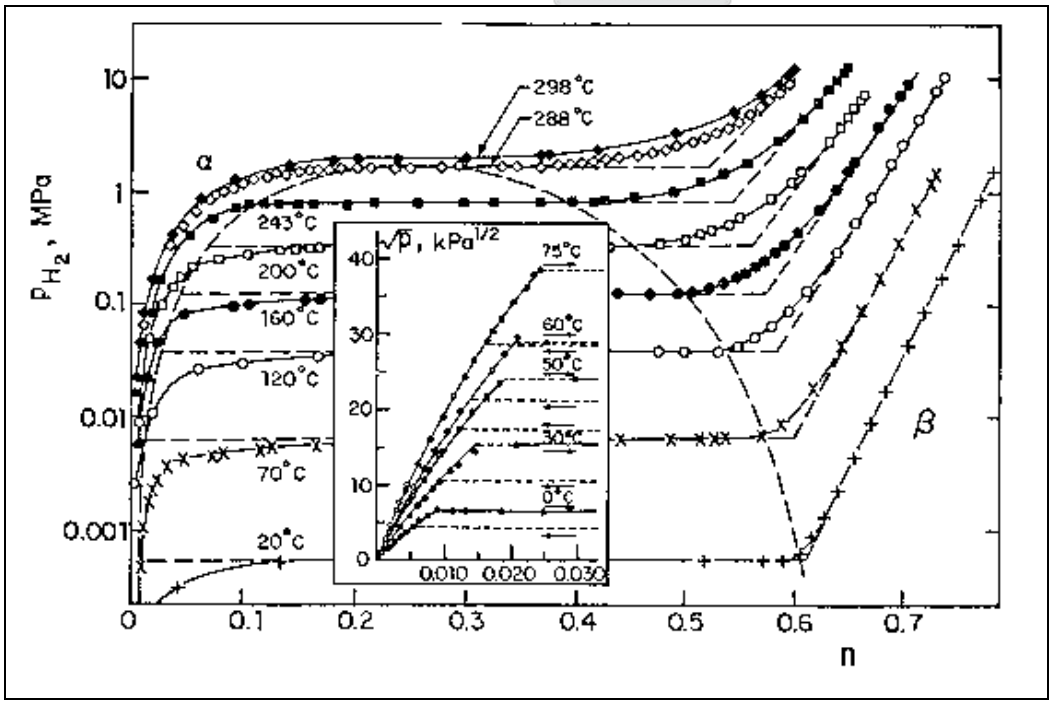


**Figure 2.6: Equilibrium solubility isotherms of $PdH_n$ for bulk Pd (Shu et al., 1991)**

## 2.6 PALLADIUM AND PALLADIUM ALLOY MEMBRANES

In recent years, there has been an increasing interest in developing palladium based membranes applied to versatile fields, such as hydrogen separation, hydrogenation, dehydrogenation, methane reforming, etc. Palladium and palladium membranes have consequently received growing attention for separation and purification of hydrogen, largely due to the unique permselectivity of palladium to hydrogen and good mechanical stability. However, the palladium foil suffers from the discontinuous lattice expansion due to α-β phase transition at temperature below 573 K in hydrogen atmosphere, namely hydrogen embrittlement. As reported in the literature, addition of group IB metals (e.g. Ag and Cu) into palladium membrane can prevent hydrogen embrittlement and also increase the hydrogen flux. Uemiya et al. (1995) demonstrated the palladium membrane alloying with 23% silver exhibited maximum hydrogen permeability. Recently, current developments look at the employment of composite membranes in which the palladium or palladium alloy is deposited as a thin film onto a porous ceramic or metal substrate. The introduction of alloying elements into the palladium membranes has been used to improve their resistance to hydrogen embrittlement. Such composite membranes (with a thin palladium film on a porous substrate) have good stability and reduced material costs, but their main attribute is in providing a structure possessing both higher hydrogen fluxes and better mechanical properties than the thicker metal membranes. Much effort on promoting the hydrogen permeation rate of palladium alloy membranes have been reported by Cheng and Yeung (1999), Keuler et al. (2000, 2002), and Nam and Lee (2001).



### 2.6.1 PREPARATION OF PALLADIUM MEMBRANE

Initial work on palladium membranes used foils, typically 50 μm or thicker. The advances made in preparing inorganic membranes have shifted research away from foils towards composite membranes with much thinner palladium layers. Not only is this cheaper, but it also allows for a large increase in hydrogen flux through the film. Composite palladium membranes are prepared by depositing palladium or palladium alloys on a multi-layer inorganic membrane support. Several thin film deposition techniques have been developed to deposit thin palladium layers with minimum defects.

Prior to any deposition, the membrane support needs to be thoroughly cleaned. Different thin film deposition techniques will be discussed briefly in the next few paragraphs. More detail on preparing thin films can be found in Keuler (1997).

#### 2.6.1.1 Wet impregnation

This technique is not suitable for preparing dense metal layers on inorganic supports. The metal is deposited in the pores of the membrane and often these membranes are used as contactors. Cannon et al. (1992) prepared Pd-impregnated porous Vycor glass membranes. The change in membrane pore size was minimal. Porosity control and uniform impregnation were some problems encountered. The metal served as a catalyst and not as a separator. Uzio et al. (1993) found that the membrane permeability was not changed after depositing Pt through ion exchange on an alumina membrane (Societé des Céramiques Techniques or SCT multi-layer membrane with a 4 nm γ-alumina top layer). For the membranes tested by Uzio et al. (1993), the diffusion mechanism remained Knudsen diffusion after depositing Pt on an alumina membrane.

#### 2.6.1.2 Sol-gel process

Brinker and Scherer (1990) described sol gel chemistry. Particles of a few nanometers in size can be made and deposited on a support membrane. The gel is applied onto the membrane by slip casting. The organic components in the gel are burned off during the firing stage, and the result is an inorganic membrane support with a metal or oxide layer deposited on it.

Several attempts have been made to prepare Pd or Pt composite membranes by the sol gel method. Xiong et al. (1995) prepared Pd/γ-alumina membranes of which the pore size varied between 5.5 and 6.5 nm for the different Pd concentrations employed, indicating that there was little success in reducing the pore size. Vitulli et al. (1995) prepared a $Pt/SiO_2$ layer by the sol gel process on a SCT multi-layer alumina support. The resultant membrane showed Knudsen diffusion properties with a hydrogen to nitrogen selectivity of less than 3.

#### 2.6.1.3 Vapour deposition techniques

There are two basic types of vapour deposition techniques for preparing thin films: chemical and physical vapour deposition. Physical vapour deposition can be through either evaporation or sputtering.

- Physical vapour deposition

With physical vapour deposition, complex alloys can be prepared, the deposition rate can be accurately controlled and very thin films (< 1 μm) can be prepared, but deposition on non-flat surfaces poses problems. Chemical vapour deposition can be performed inside tubes, but there is a large loss of vapour through the membrane in the initial stages (Morooka et al., 1995).

Evaporation can be performed with resistive heating, but it is far less common than sputtering. During sputtering, atoms from the target are dislodged through ion bombardment by an inert gas and deposited on the substrate. Argon is most frequently used. Key parameters during sputtering are the sputtering time, plasma power, substrate temperature and target to substrate distance. Jayaraman et al. (1995a, b) investigated the effects of some of those parameters on the quality and permeance of the sputtered film. Gryaznov et al. (1993) prepared complex alloys of palladium and one or more of Ru, Co, Pb, Mn and In on porous metal discs. All examples encountered in literature for palladium sputtering on porous supports used discs as the substrate.

- Spray pyrolysis

Spray pyrolysis is similar to sputtering. Li et al. (1993) rotated capillary membranes in a high temperature flame to deposit palladium and silver on the outer surface of the membrane. Palladium and silver nitrate were atomised and the aerosol fed with oxygen to a hydrogen-oxygen flame. The metal condensed on the membrane to form a metal layer.

- Chemical vapour deposition

For chemical vapour deposition (CVD), a metal salt is heated and deposited on the substrate. Palladium acetate is commonly used (Morooka et al., 1995) as the metal salt. CVD reactors are described by Xomeritakis (1996). Typical sublimation conditions for palladium acetate are temperatures between 400 °C and 500 °C and a reduced pressure in an argon atmosphere. Palladium chloride can also be used for CVD. The detailed experimental conditions have been given by Xomeritakis (1996). $PdCl_2$ was reduced with hydrogen. The reduced pressure was applied on the one side of the tube and the layer deposited on the other side of the tube. There was some deposition of palladium inside the pores. Layers prepared by CVD are typically thicker than those prepared by sputtering.

#### 2.6.1.4 Electroplating

Metals and alloys can be plated on a conducting substrate that acts as a cathode. Ceramics and plastics need to be treated before they can be electroplated. The metal cations are suspended in solution and reduced by an external current passing through the electrolyte. The cation concentration, bath temperature and current density determine the deposition rate. Even deposition on large surfaces is difficult due to a variance in current density and a declining metal ion concentration in the plating bath. A method for plating Pd and its alloys on porous supports was described by Itoh and Govind (1989).

In a more recent study, Nam et al. (1999) used a vacuum electroplating technique to deposit palladium on a modified porous stainless steel support. A submicron Ni layer was dispersed on the surface of the porous stainless steel support (0.5 μm pore size) under low vacuum and then sintered at 800 °C for 5h under high vacuum. A thin copper layer was deposited on the Ni and finally a Pd layer was electroplated on the copper under vacuum. The film was about 1 μm thick with 78 wt % Pd and 22 wt % Ni. Hydrogen to nitrogen selectivity varied between 500 and 5000 at temperatures over 350 °C.

#### 2.6.1.5 Electroless plating

Electroless plating is an autocatalytic oxidation-reduction reaction in which metal ions are reduced and deposited as metal atoms. It is similar to electroplating, but no external current is supplied. A detailed discussion can be found in Keuler (1997). It can be applied onto any material that has been properly pretreated. Some materials that have been electroless plated are porous Vycor glass (Yeung et al., 1995a; Uemiya et al., 1991), porous stainless steel (Shu et al., 1993) and porous alumina (Collins and Way, 1993; Yeung and Varma 1995b). The main advantages and disadvantages of electroless plating are listed by Keuler (1997). The advantages of this process can be summarised as:

- The technique is quick, simple and inexpensive.
- Dense, non-porous films of even thickness can be prepared on any shape.
- There is good metal to ceramic adhesion.



The main disadvantages are:

- Impurities might form in the metal layer when using certain reducing agents. Using sodium hypophosphite as reducing agent causes a 1.5% phosphor deposition (Loweheim, 1974,) and using boronhydride results in a 3-8% boron deposit (Shipley, 1984). Hydrazine gives very pure deposits, but the deposition rates tend to be slow (Athavale and Totlani, 1989).
- Thickness control is difficult and costly losses might occur due to the decomposition of the plating solution (Shu et al., 1991).
- Co-deposition with other metals to form alloys has not been very successful so far. Deposition of separate metal layers and subsequent alloying has also proven to be very difficult.

## 2.7 ELECTROLESS PLATING

Electroless plating is a controlled autocatalytic deposition of a continuous film on the surface of a substrate by the interaction of the metal and a chemical reducing agent. For palladium membrane preparation using the electroless plating technique, palladium particles are produced by reduction from the plating solution containing amine-complexes of palladium in the presence of reducing agents. These particles then grow on palladium nuclei which have been pre-seeded on the substrate surface through a successive activation and sensitisation procedure and which also act as a catalyst for the reduction of the palladium complexes. This creates the autocatalysed process of electroless plating.

### 2.7.1 SUBSTRATE PRETREATMENT

As mentioned earlier (see Section 2.6) the substrate needs to be thoroughly cleaned before any thin film deposition technique can be successfully applied. For electroless plating on non-conducting surfaces (ceramics and plastics), the surface needs to be activated prior to plating. There are two procedures for catalysing the surface to be plated (Feldstein, 1974). Both processes employ palladium and tin salts. In the older process the substrate is first placed in a tin chloride solution (sensitising step) and then in a palladium salt solution (activation step). For the exchange process, a colloidal solution containing both palladium and tin salts is required.

Palladium ions are reduced and Pd nuclei are deposited on the substrate. Models for nuclei growth on the substrate have been developed by Cohen et al. (1971). Several pretreatment solutions are listed (Osaka and Takematsu, 1980) in literature and have been tested and evaluated. The two step process deposits more metal than the exchange process does and there is a higher Pd content in the deposit. This is favourable for preparing high purity deposits.

### 2.7.2 ELECTROLESS PLATING SOLUTION COMPOSITION

An electroless plating solution has a few basic components:

- a metal salt of the required metal than needs to be deposited,
- a reducing agent,
- a pH regulator, and
- a stabiliser that forms a complex with the metal ions and allows for a slower metal release from the solution.

Not all metals can be electroless plated, but metals that form good hydrogenation-dehydrogenation catalysts can be plated. A universal plating mechanism is described by Van den Meerakker (1981).

Ethylene di-amine tetra acetate (EDTA) is most commonly used as stabiliser with hydrazine or sodium hypophosphite as the reducing agent. Ohno et al. (1985) lists five reducing agents that can be used for various metal depositions. The amine complex of palladium is used for electroless plating: $(NH_3)_4PdX$, with X = $Cl_2$ or $NO_3$.

Rhoda (1959) developed an autocatalytic reaction process for the deposition of palladium by means of electroless plating. The tendencies for a homogeneous reduction of palladium ions and a high degree of solution instability were overcome by using the disodium salt of EDTA as a stabiliser. The plating solution employed by Rhoda, consisted of a palladium-amine complex, a reducer and a stabilising agent as basic ingredients. Palladium deposition occurs according to the following two simultaneous reactions (Mouton, 2003).

- Anodic reaction:

  $N_2H_4 + 4OH^- \rightarrow N_2 + 4H_20 + 4e^-$ (2.9)
- Cathodic reaction:

  $2Pd^{2+} + 4e^- \rightarrow 2Pd^0$ (2.10)
- Autocatalytic reaction:

  $2Pd^{2+} + N_2H_4 + 4OH^- \rightarrow 2Pd^0 + N_2 + 4H_2O$ (2.11)

During the electroless plating, if the reactants in the plating solution match the ratio in equation (2.11), $Pd^{2+}$ will completely turn to Pd metal.

Furthermore, different plating characteristics are observed when plating the inside and the outside of porous tubes. Keuler et al. (1997) investigated the interaction between various plating variables and their effect on solution stability.

### 2.7.3 RECENT ADVANCES IN ELECTROLESS PALLADIUM PLATING

With the conventional electroless plating technique, membrane selectivity drops fast when palladium films are thinner than 5 μm. The deposit tends to be columnlike and defects are present in the thinner films. Research has focussed on trying to make films thinner, modify defects and yet maintaining high selectivity.

Yeung et al. (1995a, 1995b) studied the application of osmotic pressure during electroless plating. They used porous Vycor membranes as well as α/γ-alumina membranes as supports. Yeung and co-

workers found that the osmotic pressure made the Pd coatings denser, nonporous, thinner and with a smoother surface morphology.

Li et al. (1997, 1999) used a similar approach to repair defects in their electroless plated Pd films. Porous stainless steel (0.1 μm pore size) and α-alumina (0.16 μm pore size) membranes were used as supports. An initial Pd coating was applied and then one or more coatings were added under osmotic pressure with NaCl as solute. This resulted in film densification and defect minimisation.

Zhao et al. (1998) used a different pretreatment process to the traditional Pd/Sn activation and sensitisation process. The porous alumina substrate was activated by a Pd(II) modified boehmite sol. The gel-coated substrate was dried, calcinated at 600 °C and then reduced in hydrogen at 500 °C. Electroless plating was performed on those activated substrates which they claimed had a smoother surface and more uniform distribution than those prepared by conventional pretreatment. After using very high hydrazine concentrations, they observed that the electroless Pd coating consisted of much finer particles and this resulted in a more compact film.

Zheng (2000) prepared palladium–ceramic composite membranes on porous α-$Al_2O_3$ supports by electroless plating. A novel hydrothermal method was used to control the systemic pressure for the fabrication of palladium membrane. Palladium membranes with a pore size of 0.36 mm were prepared by electroless plating under hydrothermal conditions. The pore size shrinkage of the hydrothermally deposited palladium membrane is significantly higher than that produced under conventional conditions.

Tong and co-workers (2005) stated that an improved electroless plating method using aluminum hydroxide gel as a modification material has been developed for the fabrication of thin Pd membranes on MPSS substrates. The membrane preparation procedure consisted of preparation of filling materials, material filling into the macro pores of the substrate, electroless plating of thin Pd membrane on the filled substrate, and recovery of the macropores of the substrate. The macropores inside the substrate can be completely filled with aluminum hydroxide gel. A Pd membrane as thin as 6 μm is deposited on the dense substrate by the electroless plating. A stable Pd membrane with high hydrogen permeability can be prepared by introduction of Pd seeds in the hydroxide gel.

## 2.8 PALLADIUM MEMBRANE TEMPERATURE STABILITY

Some work has been done on the long term stability of metal composite membranes (Buxbaum and Kinney, 1996), where palladium is coated onto other refractory metals. Very few papers have been published on the long term stability of palladium or palladium alloys deposited on porous supports and on alloying procedures.

Paglieri et al.(1999) studied the high temperature stability of Pd composite films prepared by electroless plating. Plating was performed on the inside of a 200 nm α-alumina support. At temperatures of 550 °C and above, the membranes failed after a few days and the separation factors dropped to the Knudsen level. Removing tin from the pretreatment procedure in electroless plating reduced the problem of membrane failure, but substantial selectivity decline still occurred above 550 °C. At 450 °C and 500 °C, the membranes remained fairly stable for a number of weeks, and the time of stability depended on the Pd film thickness. It was found that the amount of time to fail was proportional to the Pd film thickness and that the same failing mechanism prevailed for all thicknesses. Possible reasons for failing were:

- Impurities might be trapped at the Pd-alumina interface during pretreatment and plating, which later result in pore formation.
- Differences in thermal expansion of Pd and alumina can cause cracking.
- Residual porosity in the Pd film can transform into pores.

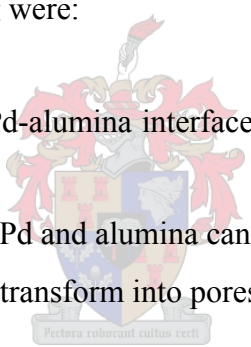


## 2.9 DEACTIVATION OR POISON OF PALLADIUM MEMBRANES

Palladium and palladium alloy membranes perform well when exposed to only pure hydrogen. The presence of other gases may severely impair hydrogen transport through the membrane. Although this field has not been extensively studied, some investigators have reported important findings. McBride and McKinley (1965) studied the effects of about 50% CO, $H_2S$, $CH_4$ and $C_2H_4$ in hydrogen. They reported that all gases showed some decrease in hydrogen permeance, with $H_2S$ giving the worst result. They concluded that at lower temperatures, molecules adsorb on palladium to decrease the sites available for hydrogen adsorption. At high temperatures a thin contaminant layer (coking) may form on the palladium. Antoniazzi et al. (1989) studied membrane deactivation caused by $H_2S$. They concluded that $H_2S$ poisoning was irreversible and that the reduction in hydrogen permeance through the Pd foil fell by about 1% for every ppm $H_2S$ present in the feed.

A number of studies have focussed on the effects of carbon monoxide on hydrogen permeance (Yoshida et al., 1983; Sakamoto et al., 1996) through palladium and palladium alloys. The general conclusion was that the operating temperature of the membrane in the presence of CO should be above 350 °C, to prevent CO adsorption and loss of hydrogen flux.

Jung et al. (2000) studied hydrogen permeance through palladium in the presence of steam, methane, propane and propylene. Propane and methane had a negligible effect on the hydrogen flux through the palladium film. Propylene caused severe flux decline, which dropped further with time. A carbonaceous layer was formed on the Pd due to the dehydrogenation of propylene. Steam had both a positive and a negative effect. Steam adsorbed strongly on palladium to decrease the available surface for hydrogen adsorption and thus, the hydrogen flux through the film. On the other hand, steam volatilised carbon species on the palladium surface to reduce coking and improve the hydrogen flux.

## 2.10 PERMSELECTIVITY OF PALLADIUM MEMBRANES

A comparison of results obtained recently for hydrogen flux measurements and hydrogen selectivities for Pd and Pd/Ag membranes obtained by electroless plating and by MOCVD (metal organic chemical vapour deposition) are presented in Table 2.5. Electroless plating tends to give higher fluxes and also produces larger values of the $H_2/N_2$ selectivities. An interesting feature is that the pressure exponent values are either 0.5, or close to this value, for the membranes prepared by electroless plating, but unity for those prepared by MOCVD. The tendency to diffusion control, suggested by the results for the electroless plated membranes, may be a function of the greater thickness of these structures, while for the thinner MOCVD membranes the fluxes are primarily controlled by first-order surface processes.

Most of the research effort (Hughes, 2001) has been concentrated on the use of porous alumina and porous stainless steel as substrates onto which the Pd deposited, although silica, porous glass, some polymers and other porous metals have also been used to a minor extent. A comparison of porous stainless steel and α-alumina supports for both Pd and Pd/Ag given in Figure 2.6, in the form of Arrhenius plots. The thickness of the deposited layers was about 10 μm in each case. Activation energies almost identical for all three systems, indicating that the nature of the porous support does not affect the mechanism. However, it appears that the porous stainless steel substrate produces lower fluxes than the porous alumina, despite having a large pore size.

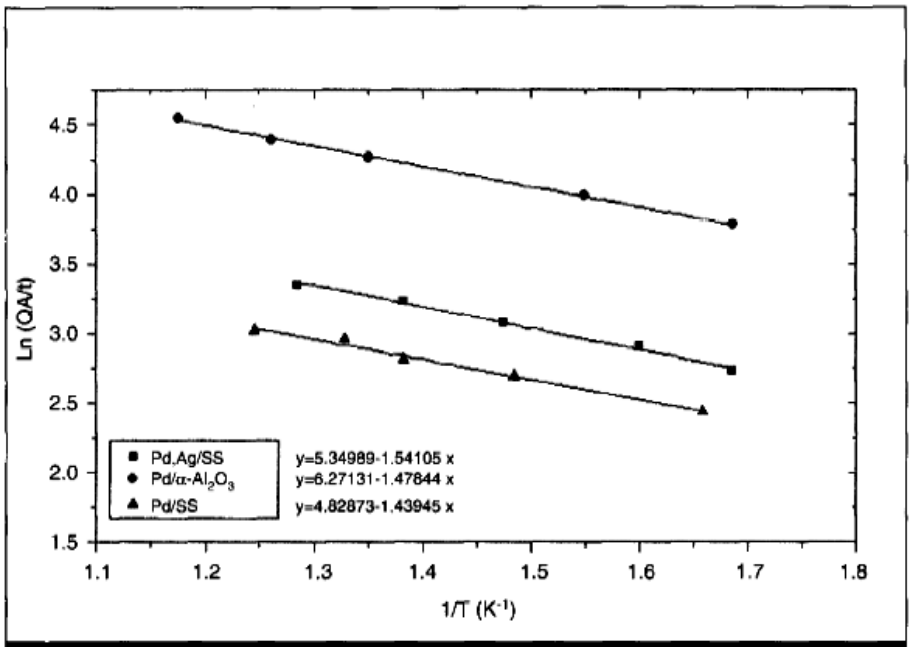


**Figure 2.7:** **Comparison of activity for three membranes (Hughes, 2001)**

**Table 2.5:** **Hydrogen fluxes and selectivities of Pd and Pd/Ag membranes (Hughes, 2001)**

| **Membrane** | **Preparation method** | **Pd film thickness (μm)** | **$H_2$ flux (μmol/$m^2$/s/Pa)** | **Selectivity ($H_2/N_2$ or $H_2$/He)** | **Pressure exponent: n [see equation (2.7)]** | **T (°C)** | |
|---|---|---|---|---|---|---|---|
| $Pd/Al_2O_3$ | Electroless plating | 17 | 2.49 | >1000 | 0.573 | 500 | Collins & Way (1993) |
| Pd-Ag(23%) on $Al_2O_3$ | Electroless plating | 5.8 | 4.7 | - | 0.5 | 400 | Kikuchi & Uemiya (1991) |
| Pd/Stainless steel | Electroless plating | - | 1.0 | 5000 | 0.5 | 350 | Mardilovich (1998) |
| Pd/Stainless steel | Electroless plating with osmosis | - | 9.1 | 10000 | 0.5 | 560 | Yeung & Varma (1995b) |
| $Pd/Al_2O_3$ | MOCVD | 3.5 | 0.9 | 1000 | 1 | 300 | Xomeritakis & Lin (1996) |
| $Pd/Al_2O_3$ | MOCVD | 0.5-1 | 0.05-1.0 | - | 1 | 350-450 | Xomeritakis & Lin (1998) |
| Pd/sol-gel $Al_2O_3$ | MOCVD | 0.5-5 | 0.1-0.2 | 200-300 | 1 | 300 | Collins & Way (1993) |

## 2.11 APPLICATIONS OF INORGANIC MEMBRANES

There are many advantages and disadvantage of using inorganic membranes for separation reactions. Keuler (1997) gave an extensive list of these advantages and disadvantages. More advantages and disadvantage were given by Armor (1995). Inorganic membrane technology has been fully commercialised and is used in many different industries. These include food processing, processing of beverages, drinking water, biotechnology, pharmaceuticals, waste oil treatment and petrochemical processing. Hsieh (1989) and Hsieh (1996) discussed these and many other specialised applications. Pd alloy metal membranes are commercially used as hydrogen purifiers (Hsiung et al., 1999). The present study will concentrate on a class of modified inorganic membrane called catalytic membranes, and more specifically on palladium-based catalytic membranes.

## 2.12 PALLADIUM MEMBRANE REACTORS

Considerable interest has been expressed in recent years in the concept of process intensification, one important aspect of which is the potential for combining the reaction and separation stages of a process in one unit. Apart from the benefit inherent in cost reduction of plant and maintenance, there is also the potential attainment of higher conversions and product yields (Hughes, 2001).

Although most research effort has been devoted to obtaining higher conversions and overcoming the limits imposed by equilibrium, it is often of more practical application to use the membrane to operate at the same conversion, but at a lower temperature. This means the reaction selectivity can be improved by minimising side reactions which are more prevalent at a high temperature, and in particular, by limiting the amount of carbonaceous deposits which would reduce catalyst activity (Hughes, 2001).

The two main areas of application considered for catalytic membrane reactors are those involving the removal or addition of hydrogen through a selective membrane, or the use of porous membranes to control the feed rate during partial oxidation reactions. Pd is still the dominant material for this purpose. This is because of its considerable solubility for hydrogen. The pure Pd metal absorbs 600 times of its volume at room temperature, and the various Pd alloys absorb comparable quantities (Hughes, 2001).

For use in membrane reactors the following requirements must be met:

- the membrane should possess a high hydrogen permeation flux,
- should have a high selectivity for hydrogen,
- must be resistant to poisons,
- must be durable, that is, it must have a long service life, and be resistant to temperature cycling, and
- must be capable of adequate sealing in the membrane reactor.

## 2.13 SUMMARY

This chapter introduced the background for the remaining section of this thesis. It mainly presents the various types of inorganic membranes that are currently available. The main advantages and disadvantages of using inorganic membranes as well as the areas of application have been mentioned. The different separation mechanisms through porous membranes and non-porous membranes were discussed. Palladium and palladium alloy membranes were discussed in more detail, with specific attention being given to the palladium-hydrogen system. Different methods by which to prepare palladium composite membranes were described. Electroless plating was discussed in detail, covering substrate cleaning, pretreatment and the actual plating process. Recent advances in electroless plating were then mentioned. Finally, Pd membrane reactor was briefly described.



According to the literature study in this chapter, it was found that growing attention has been paid to electroless plating with vacuum or osmosis. Keuler (2000) applied a vacuum on the shell side of the plating reactor during the electroless plating without precisely measuring it. Moreover, there are few publications or papers focusing on the influence of the support membranes on the electroless plating, methods of pre-cleaning before pretreatment, the vacuum applied during electroless plating, post-cleaning, heat treatment after plating. Moreover, the morphological structures of palladium composite membranes also influences the permselectivity of the palladium composite membranes where $H_2$ flows through. Therefore, the factors mentioned above, which affect the preparation and permselectivity of Pd composite membranes, have been investigated in this project.

# CHAPTER 3: BASIC EXPERIMENTAL PROCEDURES

Chapter 3 consists of four sections. The first section (3.1) focuses on the methods for characterisation of the support membranes, prior to electroless plating. The second section (3.2) details the preparation procedures for palladium composite membranes using a modified electroless plating technique. The third section (3.3) describes the heating methods after palladium electroless plating has been achieved. The fourth section (3.4) describes permeance testing, using hydrogen and nitrogen, and analytical characterisation techniques performed on the prepared palladium composite membranes.

## 3.1 SUPPORT MEMBRANE

This section provides the basic information of support membranes, and describes the procedures for characterisation of support membranes by the bubble point test, bubble point screening test, and membrane permeance testing.

### 3.1.1 SUBSTRATES OR SUPPORT MEMBRANES

The support membranes, i.e. the substrates utilised in this study, were macroporous α-alumina ceramic membranes, purchased from Pall Exekia Corporation, France. The membranes comprise three α-alumina layers, whose structure is illustrated in Figure 3.1.

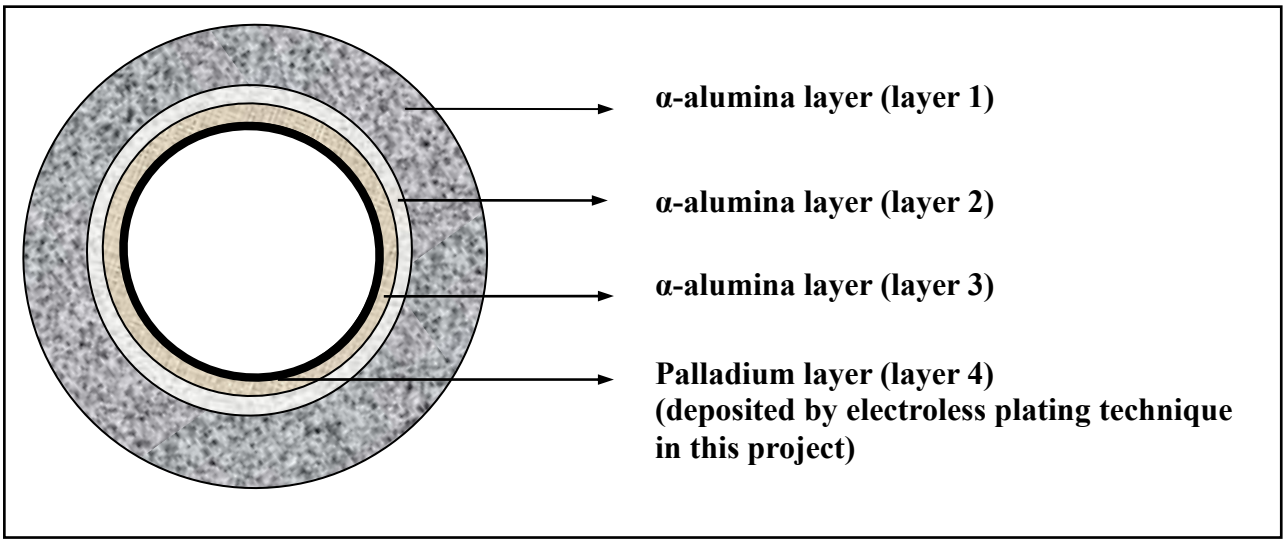


**Figure 3.1: α-alumina ceramic membrane structure (Pall Exekia)**

The α-alumina ceramic membranes had a length of 150 mm, an outside diameter of 10 mm and an inside diameter of 7 mm. The innermost layer had a pore size of 200 nm. Further characteristics relevant to the pore diameter and thickness of each layer are presented in Table 3.1. Pictures of the uncoated (blank) support membrane and Pd coated membrane can be seen in Figures 3.2 and 3.3 respectively.

**Table 3.1: Characteristics of a α-alumina ceramic membrane (Pall Exekia)**

| | Description of layer | Pore diameter (μm) | Layer thickness (μm) |
|---|---|---|---|
| **Layer 1** | α-alumina | 12 | 1500 |
| **Layer 2** | α-alumina | 0.8 | 40 |
| **Layer 3** | α-alumina | 0.2 | 20 |
| **Layer 4** | Palladium (deposited by electroless plating technique in this project) | 0 | 1.7 - 4 |

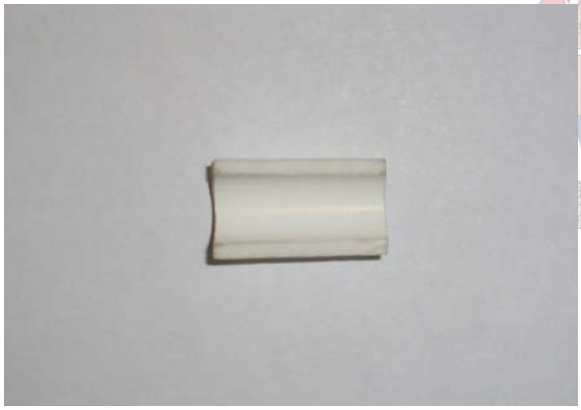

**Figure 3.2: Uncoated support membrane (blank)**

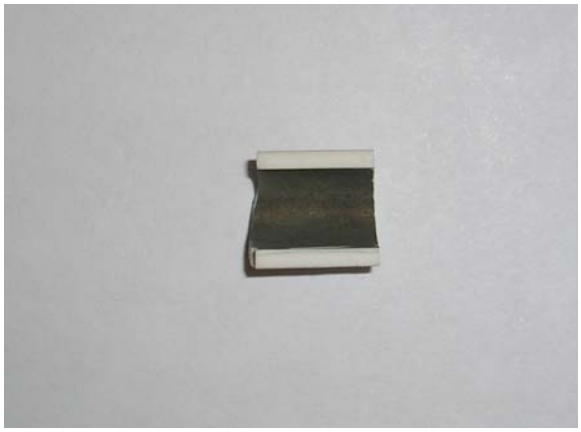

**Figure 3.3: Pd coated membrane**

In order to obtain a proper membrane reactor sealing, the outside surface at the ends of the support membrane had to be sealed with enamel prior to plating. Enamel was applied along a length of 10~15 mm at both ends on the outer surface of the support membrane. The membrane ends were first dipped into an enamel slurry, after which they were calcined (Keuler, 2000). The manufacturer of the substrates completed this procedure. Two or three layers of enamel, which were non-porous, were applied to obtain a good sealing. (See Figure 3.4)

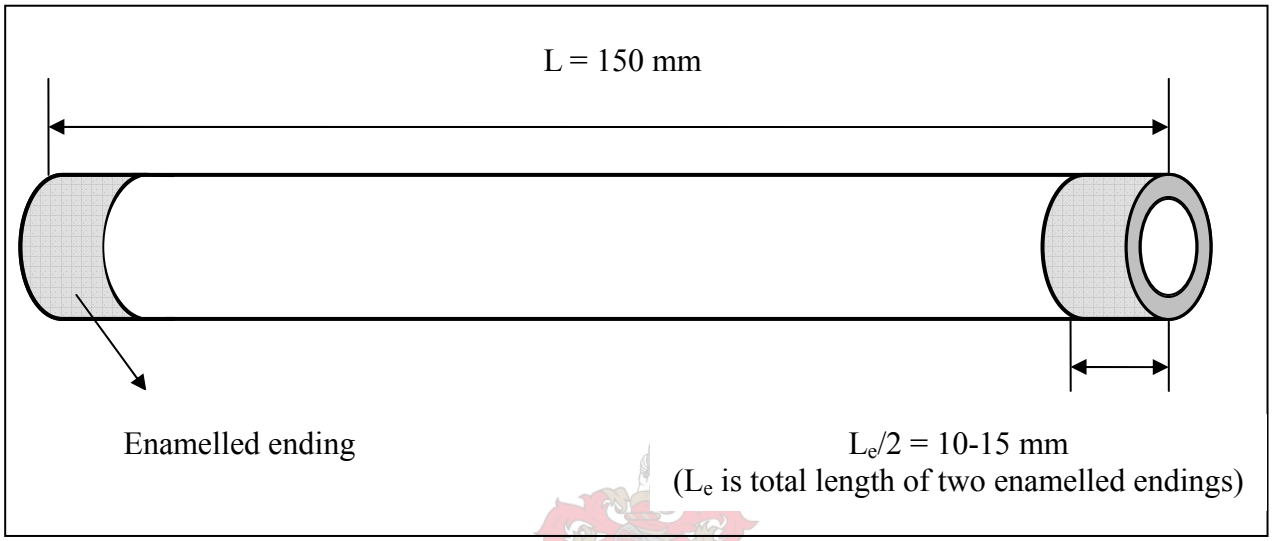


**Figure 3.4: A support membrane with enamelled endings**

Two similar sets of support membranes were used in this study. One set of membranes was purchased in 2004 (namely membranes 1/30, 2/30, 3/30, 4/30, 5/30, 6/30, 10/30, 12/30), and the other set of membranes was purchased in 2005 (memebranes 1/17, 2/17, 4/17, 5/17, 6/17).

Some additional information about the support membrane is summarised below.

- Volume of substrate (or support membrane):

$$V_m = (L - L_e) \times (\pi \times D_i^2) / 4 \qquad (3.1)$$

- Surface area of substrate (or support membrane) for plating:

$$A_p = \pi \times (L - L_e) \times D_i \qquad (3.2)$$

$l$ ------- Thickness of palladium layer [m]

$d_{Pd}$ ------- Density of palladium (12023 kg/m$^3$) [kg/m$^3$]

| | | | |
|---|---|---|---|
| $V_m$ | ------- | Volume of support membrane | [$m^3$] |
| $A_p$ | ------- | Surface area of support membrane for plating | [$m^2$] |
| L | ------- | Length of support membrane | [m] |
| $L_e$ | ------- | Total length of both enamelled endings | [m] |
| $D_i$ | ------- | Inner diameter of membrane tube | [m] |

Therefore, according to equations (3.1) and (3.2), the necessary results could be obtained. The volume of substrate for plating in this study is illustrated in Table 3.2. Sample calculations of $S_p$ and $V_p$ for membrane (1/17) are listed below.

- Volume of substrate (or support membrane):

  $V_m = (L - L_e) \times (\pi \times D_i^2) / 4$ = (15-2.2) x 3.14 x $0.7^2/4$ = 4.9235 $cm^3$

- Surface area of substrate for plating:

  $A_p = \pi \times (L - L_e) \times D_i$ = 3.14 x (15-2.2) x 0.7 = 28.1344 $cm^2$

**Table 3.2: Basic information of the α-alumina ceramic membranes used in this study**

| Identification of Membrane | Length (L-$L_e$) (cm) | Surface Area ($cm^2$) $A_p$ | Volume of Support membrane ($cm^3$) $V_m$ | Mass of support membrane prior to pretreatment (g) |
|---|---|---|---|---|
| **Membrane Set 1 (purchased in 2004)** | | | | |
| **1/30** | 12 | 26.376 | 4.6158 | 16.7503 |
| **2/30** | 12 | 26.376 | 4.6158 | 16.7454 |
| **3/30** | 12 | 26.376 | 4.6158 | 16.7503 |
| **4/30** | 12 | 26.376 | 4.6158 | 16.9204 |
| **5/30** | 12.8 | 28.1344 | 4.9235 | 16.7111 |
| **6/30** | 12.1 | 26.5958 | 4.6543 | 16.9009 |
| **10/30** | 12 | 26.376 | 4.6158 | 16.6800 |
| **12/30** | 12 | 26.376 | 4.6158 | 16.9639 |
| **Membrane Set 2 (purchased in 2004)** | | | | |
| **1/17** | 12.8 | 28.1344 | 4.9235 | 17.3584 |
| **2/17** | 12.8 | 28.1344 | 4.9235 | 16.6977 |
| **4/17** | 12.8 | 28.1344 | 4.9235 | 16.6826 |
| **5/17** | 12.7 | 27.9146 | 4.8851 | 17.0170 |
| **6/17** | 12.8 | 28.1344 | 4.9235 | 16.9598 |

### 3.1.2 BUBBLE POINT SCREENING TEST

It was found in this study that the bubble point screening test provides a simple and effective means for visualising the locations of defects on the surface of the support membrane. The apparatus was manufactured in the workshop of the Department of Process Engineering at the University of Stellenbosch. The equipment is shown in Figure 3.5 and Figure 3.6.

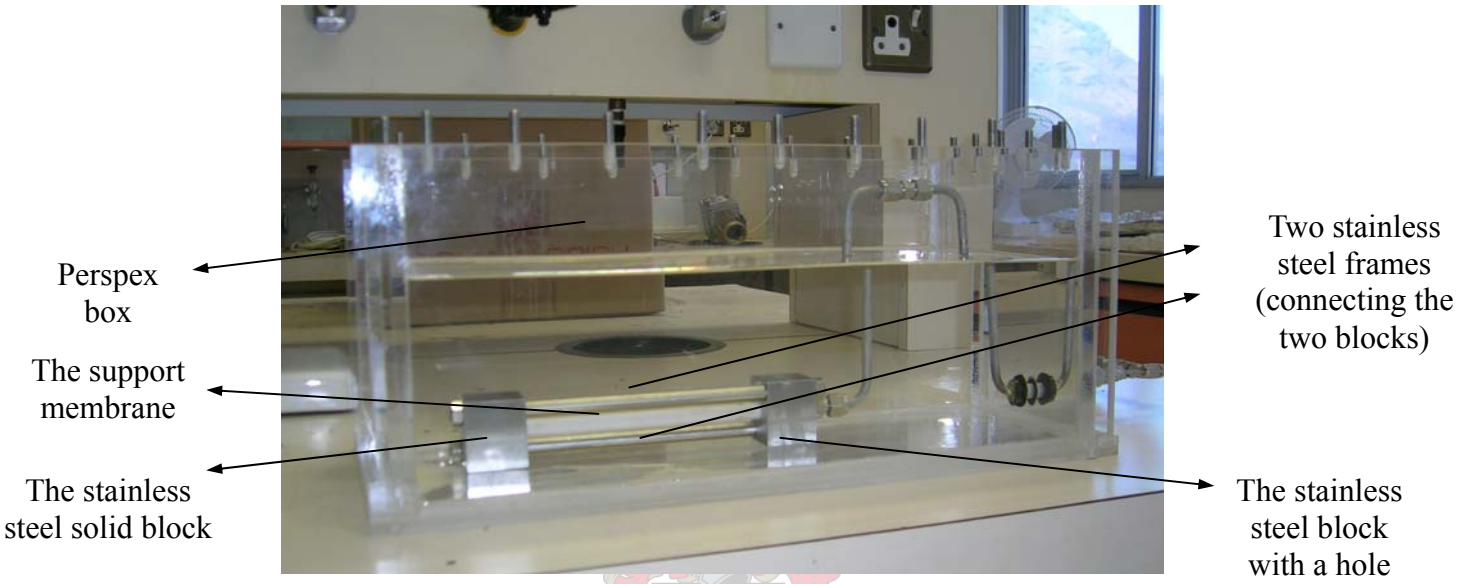


**Figure 3.5: The bubble point screening test setup**

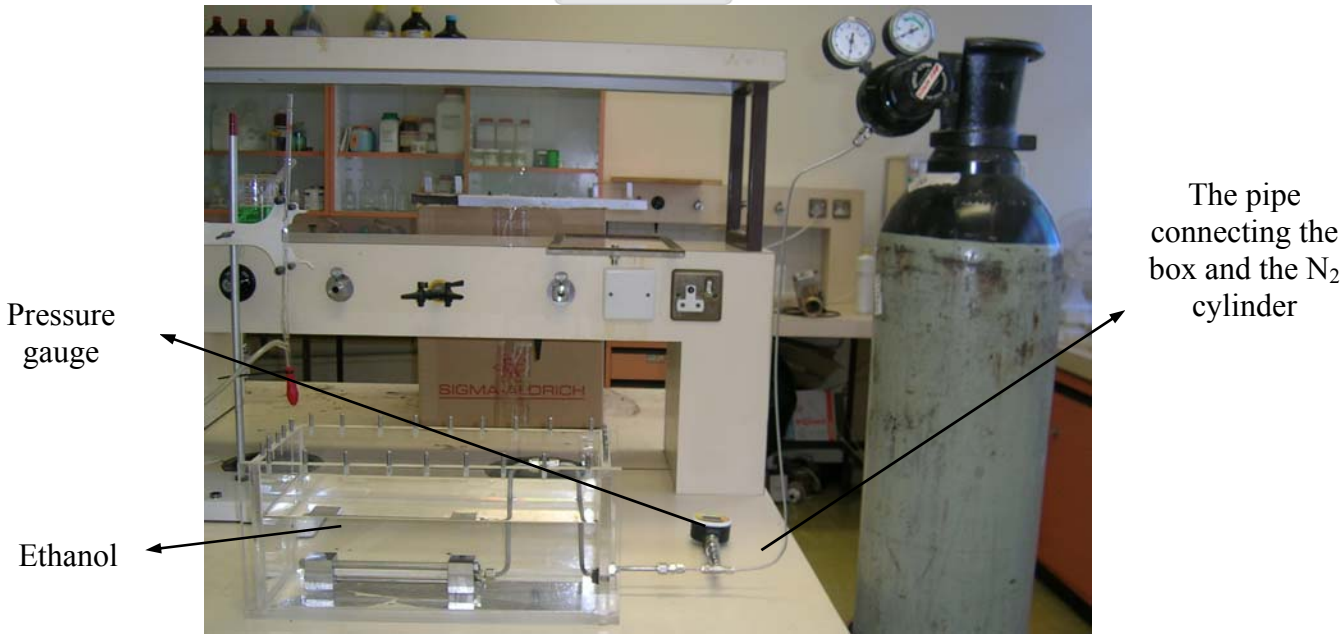


**Figure 3.6: The whole apparatus of bubble point screening test**

The main box, made of Perspex, was completely sealed, except for the top. Two stainless steel blocks, connected by stainless steel frames, were used to grip a support membrane between them. One block was solid, while the other had a hole in the middle. The latter block was connected using a pipe through the box, which linked the box and the nitrogen cylinder. A pressure gauge was fitted to the pipe to measure the pressure on the tube side of the membrane when nitrogen was forced into it.

Prior to starting the bubble point test, a dry support membrane was sealed with two rubber o-rings at both ends, and then placed between the two supporting blocks. The membrane was held between the blocks by tightening the nuts (without breaking the membrane). The frame and block were then placed into the main Perspex box, which was filled with ethanol (99.99 wt %) to completely immerse the membrane. (Nitrogen hardly dissolves in 99.99 wt % pure ethanol). When nitrogen was fed into the membrane by gradually increasing the feed pressure, any nitrogen gas that emerged from the pinholes in the membrane formed visible bubbles in the ethanol. Increasing the pressure made it possible to observe from which locations in the membrane the bubbles were emerging from. A number of pictures were taken for the test in order to record the quantity of the bubbles, and thus the locations of the defects. The results were recorded to compare the quality of the substrate, which could provide additional information helping to analyse the influence of the substrate on the electroless plating.

### 3.1.3 PERMEABILITY TEST OF SUPPORT MEMBRANES

A permeability test, using nitrogen at room temperature, was performed on the support membranes to obtain further information of the nitrogen permeability of substrates.

After the bubble point test, the membrane was rinsed in distilled water for 30 minutes to remove all the contaminants. A mechanical stirrer (Heidolph) (See Figure 3.7) operating at a stirring speed of 1300 rpm was used. The membrane was then dried in an oven overnight (14 to 16 hours) at 120 °C. The mass of the membrane was subsequently recorded after the membrane had cooled down to 60 °C.

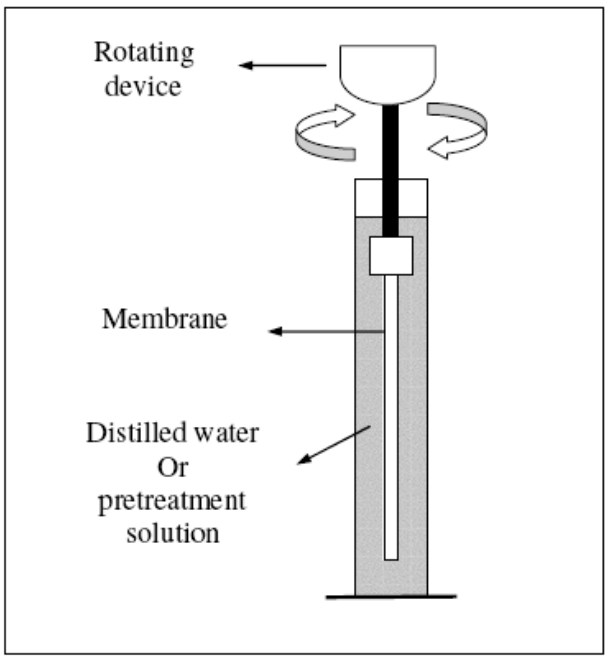


**Figure 3.7: Stirrer (Heidolph) for membrane pre-cleaning before pretreatment, surface pretreatment and membrane post-cleaning after plating**

Afterwards, the permeability test was performed at room temperature (13~22 °C, depending on ambient temperature) to investigate the nitrogen permeability of the support membrane. The reactor used for the permeability test is illustrated in Figure 3.8. The fluctuating ambient temperature does not affect the outcome of the pretreatment. The temperature in the laboratory was measured while the permeability test was being conducted.

The reactor was made of stainless steel, and was manufactured in the workshop of the Department of Process Engineering in the University of Stellenbosch. Two graphite o-rings were used to obtain an effective seal with the membrane. The o-rings had dimensions of 10.4 by 17.9 mm, a thickness of 5 mm and a density of 1.6 g/cm³. They were purchased from Coltec Industries (Le Carbone Loraine) Lyon, France. Two nuts were bolted into the reactor ends to seal the membrane by squeezing two fittings into the graphite o-rings. Each of the two fittings had an angle at the bottom side which wedged the graphite o-ring in place (see Figures 3.9 and 3.10). When the two nuts were tightened, the two fittings forced the graphite rings to move forward and sideways, thus pushing the graphite rings against the enamelled membrane endings, and achieving a proper seal. If the nuts are sufficiently and appropriately tightened, a very good seal can be obtained. Over-tightening results in either breaking or cracking of the membrane.

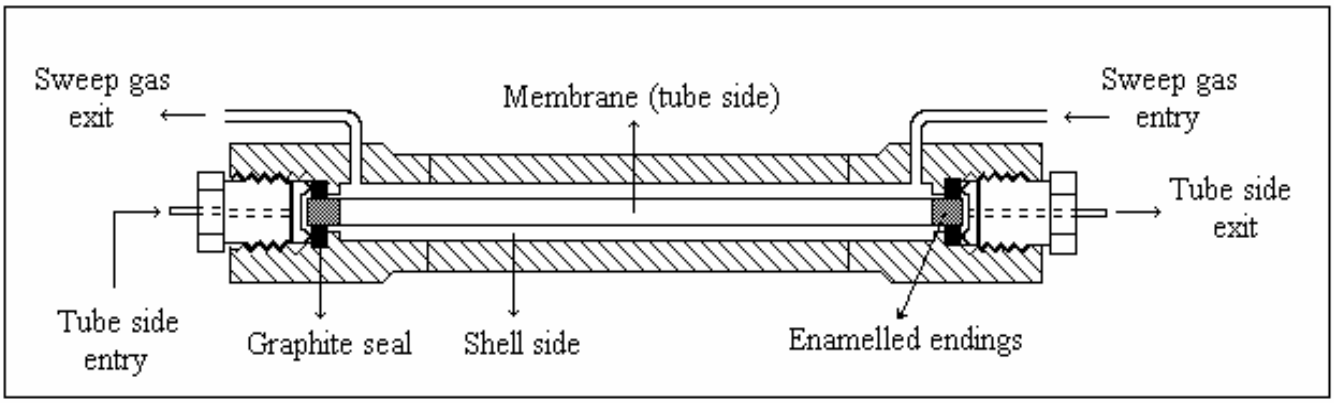


**Figure 3.8:** **Membrane reactor used to test the membrane permeability**

**Figure 3.9:** **Top view of the two modified fittings**

**Figure 3.10:** **Side view of the two modified fittings**

The membrane was placed inside the reactor, and the two graphite rings were placed evenly at the ends (see Figure 3.8). The nuts were then tightened moderately until they screwed about 4 mm into

the graphite ring at each end. This was tested several times without breaking or cracking the membrane. This whole tightening procedure was performed in the workshop. The membranes must be supported horizontally on the working bench while being tightened. The two nuts were tightened equally, so that the membrane would not be over-squeezed at one end. Occasionally, the reactor had to be re-opened and slightly shifted, to make sure that the membrane was uniformly seated.

In the second year of this study, rubber o-rings were applied to seal the support membrane inside the reactor, thus replacing the graphite rings. As the permeation test was done under room temperature, there was no concern about cracking of the rubber rings. A better sealing of the membrane was obtained when using the rubber rings due to their softness and flexibility. Moreover, rubber rings are much cheaper than graphite rings.

For nitrogen testing, the shell gas exit and tube side exit (see Figure 3.8) of the reactor were closed off. The feed nitrogen was forced through the support membrane by gradually increasing the pressure. The flow rate of the permeating gas was measured using two flow meters. One of the flow meters was a 0 to 50 ml bubble flow meter (manufactured in the Chemistry Department) for measuring high-pressure gas flow rates (see Figure 3.11), and the other was a gas flow meter (wet type laboratory gas and air metres, Alexander Wright & Co. (Westminster), Ltd) for gas flow rates at low pressure ($\leq$ 65 mbar) (see Figure 3.12). After the support membrane was tested and analysed, a record of the pore size, pore distribution, locations of defects and nitrogen permeability of the support membrane could be kept to assist with the analysis of their influence on the preparation of Pd composite membranes.

**Figure 3.11: Bubble flow meter (total volume of 50 ml) for gas flow rate at high pressure**


**Figure 3.12: Gas flow meter for gas flow rate at low pressure**

### 3.1.4 BUBBLE POINT TEST

Preparing membranes with better separation characteristics for specific industrial or laboratory applications is important for the continued development of membrane technology. In this study, it is recognised that the pore size and pore structure of the support membrane influences the quality of

the palladium composite membrane layer that is coated on the support's inside surface. In light of this, the support membranes need to be non-destructively characterised before any Pd is deposited.

An easy, fast and inexpensive method for determining the maximum pore size and the pore size distribution is offered by the bubble point technique.

The support membrane was immersed in ethanol overnight, and a bubble point test was subsequently performed. The support membrane (its pores filled with ethanol) was placed and sealed in a stainless steel reactor module, the same as used in section 3.1.3 (see Figure 3.7). Nitrogen was forced through the support membrane by increasing the feed pressure. The equation for determining capillary pressure (Iojoiu, 2004) corresponding to the pore size of the membrane was obtained from Laplace's law, assuming perfect wetting and a mono-disperse cylindrical cross section. While these assumptions are a simplification of the real case, the values obtained give a correct order of the capillary pressure applicable for the membrane layer. The pressure applied on the membrane and the flow rate of the nitrogen was recorded to calculate the pore diameter of the defects by Laplace's law. More detailed experimental mechanisms are discussed in section (4.3.3).

## 3.2 MEMBRANE PRE-CLEANING BEFORE PRETREATMENT

The support membrane was cleaned before plating, using three different methods to remove all the contaminants. The mass of the support membrane was recorded before and after the membrane cleaning for comparative purposes.

### 3.2.1 MEMBRANE CLEANING METHOD 1

The membrane was rinsed in distilled water for 30 minutes using a stirrer at a stirring speed of 1300 rpm to remove all contaminants. As illustrated in Figure 3.7, one end of the support membrane was connected to the stirrer, and the other end was immersed in distilled water. To ensure proper cleaning of both ends of the support membrane, it was removed from the stirrer after 15 min, inverted and then rinsed again. Thereafter, the membrane was dried at 120 ºC overnight (14-16 hours; above boiling point of water) in an oven to ensure that all the solution concealed in the pores of the membrane could evaporate. The temperature should not be higher than 120 ºC, to prevent any potential changes in the membrane structure at higher temperatures. The mass was recorded the next day when the membrane had cooled down to room temperature.

### 3.2.2 MEMBRANE CLEANING METHOD 2

The support membrane was first washed in an ultrasonic bath (Elma, TranssonicT460/H, Wirsam Scientific, constant frequency of 35 kHZ) for 10 min at room temperature. The membrane was then rinsed in distilled water for 30 minutes using a stirrer at a stirring speed of 1300 rpm to remove all the contaminants (See Figure 3.7). The membrane was subsequently dried at 120 ºC overnight (14~16 hours) in an oven. Both ends of the membrane must be washed. The mass was subsequently recorded when the membrane had cooled down to room temperature. The membrane cleaning was completed as outlined in Table 3.3. .

**Table 3.3: Membrane cleaning procedures, method 2**

| Setup | Liquid or solution | Time (min) | Speed/Frequency | Direction |
|---|---|---|---|---|
| Ultrasonic bath | Distilled water | 10 | 35 kHZ | - |
| Stirrer | Distilled water | 30 | 1300 rpm | 15 min for each ends |

### 3.2.3 MEMBRANE CLEANING METHOD 3

The support membrane was stirred in succession with dilute sodium hydroxide solution, dilute hydrochloric acid solution, and finally distilled water to remove organic contaminants (Hou and Hughes, 2001). Sodium hydroxide assists with removing organic contaminants and hydrochloric acid assists with the removal of inorganic contaminants. See the procedures in Table 3.4. After cleaning, the membrane was dried at 120 ºC overnight (14~16 hours) in an oven. The mass was subsequently recorded after the membrane had cooled down to room temperature.

**Table 3.4: Membrane cleaning procedures, method 3**

| Setup | Liquid or solution | Time (min) | Speed/Frequency | Direction |
|---|---|---|---|---|
| Stirrer | 0.5 mol/l NaOH | 30 | 1300 rpm | 15 min for each end |
| Stirrer | 0.5 mol/l HCl | 30 | 1300 rpm | 15 min for each end |
| Stirrer | Distilled water | 60 | 1300 rpm | 30 min for each end |

## 3.3 MEMBRANE PRETREATMENT SOLUTIONS AND PROCEDURES

Wu, Xu and Shi (2000) proposed that the mechanism of the electroless plating technique is based on the controlled autocatalytic reduction of metastable metallic salt complexes on the target surface. The reduction of a cathodic metal and the oxidation of an anodic reductant take place simultaneously. Due to the fact that the common substrates, such as microporous glass, silver

support, porous stainless steel, and ceramic membranes, are not active enough to initiate the redox reaction, pretreatment of the support membrane is required for activation with palladium nuclei. This would catalyse the electroless plating reaction. Thus, the process of palladium electroless plating involves a necessary pretreatment and electroless deposition.

### 3.3.1 PREPARATION OF PRETREATMENT SOLUTION

The traditional activation procedure comprises two steps, using a palladium salt and a tin chloride salt. In this study, the palladium (II) chloride salt was bought from Fluka, South Africa, and the tin chloride salt was purchased from Aldrich, South Africa. See the pretreatment solution composition in Table 3.5. Both this study and that done by Keuler (2000), much less $SnCl_2$ was used than Li (1996) to avoid the excess $SnCl_2$ from forming impurities on the activated Pd surface. A ratio of 1.1:1 (Sn:Pd) was used in this study.

The pretreatment solution was prepared according to the data in Table 3.5. 270 ml of fresh tin chloride solution was prepared for each membrane, while 1000 ml of palladium chloride solution was prepared for each of the three membranes. After preparing the solutions they were allowed to stand overnight (at least 15 or 16 hours). It was observed that $PdCl_2$ (g) (99.99 wt %) did not dissolve in distilled water, so a method was developed to prepare a proper palladium solution (see section 3.3.1.2).

**Table 3.5: Pretreatment solution composition**

| | Li (1996) | Keuler (2002) | This study (2005) |
|---|---|---|---|
| **Sensitising solution (per litre)** | | | |
| 37 wt % HCl (ml) | 1 ml/l | - | - |
| $SnCl_2.2H_2O$ (g) (99.99 wt %) | 5 g/l | 0.45 g/l | 0.45 g/l |
| **Activation solution (per litre)** | | | |
| 37 wt % HCl (ml) | 1 ml/l | - | 1 ml/l |
| 23 wt % $PdCl_2$ | - | 1.4 g/l | - |
| $Pd(NH_3)_4CI_2$ | $5.0 \times 10^{-4}$ M | - | - |
| $PdCl_2$ (g) (99.99 wt %) | - | - | 0.3215 g/l |
| Sn to Pd molar ratio | 44 | 1.1:1 | 1.1:1 |

### 3.3.1.1 Preparation of $SnCl_2$ solution

As 270 ml of fresh $SnCl_2$ solution was required for each membrane, 0.1215g of $SnCl_2.2H_2O$ (g) was dissolved in less than 200 ml distilled $H_2O$. More distilled $H_2O$ was then added until the volume of the solution was 270 ml. $SnCl_2.2H_2O$ (g) dissolves easily in distilled water. Fresh tin solution was prepared for every membrane due to its unstable nature. After the solution was prepared, it was stored in a fridge to prevent decomposition.

### 3.3.1.2 Preparation of 1000 ml of $PdCl_2$ solution

0.6430 ml of HCl (37 wt %) was first added to 100 ml distilled water in a 1 litre flask. 0.3215 g of $PdCl_2$ salt (99.99 wt %) was then added to the acid solution. The flask was shaken well for 2 minutes. Thereafter, an additional 500 ml of distilled water was added to the solution. The solution was placed in the ultrasonic bath for 10 min in order to accelerate the dissolution process.

The solution was allowed to stand overnight, after which it was seen to have turned bright brown with some very small particles at the bottom of the flask, which did not dissolve. As palladium salt is very expensive, any such waste is unacceptable. Thus, 0.20 ml of HCl (37 wt %) was added, and the solution was then put into the ultrasonic bath for 10 min, and left standing overnight. However, complete dissolution was still not achieved. As a result, 0.0020 ml of HCl (37 wt %) was added regularly, as outlined in Table 3.6. After each addition, the solution was placed in the ultrasonic bath for 10 min, and left for 25 min. Complete dissolution was achieved when the total amount of HCl (37 wt %) was 1.00 ml. Thereafter, more distilled water was added to the $PdCl_2$ solution until the total volume was 1000 ml (The final concentration of HCl in 1000 ml of $PdCl_2$ solution is 1 ml/l). 1000 ml of $PdCl_2$ solution was prepared at one time and used for every three membranes. It is important that the palladium chloride solution be stored at room temperature (13~25ºC), as high temperatures would cause decomposition of the solution.

**Table 3.6: Addition procedures of the HCl (37 wt %)**

| Total Amount of HCl (37 wt %) (ml) | Dissolve Time (min) | Total Amount of HCl (37 wt %) (ml) | Dissolve Time (min) |
|---|---|---|---|
| 0.6430 | Overnight | 0.8750 | 25 |
| 0.8430 | Overnight | 0.8770 | 25 |
| 0.8450 | 25 | 0.8790 | 25 |
| 0.8470 | 25 | 0.8810 | 25 |
| 0.8490 | 25 | 0.8830 | 25 |
| 0.8510 | 25 | 0.8850 | 25 |
| 0.8530 | 25 | 0.8870 | 25 |
| 0.8550 | 25 | 0.8890 | 25 |
| 0.8570 | 25 | 0.8910 | 25 |
| 0.8590 | 25 | 0.8930 | 25 |
| 0.8610 | 25 | 0.8950 | 25 |
| 0.8630 | 25 | 0.8970 | 25 |
| 0.8650 | 25 | 0.8990 | 25 |
| 0.8670 | 25 | 0.9100 | 25 |
| 0.8690 | 25 | 0.9500 | 25 |
| 0.8710 | 25 | 1.000 | 25 |
| 0.8730 | 25 | **Final concentration of HCl** | 1 ml/l |

### 3.3.2 MEMBRANE SURFACE PRETREATMENT (SURFACE ACTIVATION)

The pretreatment methods in this study were carried out according to the following three methods. The activation procedures were repeated to produce enough palladium nuclei on the support membrane surface prior to the subsequent palladium electroless plating.

#### 3.3.2.1 Membrane surface pretreatment method 1

Membrane surface pretreatment method 1 was adopted from Keuler (2000). The outside surface of the support membrane tube was wrapped with PTFE tape 3 times to ensure that only the inside of the membrane would be activated by palladium nuclei. Failure to do this would result in the outside of the support membrane surface also being activated by the pretreatment solution, which is undesirable. The equipment for pretreatment was the same as that used for membrane cleaning (see Figure 3.7). The stirring speed was set at about 1300 rpm. Approximately, 270 ml of $SnCl_2$ and 270 ml of $PdCl_2$ solution was used. The membrane was first stirred in $PdCl_2$ solution for 10 min, and

was then dipped in distilled water 10 times (1-2 second each). Subsequently, the membrane was stirred in $SnCl_2$ solution for 10 min, and was then dipped in distilled water. This sequence was repeated 3 times. More detailed procedures and sequences for pretreatment are illustrated in Figure 3.13.

After the membrane surface pretreatment, the PTFE tape was removed and the membrane was stirred in clean distilled water for 30 min to remove any residual solution in the membrane pores. This step is necessary to remove Sn-related impurities from the support membrane pores. Both ends of the membranes should be cleaned for the same reasons stated in section 3.2.1. Thus, the substrate was stirred for 15 min for each end. The membrane was then placed in an oven at 120 °C overnight and the mass of the membrane was recorded the next morning after cooling down to room temperature. The pretreatment step is a crucial prerequisite of fine electroless plating, and should, therefore, be applied carefully using the above procedures.

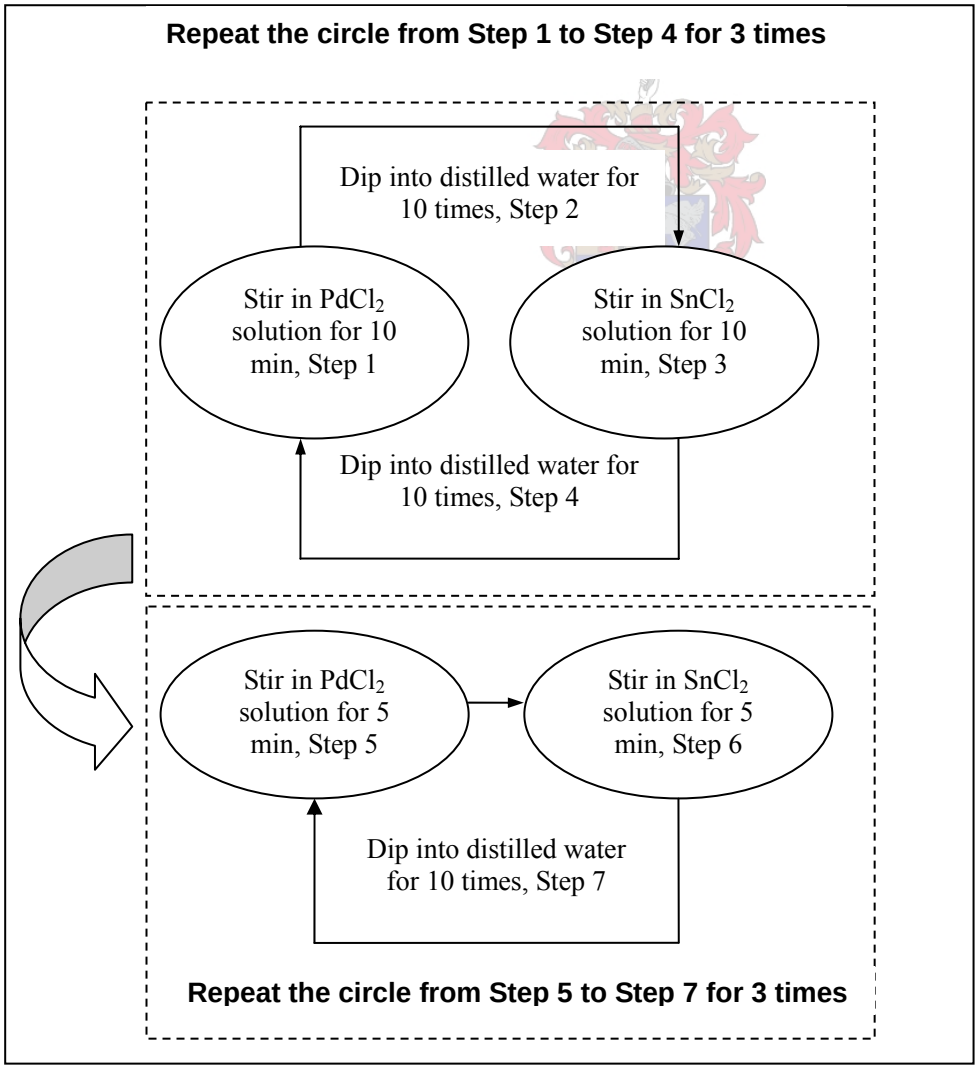


**Figure 3.13: Membrane surface pretreatment method 1**

### 3.3.2.2 Membrane surface pretreatment method 2

Method 2 was a modified version of method 1. The equipment for method 2 was the same as for method 1. Only the procedure was slightly changed. It was assumed that more palladium nuclei would be obtained if the membrane was stirred longer; this could provide a larger activated surface for palladium electroless plating, which would benefit the plating. Therefore, it was decided that for method 2, a longer time would be used for each stirring step (15 min instead of 10 min). The outside surface of the membrane tubes was wrapped with PTFE tape to ensure that only the inside of the membrane would be activated by palladium nuclei. The stirring speed was set at about 1300 rpm. Approximately, 270 ml of $SnCl_2$ and 270 ml of $PdCl_2$ solution was used. The procedure and the sequences for pretreatment are illustrated in Figure 3.14. The assumption and results are discussed in Chapter 4. After the membrane surface pretreatment, the PTFE tape was removed and the membrane was stirred in clean distilled water for 30 min. The membrane was then heated in an oven at 120 °C overnight, and the mass of the membrane was recorded the following day after cooling down to room temperature.

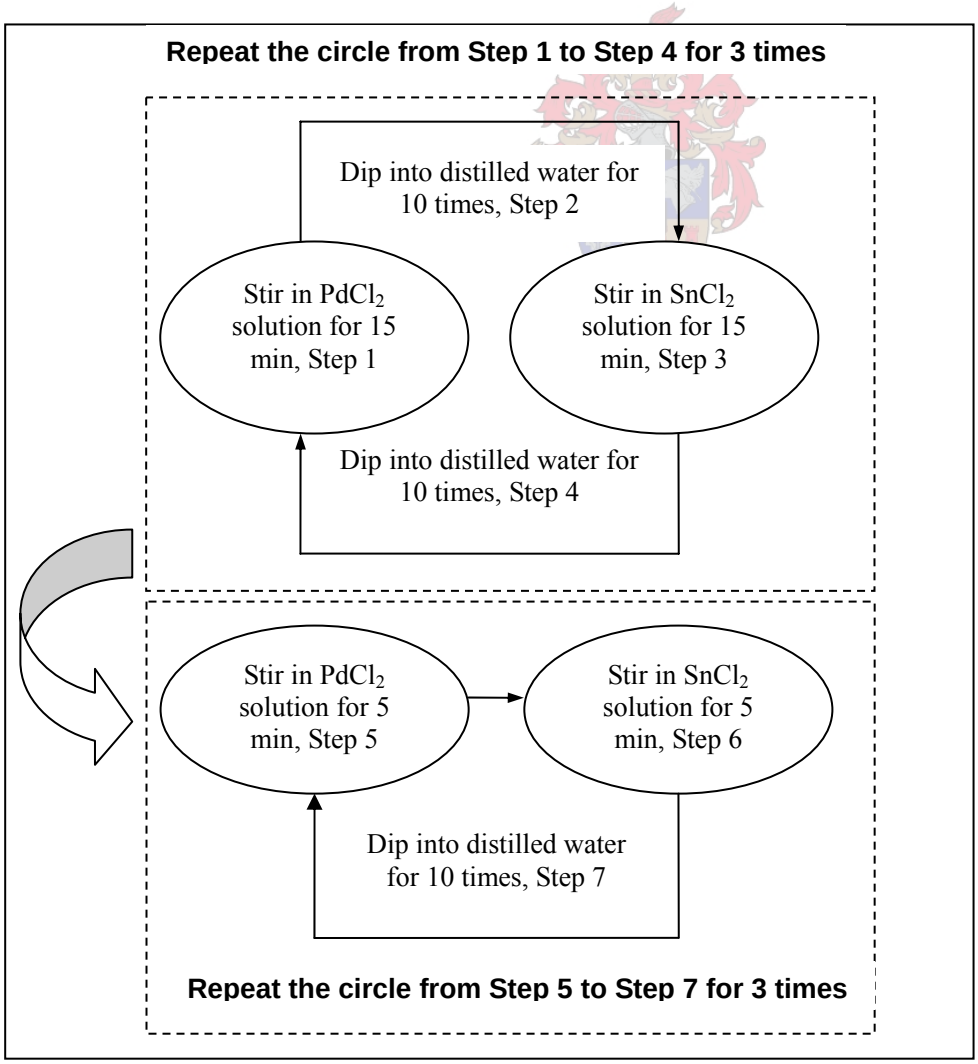


**Figure 3.14: Membrane surface pretreatment method 2**

### 3.3.2.3 Membrane surface pretreatment method 3

As the above two methods both took more than 1.5 hours to perform, they were time assuming. Therefore, a third method of pretreatment was developed in this study. The equipment for this method was the same as methods 1 and 2. Only the procedure was changed. The stirring speed was set at about 1300 rpm. Approximately, 270 ml of $SnCl_2$ and 270 ml of $PdCl_2$ solution was used. The procedures and the sequence for pretreatment are illustrated in Figure 3.15. The procedure was repeated twice from Step 1 from Step 4 for one end of the support membrane, and was then repeated twice for the other end of the membrane. In steps 1 and 3, the membrane was stirred for 15 min, because it was assumed that if the membrane was stirred slightly longer than 10 min, more Pd could be deposited on the support membrane surface, which could provide a better surface for Pd electroless plating. The results and discussion associated with this assumption are presented in Chapter 4.

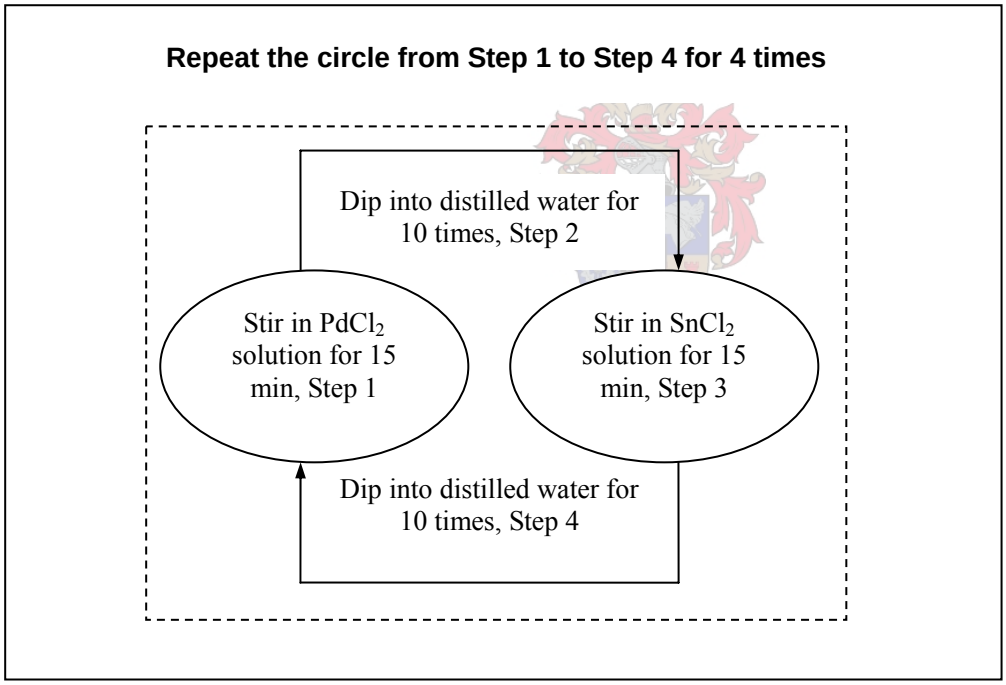


**Figure 3.15: Membrane surface pretreatment method 3**

After the membrane surface pretreatment, the PTFE tape was removed and the membrane was stirred in clean distilled water for 30 min. The membrane was then directly placed in an oven at 120 °C overnight and the mass of the membrane was recorded the following day after cooling down to room temperature.

In the above three methods, it should be ensured that both ends of the support membrane are rinsed with the pretreatment solution.

## 3.4 PALLADIUM ELECTROLESS PLATING

After the surface pretreatment, the crucial step of electroless plating of the membrane followed. The method was adopted from Keuler (2002). A 2.00 g/liter (2000 ppm) palladium solution was used for palladium electroless plating. In this study, the composition and concentration of the plating solutions were the same as Keuler's. The difference was that three different vacuums were applied on the shell side of the plating reactor to determine the optimal pressure for effective electroless plating.

### 3.4.1 PREPARATION OF THE PLATING SOLUTION

The $(NH_3)_4PdCl_2.H_2O$ (g) palladium salt, hydrazine (35 wt %), and the EDTA were all purchased from Aldrich, South Africa. The ammonia (28 wt %) was bought from Fluka, South Africa. See the plating solution composition shown in Table 3.7. The reasons for using these concentrations of Pd plating and the hydrazine were explained in detail by Keuler (2000).

**Table 3.7: Composition of the palladium plating solution for 1000 ml (2.00 g/ liter Pd in solution) (Keuler, 2002)**

| | |
|---|---|
| **$(NH_3)_4PdCl_2.H_2O$ (g)** | 4.94 |
| **28 wt % Ammonia (ml)** | 400 |
| **EDTA (g)** | 80 |
| **1.75 wt % hydrazine (ml)** | hydrazine:Pd = 0.35:1 (mol) (at the beginning of the plating)<br>increased with time |

As the palladium salt is very expensive, in order to prevent the solution from deteriorating, only 100 ml of palladium solution was prepared at any one time. 100 ml of 1.75 wt % hydrazine was prepared.

**Preparation for palladium plating solution**

About 0.494 g $(NH_3)_4PdCl_2.H_2O$ (g) was dissolved in 10 ml of distilled water, and then 40 ml of 28 wt % ammonia (ml) was added into the solution with a pipette. Then, 8 g of the EDTA was first dissolved in less than 40 ml distilled water in a beaker, and then added to the solution containing the

$(NH_3)_4PdCl_2.H_2O$ and ammonia. Additional distilled water was added until the total volume is 100 ml. Great care should be taken to prevent any wastage of the chemicals. After that, the plating solution (without the hydrazine in it) was allowed to stand for at least 12 to 16 hours prior to plating, to ensure complete dissolution of all the chemicals (Keuler, 2000).

**Preparation of 1.75 wt% hydrazine solution**

To prepare 100 ml of 1.75 wt% hydrazine solution, 5.10 ml of 35 wt % hydrazine was dissolved in 100 ml of distilled water. The solution was then allowed to stand (stabilise) for at least 12 to 16 hours prior to plating.

### 3.4.2 SAFETY ISSUES

Hydrazine is extremely toxic. $LD_{50}$ is 25 mg/kg. ($LD_{50}$ of a particular substance is a measure of how much constitutes a lethal dose. The usual terms for expressing the $LD_{50}$ are in units of mass of substance per mass of body mass). Therefore, it must be prepared in a fume cupboard with a strong extractor fan. Great caution should be taken and it is essential to wear rubber gloves, protective clothing, a respirator, as well as protective glasses. The hydrazine solution must be placed in a safe place and marked with detailed information. Ammonia has a pungent smell, so it is also suggested that the plating solution be prepared in the fume cupboard. Thus, the whole electroless plating procedure, involving palladium plating solution and hydrazine solution preparation, should also be performed in the fume cupboard with rubber gloves, protection clothing, respirator, as well as protective glasses.

### 3.4.3 PALLADIUM ELECTROLESS PLATING

The electroless plating experimental setup is shown in Figure 3.16. The water bath was heated by a heating element to a temperature of 70~73 ºC. During that time, a clean support membrane was wrapped with PTFE tape to ensure that only the inside of the membrane would be plated. The membrane was then sealed in a Teflon reactor with rubber O-rings. The bottom of the membrane was connected to a 10 mm silicon tube which was closed at its end. This helped to seal the bottom side of the membrane. On the top side of the membrane, another silicon tube of 10 cm was tightly connected to the membrane. This provided enough space so that the plating solution could cover the entire surface area of the membrane.

The Teflon reactor had a single shell-side outlet (diameter of 8 mm) for a vacuum to be drawn on the shell side. This procedure will be explained in detail in Chapter 4, where the procedures and results are discussed. An electroless plating technique with vacuum applied on the shell side of the

reactor was modified in this study (see chapter 4) to produce thin palladium films (thickness of 1.7 μm ~ 4 μm).

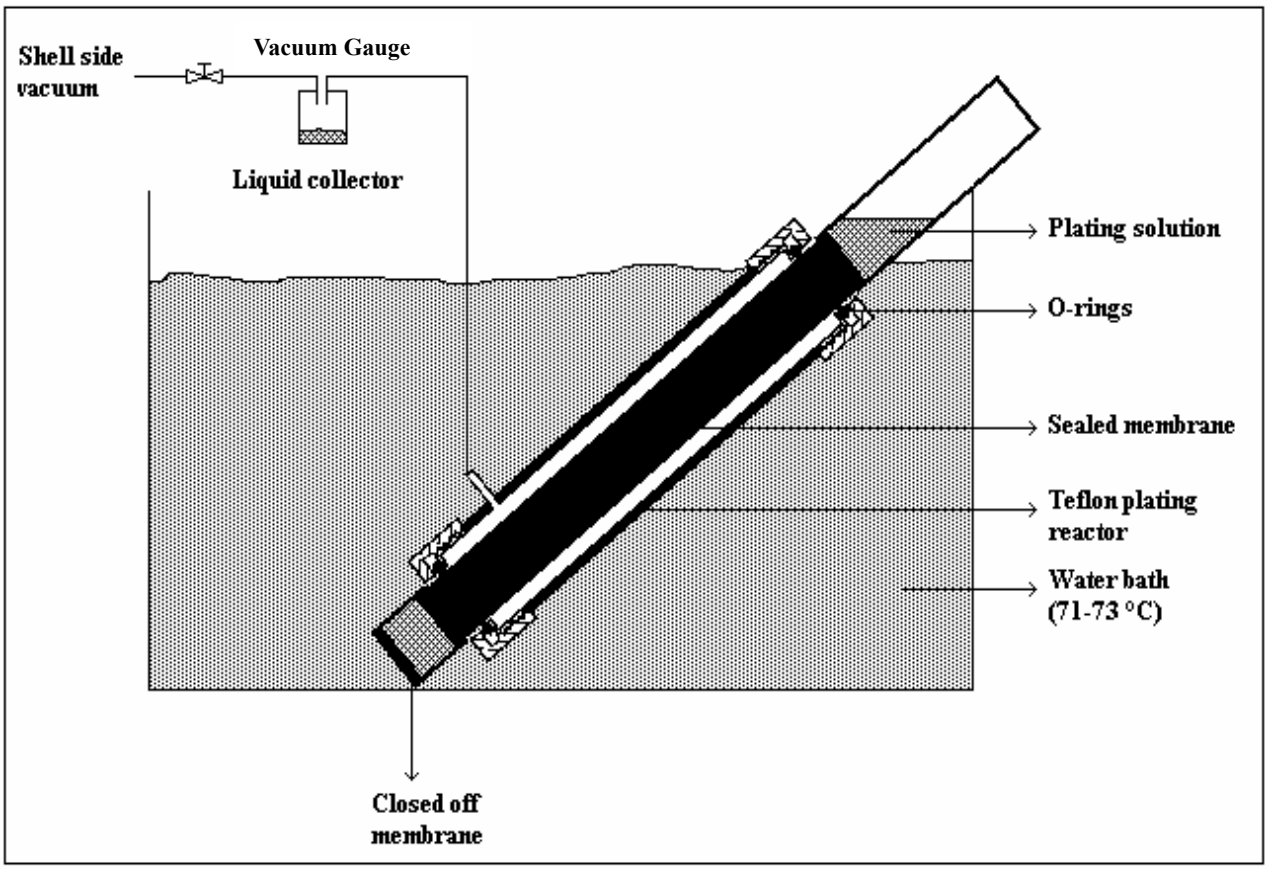


**Figure 3.16: Electroless plating equipment**

### 3.4.3.1 One micron initial palladium film preparation by electroless plating

If one micron palladium film is required, a 2.00 g/liter palladium was needed in the palladium electroless plating solution. See the calculations below.

Assume that the palladium plating solution will react completely, and that the palladium film thickness is even and smoothly distributed. Therefore, if a one micron Pd film is required, the mass of plated Pd can be calculated. Since the concentration of Pd in Pd plating solution is known, the volume of Pd plating solution that is required can be determined by calculation. However, according to the above assumptions, this is only a theoretical volume of Pd plating solution that is required for a one micron Pd layer to be plated. In practise, more Pd plating solution should be used than the theoretically calculated amount. Take membrane (1/17) as an example.

$$m_{Pd} = \pi \times D_i \times (L - L_e) \times l \times d_{Pd} \quad (3.3)$$

$l$ = 1 μm, $d_{Pd}$ = 12023 kg/m$^3$

$$\because m_{Pd} = \pi \times D_i \times (L - L_e) \times l \times d_{Pd}$$

$$= 3.14 \times 7mm \times 128mm \times 1 \times 10^{-3} mm \times 12023 \times 10^{-3} mg / mm^3 = 33.825mg$$

$\because C_{Pd}$ = 2.00 g/litre = 2.00 mg/ml

$$\therefore V_s = m_{Pd} / C_{Pd} \quad (3.4)$$

$$V_s = 33.825mg / (2.00mg / ml) = 16.913 \text{ ml}$$

| | | | |
|---|---|---|---|
| $C_{Pd}$ | ------- | Pure palladium concentration in plating solution | [g/l] |
| $d_{Pd}$ | ------- | Density of palladium (12023 kg/m$^3$) | [kg/m$^3$] |
| $D_i$ | ------- | Inner diameter of support membrane tube | [m] |
| $l$ | ------- | Thickness of palladium layer | [m] |
| L | ------- | Length of support membrane | [m] |
| $L_e$ | ------- | Total length of both enamelled endings | [m] |
| $m_{Pd}$ | ------- | Mass of plated palladium film | [g] |
| $V_s$ | ------- | Volume of plating solution | [m$^3$] |

Thus, it was known that a volume of at least 16.913 ml of plating solution should be used to produce a one micron palladium film.

An initial one micron palladium film was deposited on the inside of the membrane tube without any vacuum applied. Theoretically, 16.913 ml of plating solution should be used. However, considering the waste of solution caused by its penetration into the pores of the support membrane, and due to some experimental error, 18 ml of plating solution was used for plating. Note that the volume of the membrane that could be plated was 4.9235 ml (See Table 3.2). Thus, three consecutive platings on the membranes were performed using the 18 ml of plating solution, but by introducing 6 ml of plating solution at each stage.

The reactor, with the membrane properly fixed and sealed in place, was placed in a water bath. In addition, a beaker with water was put into the water bath. The water in the bath was heated to 70~73 ºC. The reactor was placed in the beaker and plating only commenced when the temperature of the water in the breaker was 70~73 ºC. In the first stage, 6 ml of the plating solution was introduced into the membrane using a pipette. The hydrazine was then introduced onto the

membrane tube at the beginning of the session, and after 20 min and 40 min. Thus, it took a total of 60 min for the redox reaction (for 6 ml plating solution) to complete. Thereafter, the plating solution was drained into the waste box, taking great care due to its toxicity. This procedure was then repeated with the other two stages, using 6 ml of the plating solution in each stage (therefore, a total volume of 18 ml, 6 x 3 = 18 ml, of plating solution was used to produce a 1 μm Pd layer). The whole process took 3 hours to complete. The plating procedure is essentially a batch process repeated 3 times. The quantity of hydrazine added to the plating solution is shown in Table 3.8

The hydrazine concentration was increased after each plating session in order to compensate the thermal decomposition of hydrazine, ensuring that all the Pd plating solution completed its reaction. However, an excess amount of hydrazine can increase the electroless plating rate, resulting in a coarser microstructure of the Pd film (Keuler, 2000). Therefore, the method of hydrazine addition should, as outlined in Table 3.8, should be followed precisely.

**Table 3.8: Plating procedures for the initial palladium film with hydrazine addition**

| Plating Section | Plating solution (ml) | Reaction time for 6 ml plating solution (min) | Vol. 1.75 wt % hydrazine added for 6 ml solution (μl) |
|---|---|---|---|
| **Repeat 3 times** | 6 ml | 20 | 78 |
| | | 20 | 52 |
| | | 20 | 261 |

A few tiny bubbles appeared on the surface of the plating solution (in the 10 cm silicon tube) during the plating, which was indicative of the reaction. The reactor with plating solution was shaken every 10 minutes during the reaction, especially directly after the hydrazine was introduced into the plating solution, to prevent the accumulation of the hydrazine.

The membrane post-cleaning was performed after the palladium electroless plating. It was found that membrane cleaning is as important as the plating itself, since the impurities from electroless plating definitely decrease the permeability and the selectivity of the palladium film. Thus, the membrane should be cleaned right after plating. (See the method in Table 3.9.) The membrane was then placed in an oven to dry overnight (15 - 16 hr) at 120 °C.

**Table 3.9: Membrane cleaning after plating**

| | Solution | Volume(ml) | Stirring speed (rpm) | Time (min) | Side being cleaned |
|---|---|---|---|---|---|
| Repeated 2 times | 15 wt % ammonia solution | 270 | 1300 | 30 | One end |
| | 15 wt % ammonia solution | 270 | 1300 | 30 | The other way around |
| Repeated 2 times | Distilled $H_2O$ | 270 | 1300 | 15 | One end |
| | Distilled $H_2O$ | 270 | 1300 | 15 | The other way around |

### 3.4.3.2 Second and third palladium layers plated by electroless plating

After the initial one micron palladium film was plated, a second or third palladium layer (using 6 ml of plating solution for each layer) was be plated to achieve the total desired thickness. At this stage, a range of gauge vacuums, from 10 kPa to 25 kPa (g) were applied on the shell side of the teflon reactor. This was to force the plating solution to penetrate through the pores or defects of the membrane, so as to make a defect-free palladium membrane. Keuler (2002) applied a vacuum on the shell side of the reactor, but the vacuum was not measured accurately. In this study, the vacuum was measured by a vacuum gauge, so that its precise influence on the plating could be investigated. A range of gauge vacuum, namely 10 kPa, 15 kPa, 20 kPa, 25 kPa (g), was investigated. The aim was to identify the optimal vacuum to prepare a defect-free palladium composite membrane with good metal-ceramic adhesion.



It was necessary that after each electroless plating, the membrane should be cleaned using the procedures in Table 3.9, and then dried overnight at 120 ºC in an oven. The mass of the membrane was then recorded the next morning after cooling to room temperature. Bear in mind that the palladium membrane could be tested via a permeation test using only nitrogen at room temperature after each layer was plated and dried, due to the fact that the palladium would have embrittlement in hydrogen when $T \leq 290$ ºC. The membrane, however, was only tested via permeation tests using hydrogen and nitrogen under high temperatures (350 ºC–550 ºC) and pressures (100 kPa-200 kPa) after all the desired layers were plated, not after each layer was plated. This was to prevent cracking during the permeability test under high temperatures.

## 3.5 MEMBRANE POST-CLEANING AFTER PLATING

More detailed information, specific to the palladium membrane cleaning after plating (mentioned in

section 3.4), is presented in this section. The apparatus used for membrane post-cleaning was the same as that used for pretreatment (Figure 3.7). The method was adopted and modified from Keuler (2002).

After plating, the membrane was removed from the reactor and was placed in a cylinder containing 270 ml (15 wt %) ammonia solution. The membrane was stirred at a stirring rate of 1300 rpm for one hour. This process was repeated again with fresh (15 wt %) ammonia solution, and then the membrane was stirred in 270 ml of distilled water for 30 min. The membrane was finally stirred in fresh distilled water for another 30 min. The membrane was then placed overnight in an oven at 120 °C. See the procedures in Table 3.12. (The membrane was cleaned directly after each layer was plated.)

It was essential that, after each layer had been plated, the mass be recorded so as to facilitate the calculation of the membrane thickness.

## 3.6 HEAT TREATMENT

After electroless plating and drying, there were brown spots visible in some areas on the outside of the membrane, indicative of the presence of carbon. In this study both scanning electron microscopy (SEM) with backscatter, and energy dispersive detectors (EDS) analysis were employed after the membrane was dried at 120 ºC. The results positively proved that there was some carbon on the inside of the palladium membrane layer. Carbon can cause instability of the palladium membrane. Keuler stated that the presence of carbon impurities in Pd films creates cracks when the Pd films are tested by nitrogen or hydrogen permeation tests above a temperature of 300 ºC. Thus, a heat treatment, followed by the membrane post-cleaning and drying, is definitely necessary. This is necessary to remove the carbon impurities, such as carbon obtained during plating (from the EDTA). Furthermore, the heat treatment could also assist the palladium nuclei to agglomerate to form a denser film. Three different methods of heat treatment were applied on the palladium membranes.

### 3.6.1 HEAT TREATMENT METHOD 1

Heat treatment method 1 was modified according to the heat treatment method of Keuler (2000). The heating rate used in this method was slower (rate of 1 °C/min) than Keuler's (2000) (rate of 2 °C/min). The aim was to investigate the influence of heating rate on the heat treatment. The membrane was placed in the steel stainless reactor (see Figure 3.8) and was then annealed according to the following procedure.

- Heat the Pd composite membrane at a rate of 1 °C/min in inert nitrogen gas from room temperature to 320 °C, during which time oxidation of the Pd composite membrane effected.
- Switch from using nitrogen to pure air for Pd composite membrane oxidation, and force air (the flow rate of air should be 10 $cm^3$/min) through both the tube and the shell side of the reactor, carrying out the oxidation for 2 hours.
- Switch back to inert nitrogen gas and heat the Pd composite membrane at a rate of 1 °C/min from 320 °C to 450 °C, at which temperature the reduction of the Pd composite membrane by hydrogen was then performed.
- Continue the reduction of the Pd composite membrane at 450 °C in hydrogen for 1.5 hours.
- Cool down the Pd composite membrane in inert nitrogen gas to 350 ºC and maintain this temperature for 30 min.
- Perform permeation tests on the Pd composite membrane using nitrogen or hydrogen in single-gas-testing from 350 ºC-550 ºC.

See the procedures outlined in Table 3.10.

**Table 3.10: Heat treatment procedures, method 1**

| Direction | Gas | Time (min) | T( ºC) | Gas Flow Rate | Heating Rate |
|---|---|---|---|---|---|
| Tube side | Nitrogen | 300 | 20-320 | 20 $cm^3$/min | 1°C/min |
| Tube side and the shell side | Air | 120 | 320 | 10 $cm^3$/min | Constant |
| Tube side | Nitrogen | 130 | 320-450 | 20 $cm^3$/min | 1 °C/min |
| Tube side | Hydrogen | 90 | 450 | Constant | Constant |
| Tube side | Nitrogen | 100 | 450-350 | 20 $cm^3$/min | 1 °C/min |
| Tube side | Nitrogen | 30 | 350 | 10 $cm^3$/min | Constant |

### 3.6.2 HEAT TREATMENT METHOD 2

Method 2 is detailed in Table 3.11. Compared with method 1, only the annealing time in hydrogen in method 2 was longer (3 h) than that in method 1 (1.5 h). Glazunov (1997) stated that as the annealing time, t, increased, ($t \geq 3$ h) the methane (one of the carbon impurities) peak decreased, becoming less than $10^{-12}$ A. This corresponds to the time required to attain an activated (decarburized) state of Pd, characterized by a high permeability. Therefore, in method 2, 3 hours annealing in hydrogen was applied so as to remove more of the carbon or hydrocarbon that formed

in the Pd.

**Table 3.11: Heat treatment procedures, method 2**

| Direction | Gas | Time (min) | T( ºC) | Gas Flow Rate | Heating Rate |
|---|---|---|---|---|---|
| Tube side | Nitrogen | 300 | 20-320 | 20 cm³/min | 1°C/min |
| Tube side and the shell side | Air | 120 | 320 | 10 cm³/min | Constant |
| Tube side | Nitrogen | 130 | 320-450 | 20 cm³/min | 1 °C/min |
| Tube side | Hydrogen | 180 | 450 | Constant | Constant |
| Tube side | Nitrogen | 100 | 450-350 | 20 cm³/min | 1 °C/min |
| Tube side | Nitrogen | 30 | 350 | 10 cm³/min | Constant |

### 3.6.3 HEAT TREATMENT METHOD 3

Method 3 was modified according from Keuler (2000). See the procedures outlined in Table 3.12. Compared with Keuler (2000), air was used for the oxidation of the Pd composite membrane since it was considered to be more moderate medium for the heat treatment (Ma, 2004). Using air could help prevent the membrane from cracking, which is possible when using pure oxygen.

**Table 3.12: Heat treatment procedures, method 3**

| Direction | Gas | Time (min) | T( ºC) | Gas Flow Rate | Heating Rate |
|---|---|---|---|---|---|
| Tube side | Nitrogen | 150 | 20-320 | 20 cm³/min | 2°C/min |
| Tube side and the shell side | Air | 120 | 320 | 10 cm³/min | Constant |
| Tube side | Nitrogen | 65 | 320-450 | 20 cm³/min | 2 °C/min |
| Tube side | Hydrogen | 90 | 450 | Constant | Constant |
| Tube side | Nitrogen | 50 | 450-350 | 20 cm³/min | 2 °C/min |
| Tube side | Nitrogen | 30 | 350 | 10 cm³/min | Constant |

### 3.6.4 NEW METHOD FOR HEAT TREATMENT INVESTIGATION

A new method was developed in this study. After the electroless plating, the palladium membrane was cut into two pieces. Thus, the two pieces of the same plated membrane were used in two different heating procedures. This method offered a precise way of identifying the superior heating procedure, without considering any influence of the substrate or the plating technique. The one

piece of the Pd composite membrane was treated via method 1 (see Table 3.10). The second piece was treated via method 2, shown in Table 3.11. Results and discussions with regard to these two heating procedures are presented in section 4.8.1.

### 3.6.5 ADDITIONAL HEAT TREATMENT

An additional heat treatment with hydrogen was subsequently applied on Pd composite membrane (6/17) after the permeation tests, to determine whether it could help remove more carbon impurities, as well as to test the thermal stability of the membrane in hydrogen or air at 600 °C. The membrane was heated to 600 °C in inert nitrogen gas, and then held at this temperature for 10 h in $H_2$ for further reduction and testing.

An additional heat treatment with air was applied on membrane (3/30) for 10 h for further oxidation to see whether it could reduce more carbon impurities, as well as investigating whether a denser Pd film could be obtained.

## 3.7 MEMBRANE PERMEABILITY AND PERMSELECTIVITY TESTING

Membrane permeance tests with a single gas (nitrogen or hydrogen) were performed in the reactor shown in Figure 3.8. Similar procedures were applied as those in section 3.1.3. The differences were that two graphite rings were applied to seal the palladium membrane inside the reactor, and the permeance testing was performed at 350 ºC to 550 ºC.

Some difficulty was, however, still encountered when trying to obtain good reactor-to-membrane seal. The main reason was that the enamel on the outside membrane surface was not always of uniform thickness. For testing the membrane permeability under high temperature and high pressure, the reactor and the cylindrical furnace are shown in Figure 3.17 and Figure 3.18, respectively.

The membrane was placed inside the reactor, with graphite rings at the ends, and the nuts tightened moderately (See section 3.1.3). The reactor (with the exit side closed off) was then placed in the cylindrical furnace (Figure 3.18). The reactor was connected to a pressure controller and two mass flow meters.

Figures 3.17 and 3.18 show the equipment used for high temperature membrane testing, with hydrogen and nitrogen as feeds respectively. This was also the setup for membrane heat treatment.

A thermocouple was placed in the middle of cylindrical furnace to measure the temperature of the furnace. Another thermocouple was placed in the centre of the membrane tube to record the temperature of the membrane in the reactor.

For hydrogen and nitrogen testing (Figure 3.17), one of the two shell side tubes of the reactor was closed. The reactor was operated in the dead end mode, i.e., the exit tube side was closed and the feed gas forced through the Pd film. The temperature inside the reactor was varied between 330 °C and 550 °C. A temperature controller controlled the temperature. The flow rate of the permeating gas was measured using two bubble flow meters. A zero to 100 ml flow meter was used for hydrogen measurements, and a zero to 4 ml flow meter for nitrogen. The effect of differential pressure and different temperatures on hydrogen and nitrogen permeance was studied. The external pressure should be prevented from increasing above 500 mbar.

**Figure 3.17: Reactor for testing the membrane permeability**

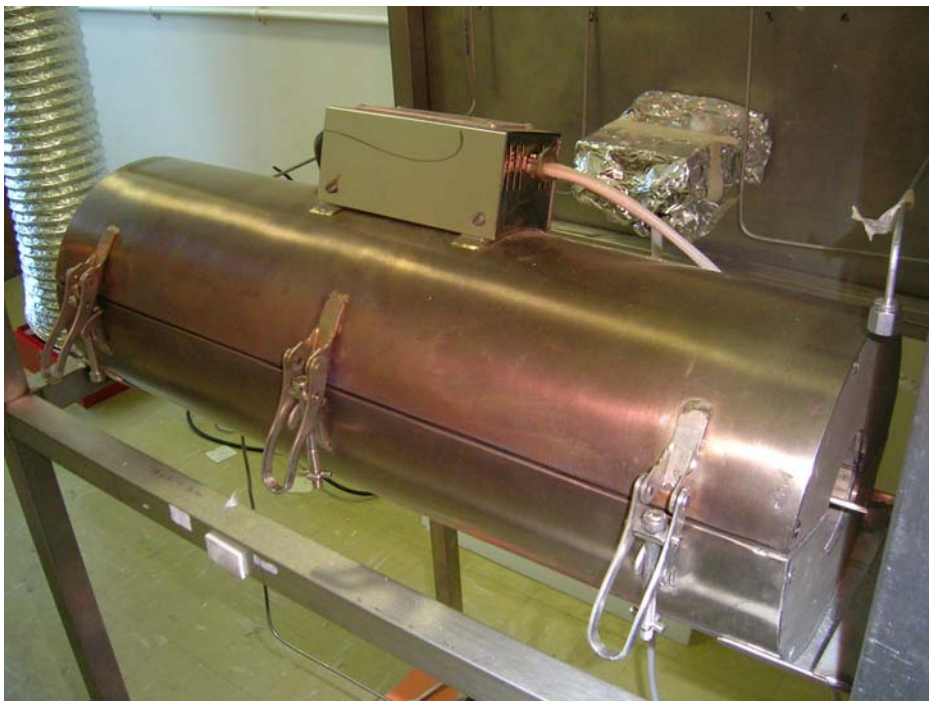

**Figure 3.18:** **Cylindrical furnace**

## 3.8 BUBBLE POINT SCREENING TEST ON PALLADIUM COMPOSITE MEMBRANES

A bubble point screening test was performed on the palladium membrane after each layer was plated (the procedure was similar to that in section 3.1.2). This was used to visualise whether there were still defects on the palladium membrane. Additionally, it was discovered that this was very helpful to observe the location of the defects. When the permeation test with nitrogen was applied on the palladium membrane (see section 3.7), it was difficult to discern whether the nitrogen is leaking from the seal of the reactor, or whether it escaping from defects present in the palladium membrane. This bubble point screening test was thus performed to determine not only whether there were still any defects on the palladium membrane, but also the locations of these defects. It thus facilitated analysis of the quality of the palladium membrane.

## 3.9 PALLADIUM FILM THICKNESS

Two methods were used to determine the amount of Pd deposited on the membrane supports. The membrane was weighed after pretreatment and dried overnight at 120 °C to get the initial mass. The membrane was weighed again after the membrane permeability testing was completed to get the final mass. The difference between the initial mass and final mass was taken as the amount of Pd deposited. From calculation, the theoretical thickness could be obtained. Another method was

to use the SEM micrographs information to acquire the real thickness.

## 3.10 ANALYTICAL TECHNIQUES

After membrane permeability tests, the surface morphology and the structural composition of the palladium membrane was examined using scanning electron microscopy (SEM, to investigate the surface morphology), energy dispersive detectors (EDS, to investigate the composition), X-ray diffraction (XRD, to investigate the composition and crystal), atomic force microscopy (AFM, to investigate the roughness and crystal sizes) and BET (Brunauer, Emmett, and Teller, to measure the porosity and surface area). The SEM, EDS and XRD analysis were done in the Department of Geology at University of Stellenbosch; AFM analysis was performed in the Department of Polymer Science, and BET analysis was performed in Department of Process Engineering. During the sample preparations and the analysis, rubber gloves were used to prevent deposition of any impurities or fingerprints onto the samples (see more detail in Chapter 6).

## 3.11 SUMMARY

This chapter covered all the experimental work performed in this study. The experimental setup and the operating procedures for the investigation of the support membranes, the preparation of the palladium membranes, permeability testing and analytical characterisations on the membranes were explained.

# CHAPTER 4: MODIFIED ELECTROLESS PALLADIUM PLATING

This chapter discusses the steps for modifying the electroless plating process on the inside surface of α-alumina ceramic membranes. Twelve palladium membranes were prepared in this study. Results and discussions are presented concerning the influence of the support membrane, the method of pre-cleaning, the modified electroless plating with vacuum, the method of membrane post-cleaning and the heat treatment procedures. Table 4.1 summarises the information for the twelve Pd membranes prepared in this study.

**Table 4.1: Pd Membranes prepared is this study**

| Identification of membrane | Surface Area for Plating $A_p$ ($cm^2$) | Volume of support membrane $V_m$ ($cm^3$) | Pd layers | Weight gain (mg) | Calculated thickness of Pd (μm) |
|---|---|---|---|---|---|
| **Membranes Set 1 (purchased in 2004)** | | | | | |
| **1/30** | 26.376 | 4.6158 | 3 | 5.4+31+30.6+40.2=107.2 | 3.37 |
| **2/30** | 26.376 | 4.6158 | 3 | 4.9+13+20.9+41.8=80.6 | 2.54 |
| **3/30** | 26.376 | 4.6158 | 3 | 5.4+31+30.6+40.2=107.2 | 3.37 |
| **4/30** | 26.376 | 4.6158 | 2 | 4.2+30+20.5=54.7 | 1.72 |
| **5/30** | 28.1344 | 4.9235 | 2 | 1.1+28+35=64.1 | 1.89 |
| **6/30** | 26.5958 | 4.6543 | 2 | 1+29+32=62 | 1.94 |
| **10/30** | 26.376 | 4.6158 | 2 | 1+41+40=82 | 2.59 |
| **12/30** | 26.376 | 4.6158 | 2 | 1+32+36=69 | 2.18 |
| **Membranes Set 2 (purchased in 2005)** | | | | | |
| **1/17** | 28.1344 | 4.9235 | 3 | 3.8+31+34+30=98.8 | 2.92 |
| **2/17** | 28.1344 | 4.9235 | 3 | 1.1+31.8+23+30=85.9 | 2.54 |
| **4/17** | 28.1344 | 4.9235 | 2 | 1.5+31+29=60.5 | 1.79 |
| **6/17** | 28.1344 | 4.9235 | 4 | 6.9+32+31+34+30=133.9 | 3.96 |

## 4.1 THEORY OF PALLADIUM ELECTROLESS PLATING

Rhoda (1959) developed an autocatalytic reaction process for the deposition of palladium by means of electroless plating. The tendency for a homogeneous reduction of palladium ions and a high degree of solution instability was overcome by using the disodium salt of EDTA as a stabiliser. The plating solution employed by Rhoda consisted of a palladium-amine complex, a reducer and a

stabilising agent as basic ingredients. Palladium deposition occurs according to the following two simultaneous reactions (Mouton, 2003):

- Anodic reaction:

  $N_2H_4 + 4OH^- \rightarrow N_2 + 4H_20 + 4e^-$ (4.1)

- Cathodic reaction:

  $2Pd^{2+} + 4e^- \rightarrow 2Pd^0$ (4.2)

- Autocatalytic reaction:

  $2Pd^{2+} + N_2H_4 + 4OH^- \rightarrow 2Pd^0 + N_2 + 4H_2O$ (4.3)

## 4.2 PARAMETERS FOCUSED ON IN THIS STUDY

**Major reasons causing failures during electroless plating**

- Impurities might become trapped at the palladium-substrate interface during pre-treatment and plating, which later results in pore formation or cracking.
- Differences in the thermal expansion of palladium and the ceramic support membrane can cause cracking under high temperatures.
- Residual porosity in the palladium film can transform into pores.



To reduce the risk of failures, and optimise the electroless plating technique, the parameters below were investigated in this study:

- Pore size, defects and permeability study of the substrates (Refer to section 3.1 in Chapter 3).
- Method of membrane pre-cleaning before pre-treatment (Refer to section 3.3 in Chapter 3).
- Method of membrane surface pre-treatment (Refer to section 3.2 in Chapter 3).
- Vacuum applied during the palladium electroless plating for the preparation of the 2nd or 3rd palladium layer (Refer to section 3.4 in Chapter 3).
- Method of membrane post-cleaning after plating (Refer to section 3.5 in Chapter 3).
- Method of membrane heat treatment (Refer to section 3.6 in Chapter 3).

Table 4.2 shows the factorial design of the experiments in 2005. Only one parameter was changed for each membrane (See Page 67).

**Table 4.2: Factorial design of experiments (study performed in 2005)**

| Identification of Membrane | Pre-Cleaning | Pretreatment ("10" refers to dip for 10 times) | Vacuum of plating | Post-cleaning | Heat treatment |
|---|---|---|---|---|---|
| **1/17** | (0.5mol/l) NaOH, 30min. (0.5mol/l) HCl, 30min, $H_2O$, 60min | **4** $PdCl_2$ 15min; $H_2O$ 10; $SnCl_2$ 15min; $H_2O$ 10 | Vacuum=20 kPa T=70-73ºC | $NH_3H_2O$, 60min, $H_2O$, 30 min | - |
| **2/17** | Ultrasonic 10min, $H_2O$, 60min | **3** $PdCl_2$ 15min; $H_2O$ 10; $SnCl_2$ 15min; $H_2O$ 10<br>**3** $PdCl_2$ 5min; $H_2O$ -- ; $SnCl_2$ 5min; $H_2O$ 10 | Vacuum=20 kPa T=70-73ºC | $NH_3H_2O$, 60min, $H_2O$, 30 min | - |
| **4/17** | (0.5mol/l) NaOH, 30min. (0.5mol/l) HCl, 30min, $H_2O$, 60min | **3** $PdCl_2$ 15min; $H_2O$ 10; $SnCl_2$ 15min; $H_2O$ 10<br>**3** $PdCl_2$ 5min; $H_2O$ -- ; $SnCl_2$ 5min; $H_2O$ 10 | Vacuum=20 kPa T=70-73ºC | $NH_3H_2O$, 60min, $H_2O$, 30 min | - |
| **6/17** | Ultrasonic 10min, $H_2O$, 60min | **4** $PdCl_2$ 15min; $H_2O$ 10; $SnCl_2$ 15min; $H_2O$ 10 | Vacuum=20 kPa T=70-73ºC | $NH_3H_2O$, 60min, $H_2O$, 30 min | **(method 1)** |
| **5/30** | (0.5mol/l) NaOH, 30min. (0.5mol/l) HCl, 30min, $H_2O$, 60min | **4** $PdCl_2$ 15min; $H_2O$ 10; $SnCl_2$ 15min; $H_2O$ 10 | Vacuum=15 kPa T=70-73ºC | $NH_3H_2O$, 60min, $H_2O$, 30 min | - |
| **6/30** | Ultrasonic 10min, $H_2O$, 60min | **3** $PdCl_2$ 15min; $H_2O$ 10; $SnCl_2$ 15min; $H_2O$ 10<br>**3** $PdCl_2$ 5min; $H_2O$ -- ; $SnCl_2$ 5min; $H_2O$ 10 | Vacuum=15 kPa T=70-73ºC | $NH_3H_2O$, 60min, $H_2O$, 30 min | **(method 1 & 2)** |
| **10/30** | (0.5mol/l) NaOH, 30min. (0.5mol/l) HCl, 30min, $H_2O$, 60min | **3** $PdCl_2$ 15min; $H_2O$ 10; $SnCl_2$ 15min; $H_2O$ 10<br>**3** $PdCl_2$ 5min; $H_2O$ -- ; $SnCl_2$ 5min; $H_2O$ 10 | Vacuum=15 kPa T=70-73ºC | $NH_3H_2O$, 60min, $H_2O$, 30 min | - |
| **12/30** | Ultrasonic 10min, $H_2O$, 60min | **4** $PdCl_2$ 15min; $H_2O$ 10; $SnCl_2$ 15min; $H_2O$ 10 | Vacuum=15 kPa T=70-73ºC | $NH_3H_2O$, 60min, $H_2O$, 30 min | - |

Table 4.3 shows the design for the experiments in 2004.

**Table 4.3: Design of experiments (study performed in 2004)**

| Identification of Membrane | Pre-Cleaning | Pretreatment ("10" refers to dip for 10 times) | Vacuum of plating | Post-cleaning | Heat treatment |
|---|---|---|---|---|---|
| **1/30** | $H_2O$, 60min | **3** 15min $PdCl_2$ / 10 $H_2O$ / 15min $SnCl_2$ / 10 $H_2O$<br>**3** 5min $PdCl_2$ / -- $H_2O$ / 5min $SnCl_2$ / 10 $H_2O$ | Vacuum=0 (for preparing the 2nd layer)<br>Vacuum=25 (for preparing 3rd layer) | $NH_3H_2O$, 60min, $H_2O$, 30 min | **(method 3)** |
| **2/30** | $H_2O$, 60min | **3** 15min $PdCl_2$ / 10 $H_2O$ / 15min $SnCl_2$ / 10 $H_2O$<br>**3** 5min $PdCl_2$ / -- $H_2O$ / 5min $SnCl_2$ / 10 $H_2O$ | Vacuum=20 kPa<br>T=70-73ºC | $NH_3H_2O$, 60min, $H_2O$, 30 min | |
| **3/30** | Ultrasonic 10min, $H_2O$, 60min | **3** 10min $PdCl_2$ / 10 $H_2O$ / 10min $SnCl_2$ / 10 $H_2O$<br>**3** 5min $PdCl_2$ / -- $H_2O$ / 5min $SnCl_2$ / 10 $H_2O$ | Vacuum=20 kPa<br>T=70-73ºC | $NH_3H_2O$, 60min, $H_2O$, 30 min | **(method 3)** |
| **4/30** | Ultrasonic 10min, $H_2O$, 60min | **3** 10min $PdCl_2$ / 10 $H_2O$ / 10min $SnCl_2$ / 10 $H_2O$<br>**3** 5min $PdCl_2$ / -- $H_2O$ / 5min $SnCl_2$ / 10 $H_2O$ | Vacuum=10 kPa<br>T=70-73ºC | - | - |

**Comments:**

- All water used was distilled water.
- Stirring speed was 1300 rpm.
- Heat treatment method 1, 2 and 3 refers to section 3.7 in Chapter 3.

## 4.3 INFLUENCE OF THE SUPPORT MEMBRANES

Substrate materials for the palladium composite membrane are selected according to their pore structure and size, porosity, mechanical and thermal stability and the surface smoothness of the substrate. Of these parameters, the pore size and smoothness of the surface of the substrate are the two key factors determining the quality of the composite membrane produced. The surface pore size should be neither too large to support a thin film, nor too small to allow the free flow of gas. Similarly, the surface should be neither too coarse to form a thin film successfully, nor too smooth to prevent adherence of the film to the substrate.

It was discovered (Ma et al., 2001) that the pore size and permeability of the substrate influence the palladium membrane. The pores size can neither be too small (to allow the gas to pass through the pores), nor too large (otherwise the surface for plating is too uneven). In addition, it was stated that the thickness of the coated palladium film strongly depends on the pore size and pore size distribution of the support. Ceramics have the advantage of a small pore size and a narrow pore size distribution. Therefore, thinner palladium films (1-2.0 μm or less) are generally formed on porous ceramic. However, the brittle nature of ceramic materials may require special configurations and supporting systems for membrane separation applications. Nonetheless, ceramics are still widely used because of their proper pore sizes, and superior thermal and mechanical properties. Asymmetric α-alumina ceramic membranes were, therefore, utilised in this study to prepare the Pd composite membranes.

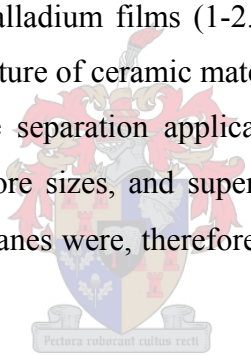


Thus, it was important to study the influence of the support membranes on the Pd electroless plating. As the support membranes should be neither cut nor destroyed during the investigations, three non-destructive methods were developed in this study to investigate the influence of the support membranes on the Pd composite membranes (see more detailed information about experimental procedures in section 3.1 of Chapter 3).

### 4.3.1 CHARACTERISATION OF THE SUBSTRATES

The support membranes, i.e. the substrates utilised in this study, consisted of three α-alumina layers, (all of them were of a macroporous nature, $D_p$ > 50 nm), and were purchased from Pall Exekia Corporation, France. The cross-section view is illustrated in Figure 3.1 (see more details in section 3.1.1).

Two similar sets of support membranes were used in this study. Set 1 was purchased in 2004 (namely membranes 1/30, 2/30, 3/30, 4/30, 5/30, 6/30, 10/30, 12/30), and Set 2 was purchased in

2005 (namely 1/17, 2/17, 4/17, 5/17, 6/17). The membranes were supposed to have an average pore size of 200 nm. However, from tests done on the support membranes it was found that the pore size of these two membrane sets did not match the manufacturer's claimed pore size of 200 nm (see further discussions regarding this in the following sections).

Figure 4.1 and Figure 4.2 are the top views of the two sets of substrates, which illustrate that both substrates surfaces had smooth structures with a great number of pores. It was observed that the support membranes of Set 2 (Figure 4.2), had a denser and smoother surface than those of Set 1 (Figure 4.1). It was thus deduced that better plating would be obtained on the membranes of Set 2. The bright spots in Figure 4.1 and Figure 4.2 were nothing more than dust particles incorporated during the preparation of the samples, which was confirmed by the EDS analysis. Therefore, membrane pre-cleaning was required to remove the dust, which would otherwise cause defects during the electroless plating.

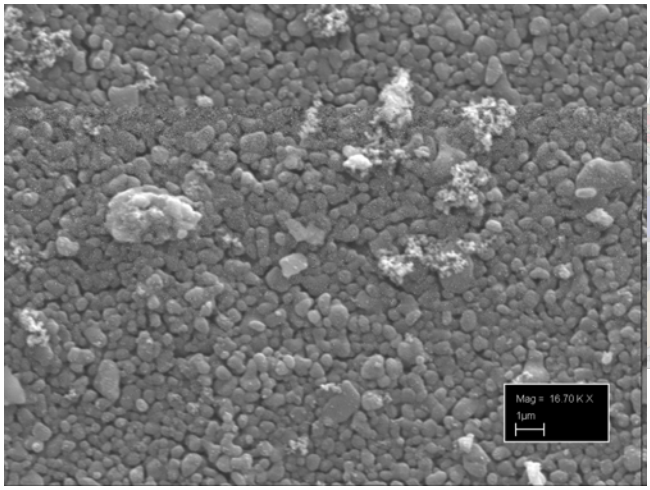


**Figure 4.1: The top view (16.70 KX) of support membrane (5/30) from Set 1**

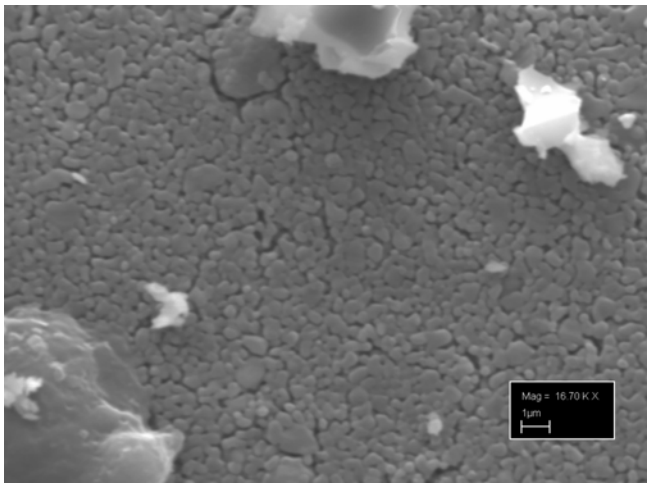


**Figure 4.2: The top view (16.70 KX) of support membrane (5/17) from Set 2**

("16.70 KX" here indicates that the SEM images were taken with a magnification of 16,700 times of the original size of the samples.)

### 4.3.2 DISCUSSION CONCERNING BUBBLE POINT SCREENING TEST

The bubble point screening test provides a good means of determining the location and quantity of defects on the support membrane surface (see experimental procedures in section 3.1.2, Chapter 3). In this study, all thirteen substrates were tested. (See Table 4.4 and Figure 4.3 for the results).

**Table 4.4: Results of bubble point screening test on the support membranes**

| Identification of Membrane | Pressure (mbar) | The first bubbles | Locations the bubbles came from |
|---|---|---|---|
| **Membrane Set 1 (purchased in 2004)** | | | |
| **1/30** | 20 | The first bubble appeared | On one of the interfaces |
| **2/30** | 50 | The first bubble appeared | In the middle of the substrate |
| **3/30** | 20 | The first bubble appeared | In the middle of the substrate |
| **4/30** | 50 | The first bubble appeared | On one of the interfaces |
| **5/30** | 34 | The first bubble appeared | On one of the interfaces |
| **6/30** | 45 | The first two bubble appeared | Close to the interface |
| **10/30** | 24 | The first bubble appeared | In the middle of the substrate |
| **12/30** | 50 | The first two bubble appeared | On one of the interfaces |
| **Membrane Set 2 (purchased in 2004)** | | | |
| **1/17** | 50 | The first two bubbles appeared | At both enamelled endings |
| **2/17** | 50 | The first two bubbles appeared | At both enamelled endings |
| **4/17** | 70 | The first bubble appeared | At one of the enamelled endings |
| **5/17** | 100 | The first bubble appeared | At one of the enamelled endings |
| **6/17** | 400 | The first two bubbles appeared | On both two interfaces |

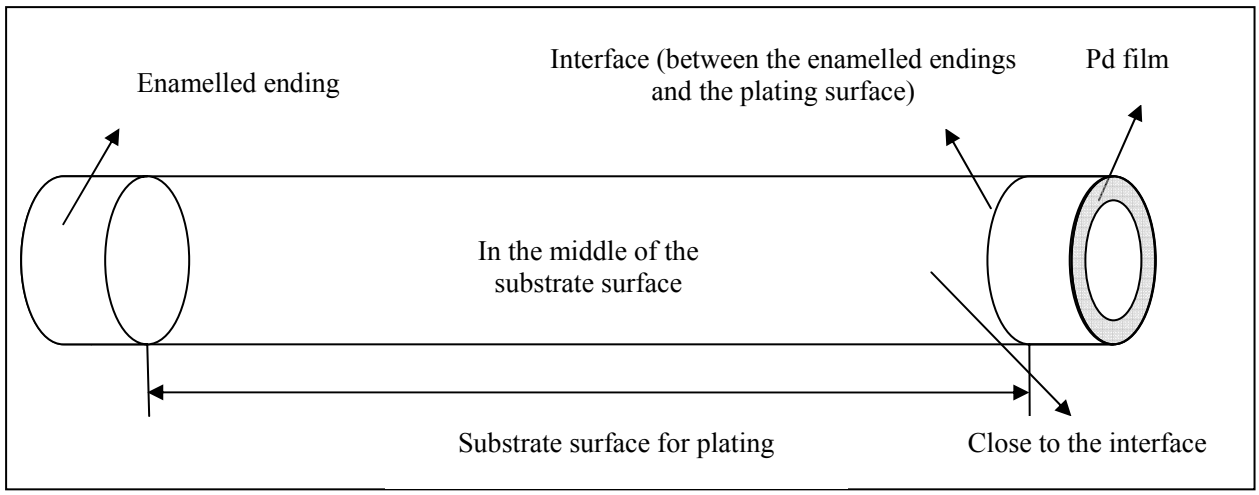


**Figure 4.3: The locations of the defects**

The membranes of Set 1 had nitrogen bubbles emerging from defects at lower pressures than those membranes of Set 2, which suggested that the membranes of Set 1 had larger pinholes/pores than membranes of Set 2. Additionally, the defects of the membranes of Set 2 were predominantly at the enamelled endings, whereas the defects of the membranes of Set 1 were either at the interfaces or in the middle of the substrates. This indicated that the membranes of Set 2 did not have as good enamelled endings as the membranes of Set 1 (enamelled endings were supposed to be non-porous). It also indicated that the membranes of Set 2 had better substrate surface (with smaller pores and smoother surface) than those of Set 1. It was assumed that the defects would be difficult to cover by Pd, and would consequently influence the quality of the Pd films. The bubble point screening tests on the Pd composite membranes subsequently proved this assumption; it was found that after the Pd films were prepared on the supports there were still defects at the interface (between the enamelled endings and the plating surface), or close to the interface.

At an increased pressure, more bubbles emerged from the pores of the support membranes. This assisted in visualising the location of additional defects, as well as the quantity of the defects. Take membrane (5/30) from the membrane Set 1 and membrane (4/17) from the membrane Set 2 for instance. When the pressure was increased to 535 mbar, only two bubbles formed during the test on membrane (4/17), whereas about 10 bubbles formed during the test on membrane (5/30). A sample picture is shown in Figure 4.4 for the bubble point screening test on membrane (5/30). Furthermore, the bubbles emerging from membrane (4/17) were closer to the enamelled endings, while the bubbles emerging from membrane (5/30) were near the interfaces and all over the surface of the substrate. This proved again that membrane (4/17) (from Set 2) had a better substrate surface (with smaller pores) than membrane (5/30) (from Set 1). It was assumed that better Pd membranes would be obtained on the substrates from Set 2 (with smaller pores) than those from Set 1. This was

confirmed by both the results of permeability test and the membrane surface analysis.

The bubble point screening test only offers qualitative analysis, thus, the next two tests of quantitative analysis were necessary.

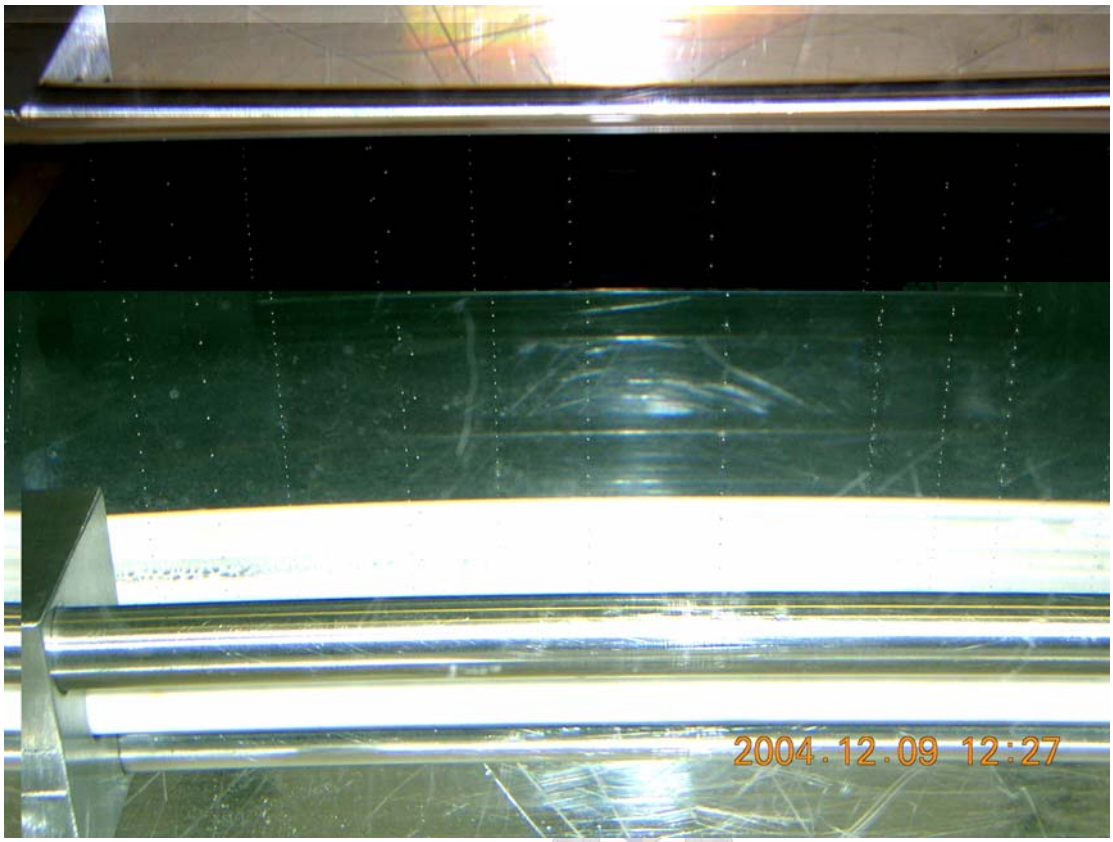


**Figure 4.4: Bubble point screening test of membrane (5/30) at a pressure of 535 mbar**

### 4.3.3 DISCUSSIONS ON BUBBLE POINT TEST

The bubble point test was utilised in this study to determine the pore size of the defects, the average pore size of the support membrane, and the pore size distributions. This method was adopted and modified from Jakobs (1997). The mechanism states that the support membrane is wetted with a liquid (fluid A), which is held in the pores by capillary forces. Another less wetting fluid (fluid B), liquid or gas, acts at increased pressure on one side of the membrane and eventually displaces fluid A.

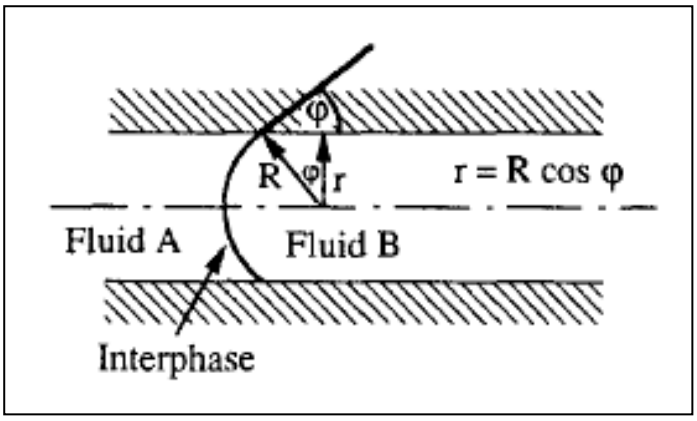


**Figure 4.5: Schematic representation of interracial meniscus in cylindrical pore, Jakobs (1997)**

The pressure difference **ΔP** (Pa) needed to expel the former liquid from a pore with radius r (μm) is given by Laplace's equation:

$$\Delta P = 2 \times \sigma \times H \qquad (4.1)$$

where **σ** is the interfacial tension (N/m) of the fluid-fluid system, and **H** is the mean curvature of the meniscus. In case of a spherical meniscus in a cylindrical pore the principal curvatures:
$\mathbf{c_1 = c_2 = 1/R}$, and the mean curvature can be expressed as, $\boldsymbol{H = c_1 + c_2/2 = 1/R = \cos \varphi / r}$. The radius of the meniscus, **R** (μm), relates to the pore radius via the contact angle, **φ**, of the fluid-fluid-membrane system as visualized in Figure 4.5, resulting in the commonly employed equation:

$$\Delta P = {(2 \times \sigma \times \cos \varphi)}/{r} \qquad (4.2)$$

Until the pressure difference over the membrane reaches the capillary pressure of the largest pores, fluid A acts like a barrier and no flow can occur. Increasing the pressure above this limit results in fluid A being expelled from the largest pores, and allows the other fluid, B, to permeate. By successively increasing the pressure, smaller and smaller pores are opened for permeation of fluid B. The ideal flow versus pressure drop curve generated in this fashion is usually 'S-shaped', as depicted in Figure 4.6, and will hereafter be referred to as the flow-pressure curve.

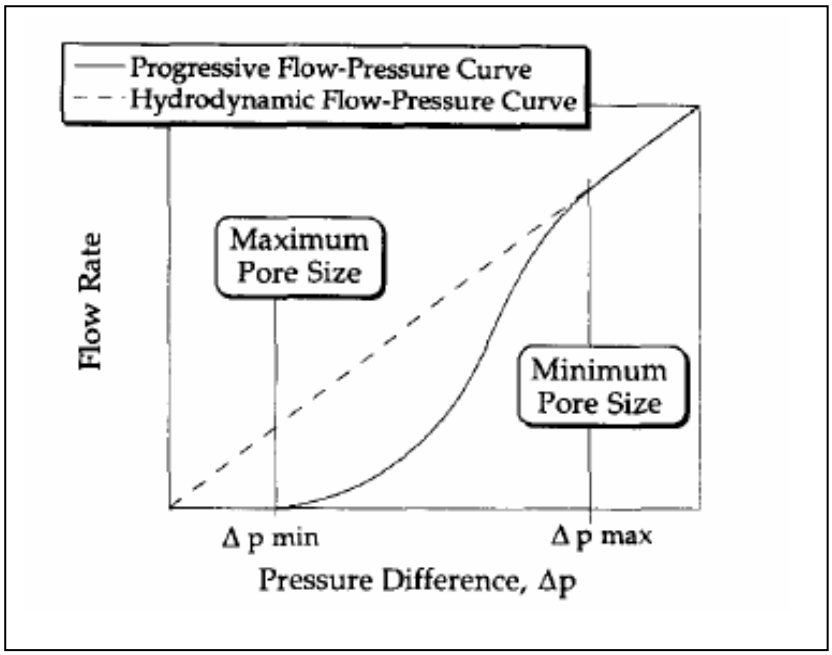


**Figure 4.6: Theoretical flow-pressure curve for the bubble point test/progressive displacement test, Jakobs (1997)**

In this study, fluid A was ethanol, and fluid B was nitrogen, i.e., the fluid system applied was an ethanol-nitrogen system.

For this system the interfacial tension, **σ** is 0.023 (n/m). Since the support membrane here was alumina ceramic, the contact angle, **φ** should be zero. Therefore equation (4.2) reduces to:

$$\Delta P = [2 \times 0.023 \times \cos(0)] / r \qquad (4.3)$$

$$\therefore r \times \Delta P = 0.046 \qquad (4.4)$$

which means:

$$D_p \times \Delta P = 0.09 \qquad (4.5)$$

where $\mathbf{D_p}$ (μm) is the pore size (or pore diameter) of α-alumina ceramic membrane, and **ΔP** (Pa) is the pressure difference.

All the membranes of Set 2 were tested and only four membranes of Set 1 (5/30, 6/30, 10/30, 12/30) were tested by this technique (see procedures in section 3.1.3 in Chapter 3). The results of the bubble point tests on the membranes of Set 1 and membranes of Set 2 are shown in Figure 4.7 and Figure 4.8.

The support membranes of α-alumina ceramics with a nominal pore size of 200 nm were analysed with the ethanol-nitrogen system. The typical flow-pressure curves for the membrane Set 1 and membrane Set 2 are shown in Figures 4.7 and 4.8 respectively. As can be seen, the measured flow-pressure curves approximately display the characteristic 'S-shape' of the theoretical model. For membrane Set 1, up to a differential pressure of 1.3 bar, no flow of nitrogen could be observed and the wetting ethanol acted as a barrier. At higher pressures the flow rate increased abruptly and converge at around 1.7 bar. For membrane Set 2, up to a pressure difference of 2.1 bar, no flow of nitrogen was observed. When the pressure was increased to 2.5 bar, the flow rate increased abruptly. Employing equation (4.5) these pressures could be related to a range of pore sizes, determining the largest and smallest pore, respectively (see Table 4.5).

The average pore size of the membranes of Set 1 is 0.35 µm, whereas, the average pore size of the membranes of Set 2 ranges from 0.25 µm to 0.35 µm. These sizes did not correspond very well with the nominal pore size of 0.2 µm stated by the manufacturer. Table 4.6 shows data of measured average pore sizes obtained by equation (4.5) and pore sizes stated by the manufacturer (Pall Exekia), as well as the error between them. Figure 4.9 is a schematic representation of some data in Table 4.6.

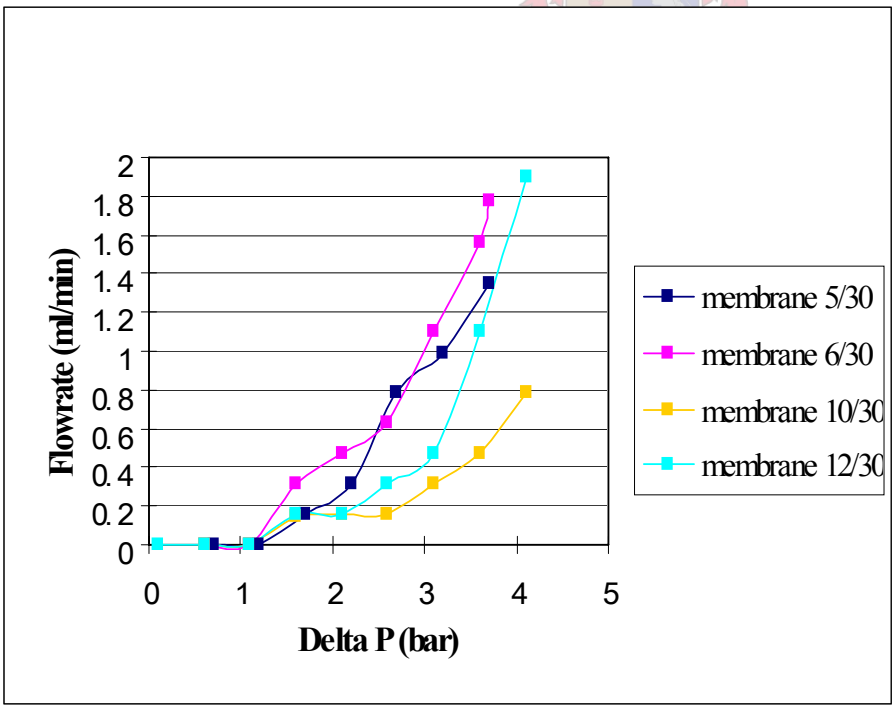


**Figure 4.7: Results of bubble point test on the membranes of Set 1, illustrating the pressure-flow curves**

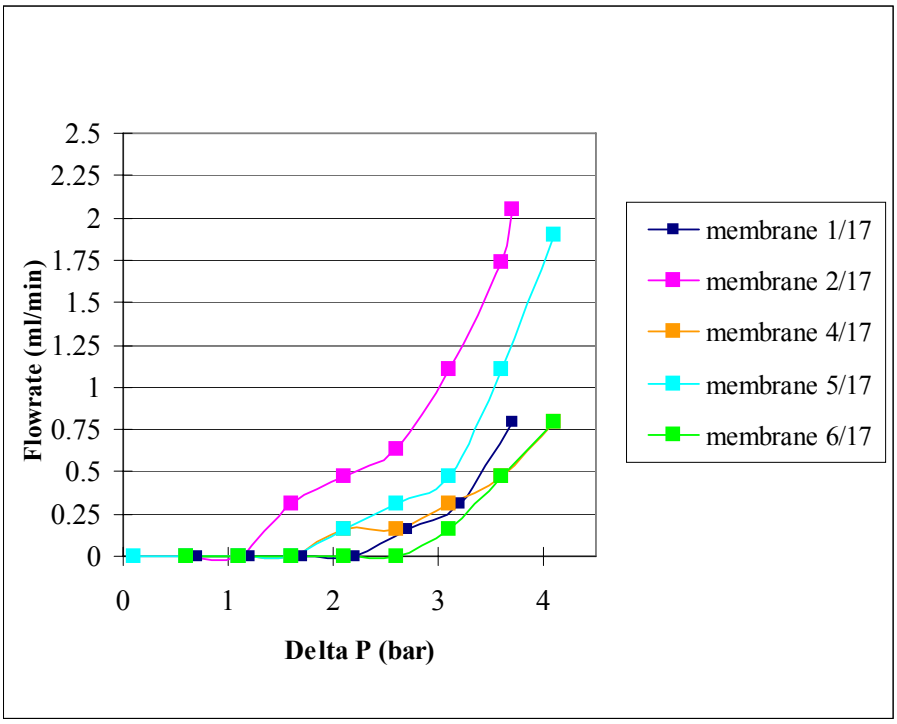


**Figure 4.8:** **Results of bubble point test on the membranes of Set 2, (Mwase, 2005)**

**Table 4.5:** **Measured pore sizes of the support membranes obtained in bubble point test**

| Identification of the membranes | The largest pore size (µm) | The smallest pore size (µm) | The Average pore size (µm) |
|---|---|---|---|
| **Membrane Set 1** | | | |
| 5/30 | 0.53 | 0.24 | 0.36 |
| 6/30 | 0.56 | 0.24 | 0.35 |
| 10/30 | 0.56 | 0.22 | 0.35 |
| 12/30 | 0.56 | 0.25 | 0.35 |
| **Membrane Set 2** | | | |
| 1/17 | 0.33 | 0.24 | 0.28 |
| 2/17 | 0.56 | 0.24 | 0.35 |
| 4/17 | 0.43 | 0.22 | 0.31 |
| 5/17 | 0.43 | 0.25 | 0.31 |
| 6/17 | 0.29 | 0.22 | 0.25 |

**Table 4.6:** **Measured pore size and pore size stated by the manufacturer (Pall Exekia)**

| Identification of the membranes | Measured average pore size (µm) | Pore size stated by manufacturer (µm) | Difference |
|---|---|---|---|
| **Membrane Set 1** | | | |
| 5/30 | 0.36 | 0.2 | 44 % |
| 6/30 | 0.35 | 0.2 | 43 % |
| 10/30 | 0.35 | 0.2 | 43 % |
| 12/30 | 0.35 | 0.2 | 43 % |
| **Average difference** | | | 43.25 % |
| **Membrane Set 2** | | | |
| 1/17 | 0.28 | 0.2 | 28.6 % |
| 2/17 | 0.35 | 0.2 | 43 % |
| 4/17 | 0.31 | 0.2 | 35.5 % |
| 5/17 | 0.31 | 0.2 | 35.5 % |
| 6/17 | 0.25 | 0.2 | 20 % |
| **Average difference** | | | 32.52 % |

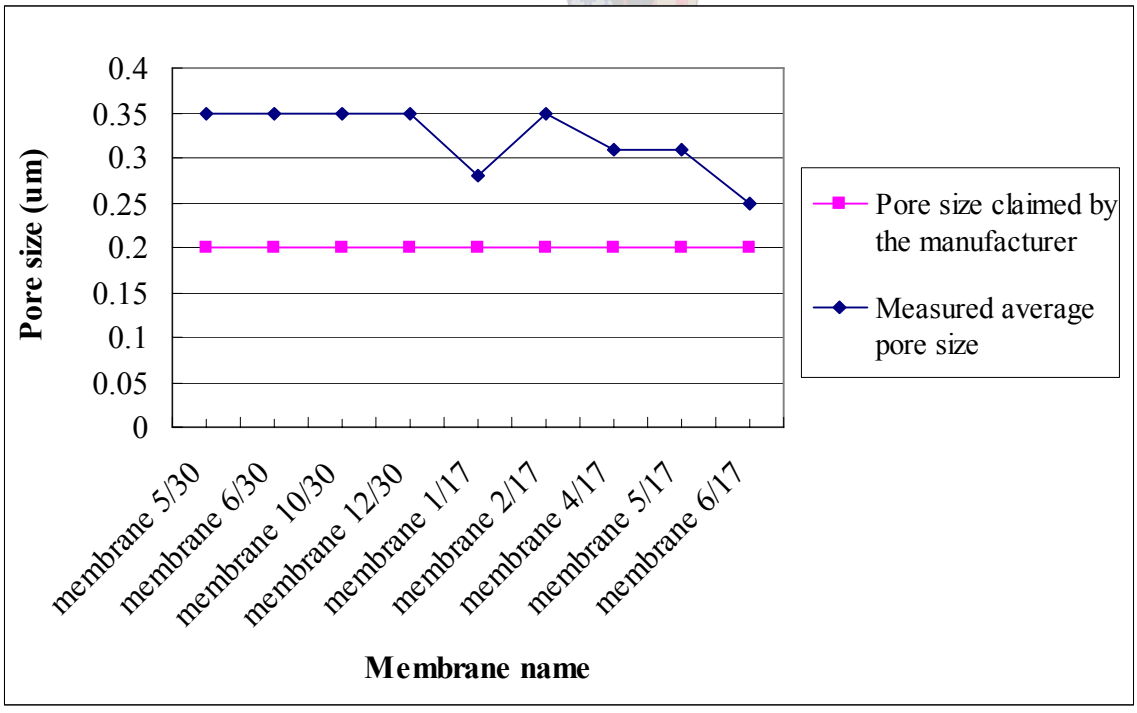


**Figure 4.9:** **Measured pore size and pore size stated by the manufacturer (Pall Exekia)**

Therefore, from the data above, it is apparent that there was a difference between the measured pore sizes and pore sizes stated by the manufacturer; the error between them ranged from 20 % to 44 %. Clearly, the pore sizes of the membrane Set 2 were smaller than those of the membranes of Set 1. It was assumed that the pore size of the support membrane had a major influence on the composite electroless plating, and better Pd composite membranes could be prepared on the supports with smaller pore sizes. This assumption was subsequently confirmed by the permeability tests on the Pd membranes using hydrogen and nitrogen. It was found that Pd composite membranes deposited on membranes from Set 2 had better permselectivity than those from membranes of Set 1.

However, the electroless plating procedure itself also influences the quality of the Pd composite membranes.

### 4.3.4 PERMEABILITY TEST ON SUBSTRATES AT ROOM TEMPERATURE

The bubble point screening test offered a visual means for identification of defects on the substrate, and the bubble point test provided some quantitative confirmation about the pore sizes. Thereafter, a permeability test was performed on the substrate to obtain information about the permeability of the substrates. Only twelve membranes were tested (Membrane 5/17 was excluded because it broke during the bubble point test).

The nitrogen feed stream was forced through the support membrane with a gradual increase in pressure. The flow rate of the permeated gas was measured using a bubble flow meter (total volume of 50 ml) (see Figure 3.11).

Figure 4.10 shows the permeability of nitrogen for eight support membranes. As can be seen, the data indicates a linear relationship between differential pressure and flow rate. Since the support membranes are macroporous, the separation mechanism of nitrogen should be a combination of laminar flow and Knudsen diffusion. For laminar flow, the gas flow rate is proportional to the pressure difference, whereas, for Knudsen diffusion, the flow rate is only proportional to the temperature. The data in Figure 4.10 thus indicates that the dominating diffusion mechanism of nitrogen through the support membrane is laminar flow.

Table 4.7 contains data for the average permeance of nitrogen at the average pressure, and provides an indication of the permeability of substrates before the Pd electroless plating. It assists with evaluating the influence of the substrates on the Pd composite membranes. Figure 4.11 presents the data in Table 4.7.

In Table 4.7, the average permeance of nitrogen for support membranes (2/17), (6/17), (6/30) and (12/30) is similar. However, after performing electroless plating on these support membranes (using a different method for each step, see Table 4.2 and Table 4.3), the permeance of nitrogen for the Pd composite membranes is quite different. Therefore, it could be concluded that the permeability of the support membrane has less of an influence on the permselectivity of the composite membranes than the electroless plating technique itself.

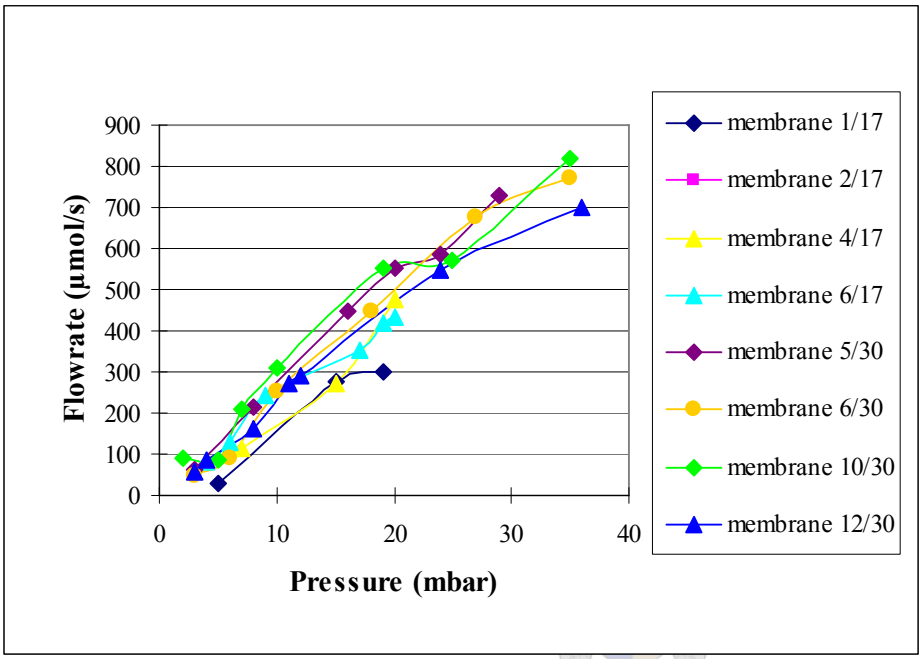


**Figure 4.10: Nitrogen permeation test of the support membranes**

**Table 4.7: Permeance of the substrates for $N_2$**

| Identification of the membranes | Average pressure (mbar) | Average permeance of nitrogen (µmol/m$^2$/Pa/s) |
|---|---|---|
| 1/17 | 13 | 47.59 |
| 2/17 | 13.33 | 83.53 |
| 4/17 | 14 | 69.5 |
| 6/17 | 12.5 | 79.076 |
| 5/30 | 16.67 | 90.769 |
| 6/30 | 16.5 | 80.614 |
| 10/30 | 14.71 | 107.44 |
| 12/30 | 14 | 81.898 |

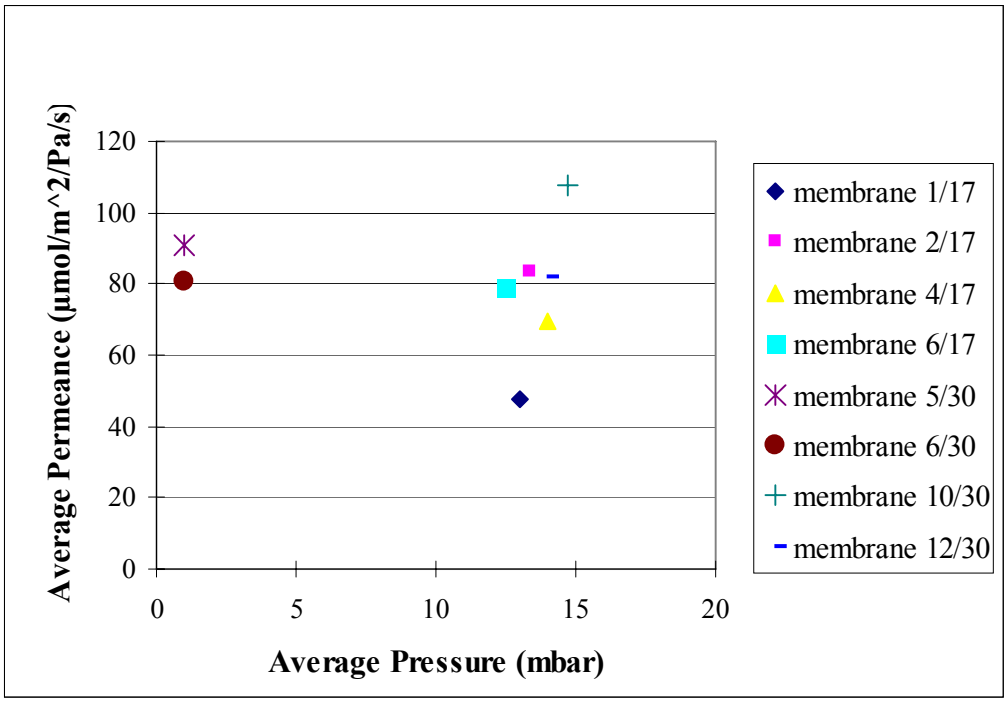


**Figure 4.11: Average permeance of nitrogen at average pressure**

## 4.4 MEMBRANE PRE-CLEANING BEFORE PRETREATMENT

During the bubble point test the support membrane was immersed in ethanol; consequently there was some residual ethanol in the membrane pores after completion of the test. Membrane pre-cleaning is necessary to remove both the organic and inorganic contaminants. Three methods were applied respectively on membranes (2/17), (4/17) and (2/30) (see Table 4.8). All the procedures applied on these three membranes were exactly the same, except the pre-cleaning procedures. Therefore, the quality of Pd membrane will highlight the effect of the pre-cleaning procedures.

Membrane (4/17) has the best selectivity of these three membranes. It appears that method 3 is more effective than the other two methods. It is assumed that the ultrasonic cleaning in method 2 simultaneously removes the contaminants and opens the pores of the support membranes. This makes the effective pore size bigger than before, and may also cause defects. It will then negatively influence the pretreatment due to the fact that this offers a coarser support surface for the pretreatment. In method 1, only stirring in distilled water cannot clean the membrane effectively. Therefore, method 3 is preferable.

**Table 4.8: Methods of pre-cleaning applied on membranes (2/17), (4/17) and (2/30)**

| Identification of the membrane | Pre-cleaning |
|---|---|
| **2/17** | Method 2 |
| **4/17** | Method 3 |
| **2/30** | Method 1 |

- method 1: stirring in $H_2O$, 60min
- method 2: Ultrasonic cleaning, 10min; stirring in $H_2O$, 60min
- method 3: stirring in (0.5mol/l) NaOH, 30 min;
  stirring in (0.5mol/l) HCl, 30min;
  stirring in $H_2O$, 60min

The membrane pre-cleaning method has rarely been published in the literature, therefore, further research is recommended.

## 4.5 MEMBRANE PRETREATMENT

The sensitisation and activation step is a very important step in determining the quality of the plated palladium membrane. Defects can result because palladium is not able to deposit on a non-activated surface due to the autocatalytic mechanism for electroless plating. Therefore, in order to obtain a defect free palladium membrane, the target surface must be seeded fully and uniformly with palladium nuclei. See the reaction during membrane surface pretreatment in equation (4.6):

$$Sn^{2+} + Pd^{2+} \rightarrow Sn^{4+} + Pd \qquad (4.6)$$

Three methods were performed in this study (see section 3.3 in Chapter 3). Take membranes (2/17), (6/17), and (3/30) for instance (see Tables 4.9 and 4.10). All the procedures applied on these three membranes are exactly the same, except for the pretreatment methods.

**Table 4.9: Methods of pretreatment applied on membranes (2/17), (6/17) and (3/30)**

| Identification of the membrane | Pretreatment |
|---|---|
| **2/17** | Method 2 |
| **6/17** | Method 3 |
| **3/30** | Method 1 |

**Table 4.10: Methods of pre-treatment**

| Method | Repeat | $PdCl_2$ | $H_2O$ | $SnCl_2$ | $H_2O$ |
|---|---|---|---|---|---|
| Method 1 | **3 times** | 10min | Dip for 10 times | 10min | Dip for 10 times |
| | **3 times** | 5min | -- | 5min | Dip for 10 times |
| Method 2 | **3 times** | 15min | Dip for 10 times | 15min | Dip for 10 times |
| | **3 times** | 5min | -- | 5min | Dip for 10 times |
| Method 3 | **4 times** | 15min | Dip for 10 times | 15min | Dip for 10 times |

After the surface pretreatment, the membrane was stirred in distilled water for 30 min, and then dried overnight at 100 °C. In method 3, the stirring-dipping cycle was repeated 4 times, and the surface turned completely black due to a uniform covering of the palladium. By this procedure, a large number of fine palladium particles were deposited on the surface. The membrane pretreated by method 1 was not uniformly covered with palladium, especially the enameled endings. It is assumed that the pretreatment time was insufficient. Method 2 is as effective as method 3, however, the procedure for method 3 is easier; thus, method 3 is preferable.

It was found that the palladium particles pretreated on the membranes of set 2 came off slightly easier than those of membranes of set 1. This has been mentioned in section 4.2, i.e. that the support membranes of set 2 had a denser and smoother surface than those of set 1 (which made it more difficult for the palladium particles to attach to the support surface during the membrane surface pre-treatment). Therefore, it is recommended that a lower stirring speed (<1300 rpm) is used in future studies on the membrane surface pre-treatment method. Alternatively, the membrane can be immersed in the pretreatment solution instead of being rinsed by stirrer. The membrane cleaning procedure after the pretreatment is obligatory, because this can remove the $Sn^{4+}$, $Sn^{2+}$ and $Cl^-$ impurities, which may otherwise form defects or pinholes on the Pd membranes.

Tanaka et al. (2005) started experimenting with pretreatment procedures without using tin. Incorporation of Sn into Pd film often results in facile delamination and defect formation, due to loss of adhesion. They concluded that the presence of tin at the alumina-palladium interface contributed to the decline of the Pd composite membrane selectivity. A procedure that eliminates tin contamination on the alumina surface is impregnation of the palladium complex, followed by reduction with hydrazine. They used palladium acetate and $[Pd(acac)_2]$ as the metal precursors, which are dissolved in either chloroform or acetonitrile. Dip and dry coating of the precursor and successive reduction of palladium with an alkaline hydrazine solution was typically carried out for seeding of palladium particles on the substrate. The reaction is expressed as follows:

$$2Pd^{2+} + N_2H_4 + 4OH^- \rightarrow 2Pd^0 + N_2 + 4H_2O \quad (4.7)$$

They claimed that the deposition of palladium on the alumina tube activated by their system is much faster than that activated by a tin chloride system. This is due to the uniform distribution of numerous Pd nano-particles, which offers more active sites and enhanced the deposition of Pd in the plating.

## 4.6 MODIFIED PALLADIUM ELECTROLESS PLATING

Previous research done by Keuler (2002) applied a vacuum during the electroless plating, and better palladium films were prepared than conventional plating techniques. However, the vacuum was not precisely measured, so it could not be reproduced and controlled well. Razima and co-workers (2001) combined electroless plating and osmosis to produce palladium composite membranes on porous Vycor glass disks. The effect of osmosis on the properties of the palladium film showed that electroless plating with osmosis allows preparation of thinner, fully dense membranes with a finer microstructure, which strongly interacts with the substrate. All these features lead to superior permeability and better thermal–mechanical properties of the composite membranes. Nam and Lee (2000) utilised vacuum electro-deposition to produce palladium/nickel membranes on substrate of disk shape stainless steel (SUS). Therefore, there has been a growing interest in the use of a vacuum or osmosis during preparation of palladium or palladium composite films. However, research on electroless plating with vacuum has been rarely performed, or published.

A technique to prepare palladium composite membranes was modified during this research, which applied an accurately measured vacuum on the shell side of the plating reactor during electroless plating. By using this method, the microstructure and thickness of the deposited film could be manipulated, and better palladium penetration into the substrate and better metal-ceramic adhesion could be achieved. It is assumed that higher permeation rates could be achieved, and denser palladium membranes could be prepared, by this method.

### 4.6.1 ELECTROLESS PLATING WITH VACUUM

After the 1 μm initial film was plated, a second or third palladium layer (using 6 ml of plating solution for each layer) was plated, depending on the total desired thickness. At this stage, a gauge vacuum was applied on the shell side of the Teflon reactor in the range of 10-25 kPa (g). The method was to force the plating solution to penetrate through the pores or defects of the membrane

where more plating solution was required to be coated. In this study, the vacuum was measured by a vacuum gauge, so that its influence on the electroless plating could be investigated. The aim was to optimise the vacuum to make defect-free palladium film with a better good metal-ceramic adhesion.

Figure 3.16 in section 3.5.3 shows the Teflon reactor, which had a single outlet with a diameter of 8 mm, for drawing a vacuum on the shell side. A thin Teflon tube with a diameter of 8 mm was wrapped with Teflon tape and then twisted tightly into the outlet. The connecting interface between the thin Teflon tube and the outlet was properly sealed, so that no liquid or gas could escape from this outlet. Vacuum was drawn on the shell side of the reactor through this outlet, and was controlled using a vacuum filter

### 4.6.2 VACUUM INFLUENCE

During the electroless plating, all the other parameters except the vacuum remained the same. See section 3.4. A range of gauge vacuum pressures (10 kPa, 15 kPa, and 20 kPa) was applied during the preparation of the second and third Pd layers.

A gauge vacuum of 25 kPa was applied during the preparation of the third layer for membrane (1/30). The results showed that a low permselectivity was obtained and the thickness of Pd film was uneven. It was assumed that the gauge vacuum of 25 kPa forced excess plating solution to penetrate the support. During the electroless plating the plating solution accumulated in the shell side of the membrane and the solution was drawn from the outlet, causing wastage of the plating solution. Figure 4.12 was taken of membrane (3/30), for which a vacuum of 20 kPa (g) was applied during preparation of the second layer. It illustrates how the palladium nuclei penetrate deeply into the pinholes of the support membrane. This assisted the Pd plating solution to penetrate into the pinholes, and reduced the defects in the support membrane. However, this decreased the film thickness in some areas of the Pd membrane and made it thinner than the theoretical data would suggest (see more details in section 6.1.4.2). Figure 4.13 is the cross-sectional view of membrane (4/30). A gauge vacuum of 10 kPa was applied during the preparation of the second layer. It is apparent that a poor Pd layer was plated on the support. The palladium does not completely cover the surface area, and the ceramic support is exposed. It is assumed that the vacuum of 10 kPa is too low. Bad permselectivity of membrane (4/30) confirmed this deduction. Figure 4.14 shows membrane (5/30). A gauge vacuum of 15 kPa was applied during preparation of the second layer. However, the Pd layer did not completely cover support membrane surface. Defects formed on the membrane and decreased the membrane permselectivity.

It was found that when the vacuum was bigger than 20 kPa (absolute), it forced excess plating solution into the pores of the support. The plating solution accumulated in the shell side of the membrane, wasting of the plating solution. When the vacuum was smaller than 20 kPa (absolute), as mentioned above, the solution did not penetrate through all the defects and the pinholes could not be completely covered. Therefore, a vacuum of 20 kPa (absolute) is suggested to prepare the Pd film (1.7-4 μm) on α-alumina ceramic support via the vacuum electroless plating technique. More details of the Pd membrane morphology and surface roughness are presented in chapter 6. Thus, thin, dense, and pinhole-free Pd composite membranes were prepared on α-alumina ceramic support with much smaller pore size and less rough surface by vacuum electroless plating.

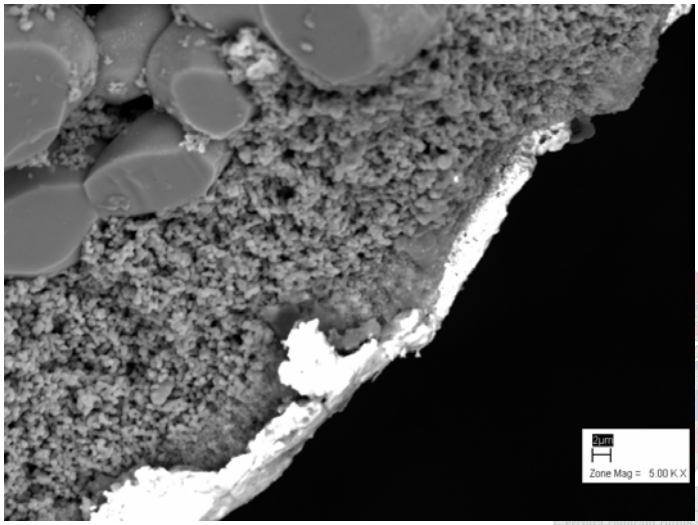


**Figure 4.12: Cross section (SEM image) of membrane (3/30), (5.00 KX)**

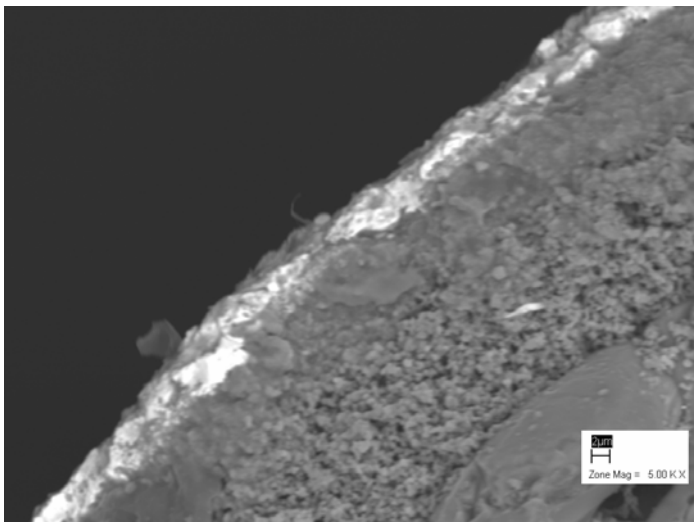


**Figure 4.13: Cross section (SEM image) of membrane (4/30), (5.00 KX)**

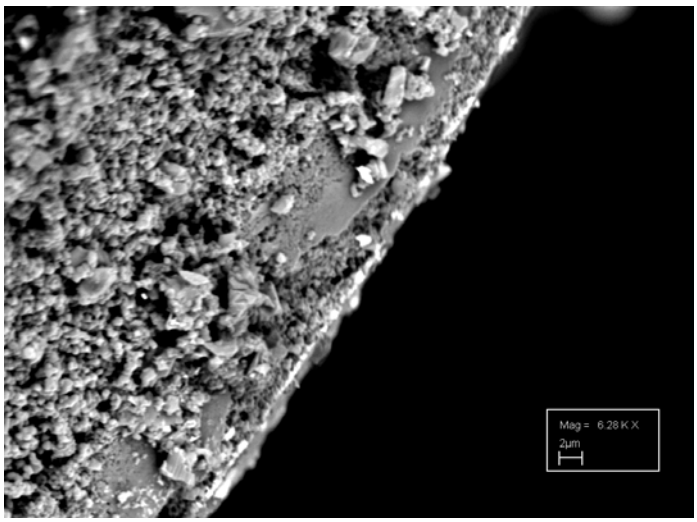


**Figure 4.14: Cross section (SEM image) of membrane (5/30), (6.28 KX)**

## 4.7 MEMBRANE POST-CLEANING AFTER PLATING

Membrane post-cleaning is essential to remove the impurities that accumulated during the electroless plating, but this has rarely been published in papers. Due to the time limitations and membrane materials (only twelve support membranes were used in this study), the method of post-cleaning has not been modified. The method of post-cleaning applied in this study was adopted from Keuler (2002).

Membrane (4/30) (with a thickness of 1.72 µm) was prepared without applying post-cleaning after the electroless plating. Impurities are prominent from EDS imaging (see Figure 4.15). The image was taken randomly of a dark spot on membrane (4/30). Atoms of Na, C, O, Al, were observed. Na and C were from EDTA, and should be removed by post-cleaning. Impurities of Al and O indicated that there were defects (pinhole) on the membrane, which should be covered by more Pd layers. Results of permeability tests show that membrane (4/30) had more defects than other membranes, and the membrane had the highest permeability of $N_2$ and lowest permselectivity of the eleven membranes. Therefore, an effective method of membrane post-cleaning should be applied after the electroless plating.

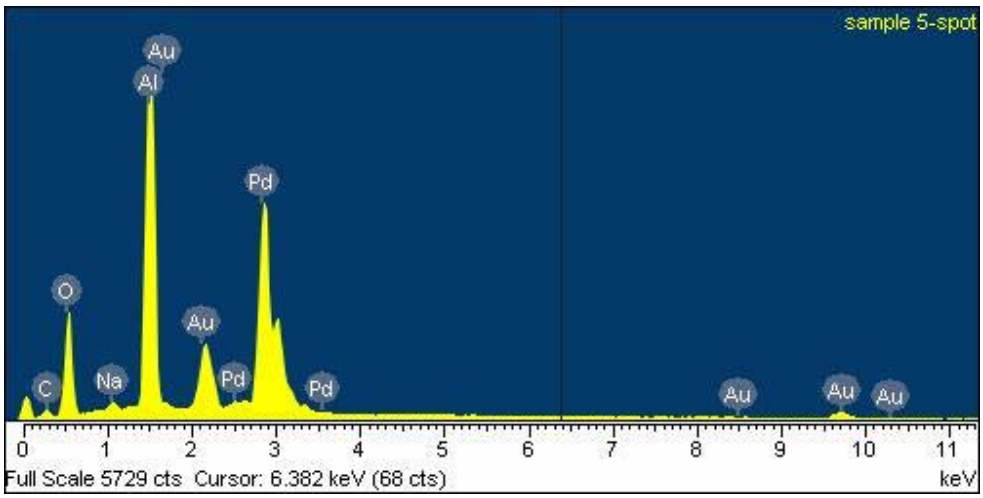


**Figure 4.15: EDS image of membrane (4/30) without post-cleaning**

The other eleven Pd composite membranes were prepared by performing post-cleaning with Keuler's method (2000) directly after the electroless plating. However, carbon impurities could still be observed by EDS analysis of most of the samples. Therefore, it is recommended that a more effective post-cleaning method should be investigated in future work.

## 4.8 HEAT TREATMENT

After electroless plating, post-cleaning and overnight drying (see sections 3.4 and 3.5), some brown spots were observed in some areas on the outside of the Pd composite membrane. This indicates the presence of carbon (Keuler, 2000). In this study, both SEM (backscatter) and EDS analysis were applied after the membranes were dried at 120 ºC. The results from some of the Pd composite membranes proved that there was some carbon, both on the inside and the outside surfaces of the palladium composite membranes. Carbon causes instability and defects on the palladium membrane, and decreases the selectivity of the palladium membrane. Furthermore, the heat treatment assists the palladium nuclei to agglomerate together to form a denser film and facilitate the adhesion between the Pd layer and ceramic support. The method of heat treatment is, therefore, essential (procedures of heat treatment used in this study are presented in section 3.6).

### 4.8.1 EFFECT OF HEAT TREATMENT

Four membranes have been annealed in this study. Take membranes (6/17) and (3/30) for example (see the procedures and methods in section 3.6).

Membrane (6/17) was annealed using method 1. It was heat treated in $N_2$ for 5 h from 20°C to 320°C, and then oxidized in air for 2 h at 320°C. The membrane was then heat treated in $N_2$ for 130

min from 320°C to 450°C, followed by reduction in $H_2$ for 1.5 h at 450°C. Finally, the membrane was cooled down in $N_2$ to 350°C and held at this temperature for 30 min. Membrane (3/30) was heat-treated using method 3. The other procedures were the same as method 1 except that the heating rate was twice that of method 1. The results suggest that a fast heating rate can cause more defects than a more moderate heating rate. Membrane (6/17) has better selectivity than membrane (3/30).

In addition, heat treatment assists Pd nuclei to agglomerate and form a denser film (see section 6.1.3).

### 4.8.2 NEW METHOD DEVELOPED TO INVESTIGATE HEAT TREATMENT

This is a new method developed for investigating the heat treatment procedures. After being plated, the Pd composite membrane was cut into two pieces, so that each piece could be exposed to a different heating procedure. This method can offer a precise way of determining which heating procedure is better, without the influence of the substrate or the plating technique. However, due to the limitation of time and materials, this procedure was only performed on membrane (10/30) in this study. Heat treatment methods 1 and 2 were performed on the two parts of the membrane, respectively. Only annealing time, using $H_2$ in method 2, is twice as longer as for method 1. Therefore, the quality of the Pd membrane after heat treatment represents the $H_2$ function during heat treatment. It was found that reduction in $H_2$ for 3 h removes more carbon impurities than reduction for 1.5 h, which is confirmed by the SEM imaging (see Figures 4.16 and 4.17). The piece annealed by method 2 had fewer dark spots (indicative of carbon) than the piece annealed by method 1.

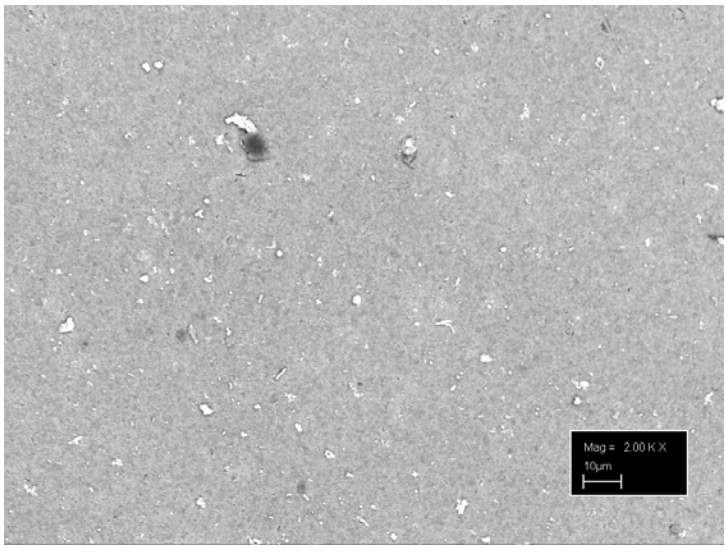


**Figure 4.16: Top view of membrane (10/30) (using heat treatment method 2), 2.00 KX**

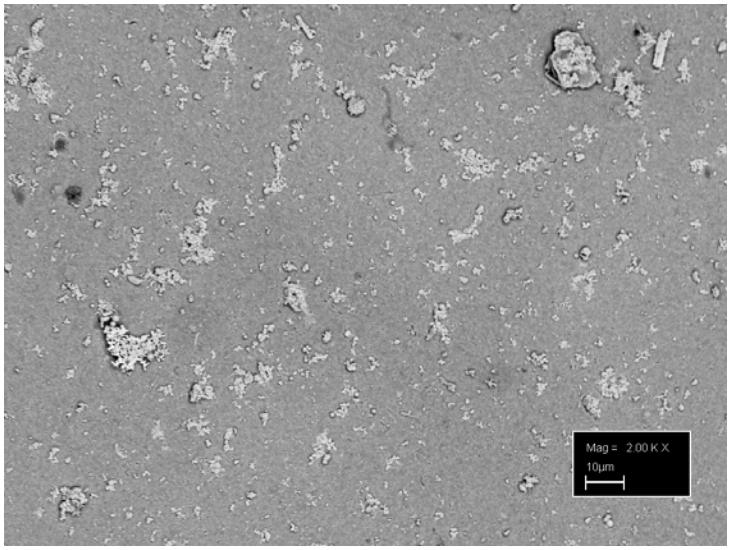


**Figure 4.17: Top view of membrane (10/30) (using heat treatment method 1) 2.00 KX**

### 4.8.3 ADDITIONAL HEAT TREATMENT

After the permeation tests, an additional heat treatment was applied on membrane (6/17) to determine whether it could facilitate the removal of more carbon impurities, as well as to test the thermal stability of the Pd composite membranes. The membrane was heated to 600 °C in $N_2$, and then held at this temperature for 10 h in $H_2$ for reduction. After the additional heat treatment, a permeability test by nitrogen was performed on the membrane. The $N_2$ permeance is an indication of the amount and type of defects on the film. The results show that heat treatment temperatures up to 550°C in $H_2$ atmosphere caused more defects to form on the membranes. Defects formed quickly, which resulted in a sharp increase in the $N_2$ permeance. $H_2$ to $N_2$ selectivity decreases rapidly, making the membrane unsuitable for separation at those high temperatures (≥600°C). This indicated that Pd composite membrane prepared in this study did not possess good thermal stability when the temperature exceeded 600 °C. Therefore, it is recommended that the Pd composite membranes prepared in this project are used only at temperatures below 600 °C.

Additional heat treatment was also applied on membrane (3/30) using air for 10 h. The XRD image (see Figure 4.18) was taken on the dark spot of membrane (3/30). Clearly, the experimental data (see Table 4.11, data in italic) does not correspond well with the theoretical PDF data. After computer analysis, it was found that the data of the impurity does not correspond to that of Sn (impurity might be imported during pretreatment) or carbon (impurity might be imported during Pd plating) or Al, or O (from support membrane). Therefore, two possible explanations are suggested here. One is that during the heat treatment, PdO formed (Ma, 2004) and it definitely affected the crystals structure of the palladium film. Thus, the data shown in XRD images no longer only

corresponds with palladium, but also with PdO. Another explanation might be that there were impurities of dust brought into the samples while preparing them.

**Table 4.11: Data for membrane (3/30)**

| No | Angle (2θ) | D space (Å) | Counts | Relative Intensity |
|---|---|---|---|---|
| 1 | 40.20 | 2.243 | 35 | 100 |
| 2 | 46.70 | 1.945 | 17 | 49 |
| ***3*** | ***52.55*** | ***1.741*** | ***13*** | ***37*** |
| 4 | 68.35 | 1.372 | 12 | 34 |

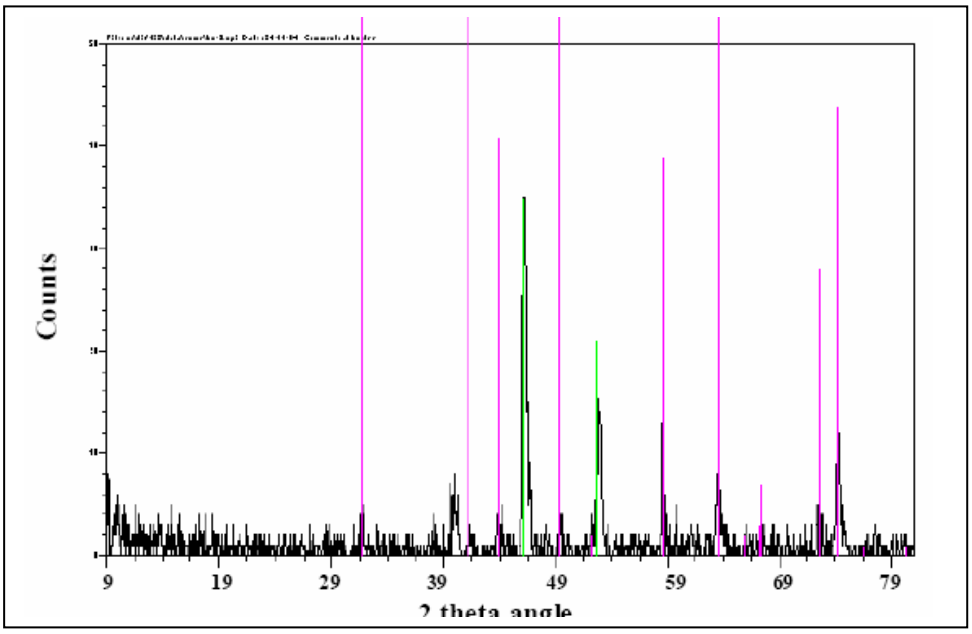


**Figure 4.18: XRD image for membrane (3/30) (the lines in green are for Pd)**

## 4.9 BUBBLE POINT SCREENING TESTS OF PALLADIUM COMPOSITE MEMBRANES

Bubble point screening tests were performed on the Pd composite membranes after the membrane permeation tests, to visualise the location of the defects. These tests showed that the defects were mainly located at the interface between the enamelled endings and the plating surfaces, or close to the interfaces. To eliminate such defects more Pd layers were coated, by applying a vacuum on the shell side of the plating reactor. Finally, when the Pd layer was more than 3 μm, no defects were found when the bubble point screening tests were performed. This is a good method to determine whether there are defects on the Pd composite membranes as well as the locations of the defects. Sometimes, the $N_2$ permeance was 2 or 3 nmol/m$^2$/Pa/s, which suggests there were defects on the

Pd films. However, no defects were observed during this test, which suggest that the $N_2$ permeation can be attributed to leaking at the membrane reactor seal, or graphite ring, and not from defects the Pd film.

## 4.10 SUMMARY

In this chapter the different steps for modification of the electroless plating process on the inside surface of α-alumina ceramic membranes are presented. Twelve palladium membranes were prepared in this study. Discussions describing the influence of the support membranes, the method of pre-cleaning, the modified electroless plating with vacuum, the method of membrane post-cleaning and the heat treatment procedures, are presented. However, due to time and material limitations, it is suggested that further attention is given to each step, particularly membrane post cleaning and heat treatment procedures.

It was found that different pores sizes and the smoothness of the support membranes had a significant influence on the Pd membranes. Better Pd composite membranes with higher permselectivity can be prepared on support membranes that contain smaller pore sizes and smoother surfaces.

Proper pre-cleaning of the support membranes is important, and an effective cleaning method was applied in this study. The preferred method is to rinse the support membranes with dilute sodium hydroxide solution, dilute hydrochloric acid solution, and finally distilled water.

After pre-cleaning, a proper membrane surface pretreatment step prior to electroless plating was essential to ensure a good quality palladium composite membrane. The support membrane surface turned completely black due to a uniform covering of palladium when using method 3 for pretreatment. The membrane was first stirred in $PdCl_2$ solution for 15 min, and was then dipped in distilled water 10 times (1-2 seconds each). Subsequently, the membrane was stirred in $SnCl_2$ solution for 15 min, and was then dipped in distilled water 10 times. These procedures were repeated 4 times. However, $Sn^{2+}$ or $Sn^{4+}$ from the pretreatment solution or residue might form impurities if the cleaning step is not performed properly. Therefore, it was imperative that the membrane is thoroughly cleaned after pretreatment.

The vacuum applied during the electroless plating on the shell side of the electroless plating reactor assists in reducing the defects. A gauge vacuum of 20 kPa (g) proved to be an optimum for

producing a good Pd coating on the α-alumina ceramic membrane (claimed pore diameter of 200 nm). Dense and smooth Pd composite membranes with high permselectivity were obtained when this vacuum was applied during the electroless plating technique.

Post-cleaning of the Pd composite membranes is important for removing carbon impurities. Membrane (4/30) was prepared without applying post-cleaning after electroless plating. The most impurities were found on this Pd film, and it had the lowest selectivity of all twelve Pd composite membranes. Due to time and material limitations, the post-cleaning has not been investigated in this study. Therefore, effective methods of post-cleaning are recommended for future work.

Heat treatment removes the carbon impurities, assists the Pd nuclei to agglomerate, and ensures better adhesion between Pd layer and ceramic supports. However, due to the different rates of thermal expansion of Pd and ceramic, the heating rate should be low (1°C/min is suggested) to prevent from membrane cracking. Furthermore, the Pd membranes cannot be exposed to $H_2$ reduction for longer than 4 hrs, otherwise, more defects are formed, which subsequently decrease the membrane selectivity In addition, if the Pd membrane contains carbon impurities, additional defects are formed during heat treatment. Therefore, it is recommended that another Pd layer be coated to cover the defects until no defects are found after heat treatment. The new method (i.e. cutting the membrane into two parts in order to apply two different heating methods) is an excellent means of investigating the morphological structure of the Pd membranes during annealing. However, in order to measure the permeability of the two parts of the Pd composite membrane, a new reactor half the size has to be manufactured. Finally, there is an assumption that further oxidation or reduction changes the surface morphology and structure of the Pd film. These changes promoted $H_2$ movement through the film, but decrease the membrane selectivity. A more detailed study is necessary to confirm this assumption.

# CHAPTER 5: MEMBRANE PERMEABILITY AND PERMSELECTIVITY

In this chapter, section (5.1) presents the theory of the separation mechanism of $H_2$ through the pure palladium films. Section (5.2) discusses the single gas testing on the Pd composite membranes using $N_2$ or $H_2$ respectively. The effects of temperature, pressure difference and film thickness on the $H_2$ and $N_2$ permeance are discussed thereafter.

## 5.1 HYDROGEN PERMEANCE THROUGH PALLADIUM MEMBRANES

The permeation of hydrogen through a dense membrane usually involves several steps in series (Lewis, 1967):

(a) dissociated adsorption of molecular hydrogen on the membrane surface.
(b) reversible dissolution of surface atomic hydrogen in bulk layer of palladium.
(c) diffusion of atomic hydrogen in the bulk palladium layer.
(d) association of atomic hydrogen into molecular hydrogen and desorption on the other surface of palladium layer.



Generally, the hydrogen permeability is expressed in terms of the permeation equation as follows:

$$J = \frac{P_{er}}{l}(P_h^n - P_l^n) \qquad (5.1)$$

where J is the hydrogen permeation flux [$cm^3/(cm^2.min$]; $P_{er}$ is the permeability constant of hydrogen through the membrane [($cm^3.cm$) / ($cm^2.min.Pa^n$)]; $P_h$ and $P_l$ are the hydrogen partial pressures on the high pressure and low pressure sides, respectively, n is a constant indicating pressure dependency (or pressure exponent). If step (c) in the hydrogen permeation through the membrane is the rate-determining step, the value of n should be 0.5 according to Sievert's law. However, if step (b) or (c) is the rate-determining step, n should be larger than 0.5.

The permeability constant $P_{er,}$ is dependent on the temperature and can be expressed using Arrhenius expression (as described in Chapter 2):

$$P_{er} = P_0 \, e^{-E_D / R_0 T} \tag{5.2}$$

where $P_0$ is the pre-exponential factor, $E_D$ is the apparent activation energy for hydrogen permeation, $R_0$ is the gas constant, and T is the absolute temperature.

The $H_2$ to $N_2$ permselectivity was determined using the following formula:

$$H_2 \text{ to } N_2 \text{ permselectivity} = \frac{H_2 \text{ permeance}}{N_2 \text{ permeance}} \tag{5.3}$$

## 5.2 SINGLE GAS PERMEATION TESTS

Single gas permeation tests were performed on the palladium membranes under positive feed pressure using $N_2$ and $H_2$. Hydrogen or nitrogen gas was introduced into the membrane tube from outside of the reactor via pipes through the mass flow controller, and the gas permeated through the membrane. The soap-bubble flow meter was used to determine the flow rate. Gas permeability and $H_2/N_2$ selectivity was determined in the experiments conducted with the individual gases. The effects of temperature, pressure difference and film thickness on permeance were thereafter investigated.

### 5.2.1 THE EFFECT OF PRESSURE DIFFERENCE

Nitrogen permeance is an indication of membrane defects or leaking. There are three factors that contribute to the measured nitrogen permeance. They are:

- Leakage through defects in the Pd film,
- Leakage at the membrane reactor seal, graphite ring, enamel interfaces, and
- Leakage at the porous membrane, or interfaces between non-porous enamel and Pd film.

The contribution of the final two factors cannot be quantified, but from experience it is known that there is at least some leakage between the membrane and the reactor seal. The measured nitrogen permeance, thus represents the maximum number of the defects.

The hydrogen flow through the composite membrane is schematically illustrated in Figure 5.1. If it is assumed that the support membrane's resistance to mass transfer is negligible (support

membrane's inner layer, $d_p$ = 200 nm), then the rate of hydrogen transport through the composite membrane will be dependant on the rate through the defects/pinholes, as well as through the dense metal film.

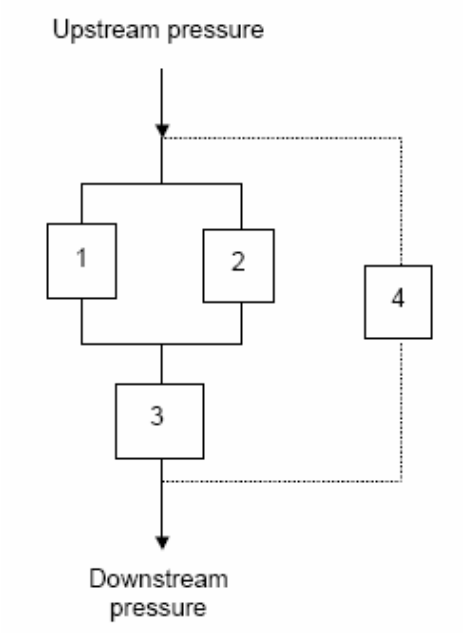


**Figure 5.1: $H_2$ flow through Pd membranes at high temperature (Van Dyk, 2005)**

1 Dense metal film
2 Metal film defects
3 Porous Alumina Support
4 Membrane/ Seal interface



#### 5.2.1.1 Nitrogen permeation tests

Figures 5.2 and 5.3 show nitrogen permeance of membrane (4/17) (with a thickness of 1.79 μm) and membrane (1/17) (with a thickness of 2.92 μm) respectively as a function of pressure and temperature. The average pressure between the tube and shell side was measured, which was the sum of the absolute pressures on the shell and tube sides divided by two. Theoretically, the average pressure should not have any effect on the nitrogen permeance (in nmol/m²/Pa/s), if it is Knudsen flow. For nitrogen, the permeance is proportional to the number of defects. Thinner films therefore have a higher nitrogen permeance than thicker films, due to the higher concentration of defects on the thinner films. The effect of film thickness on membrane performance will be discussed in more detail in section (5.2.2). Figures 5.2 and 5.3 indicate that the nitrogen permeance varied insignificantly with an increase in average pressure, confirming that the nitrogen flow through the membranes was Knudsen flow.

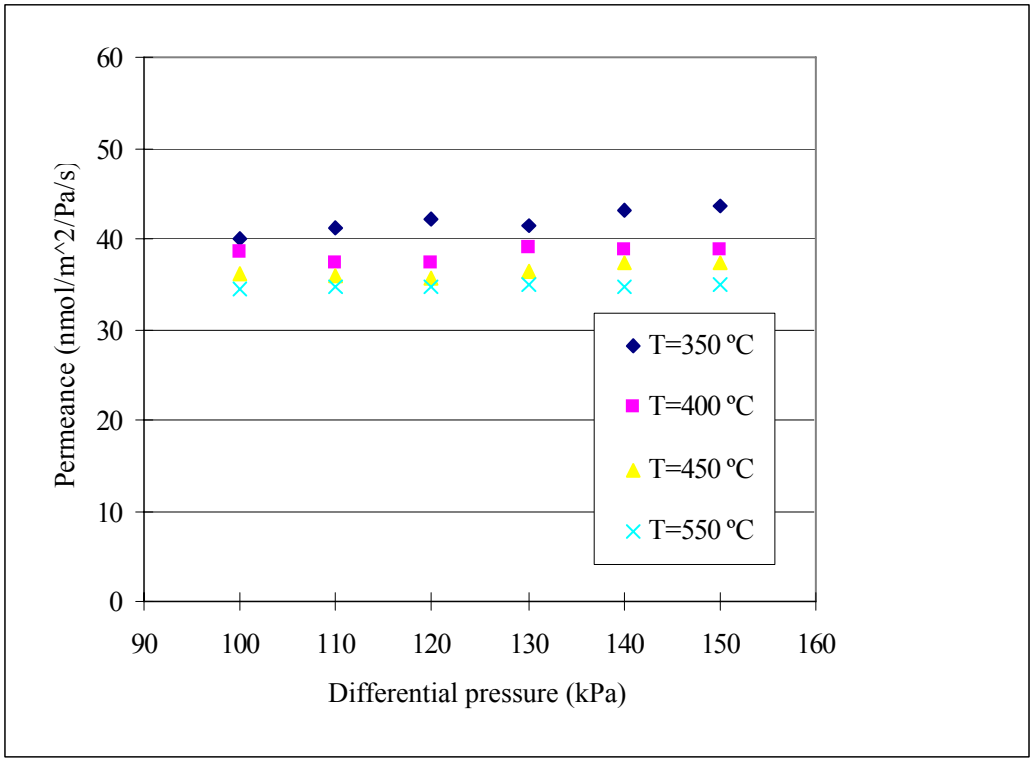


**Figure 5.2: Effect of pressure on $N_2$ permeance for a 1.79 µm Pd film (4/17)**

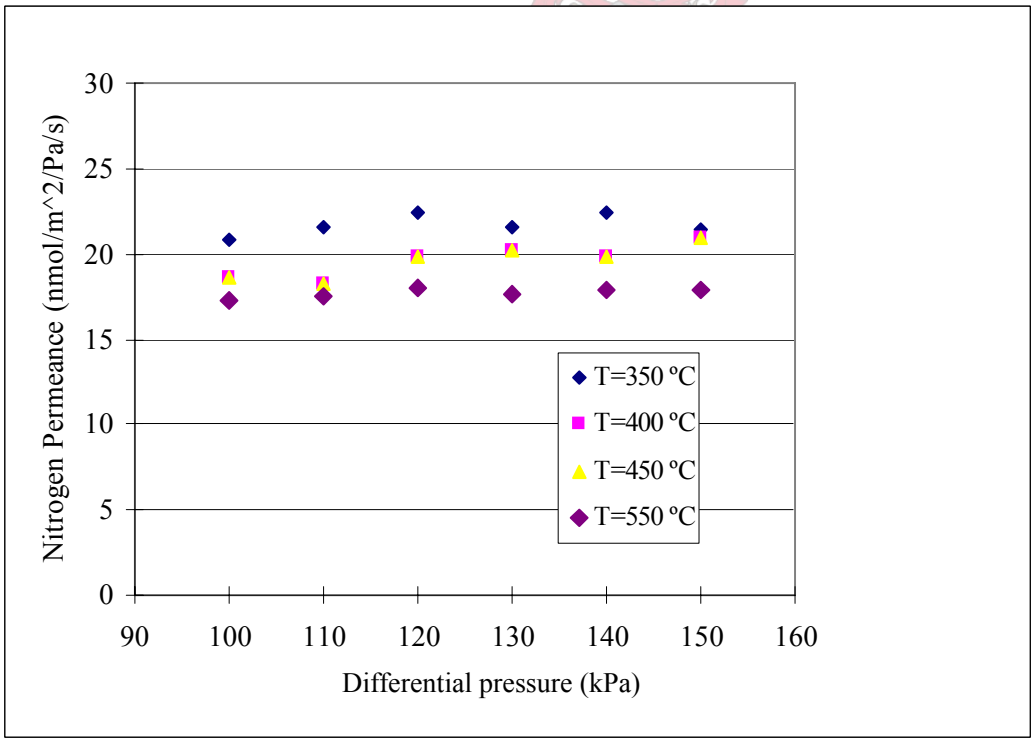


**Figure 5.3: Effect of pressure on $N_2$ permeance for a 2.92 µm Pd film (1/17)**

### 5.2.1.2 Hydrogen permeation tests

The value of n (pressure exponent) in the flux equation (6.1) was calculated for every membrane and results are listed in Appendix B. The $R^2$-value is an indication of the fit between the measured

and calculated data of n. A value close to 1 indicates a very good fit.

In this study, the value of n was close to 1. The $R^2$-values were also found to be close to 1, indicating that the calculated and measured values were in a good agreement. Dittmeyer et al. (2001) showed that membranes thinner than 4–5 µm show hydrogen pressure exponents close to 1. This indicates that step (b) or (c) (see section 5.1) is the rate-determining step. Sievert's law, where n = ½, is not applicable to the thin films synthesised in this study. Diffusion is not the rate-limiting step.

The hydrogen permeance of membranes (4/17) and (6/17) (Figures 5.4 and 5.5) did not vary considerably with pressure. The film thickness and the permeance temperature have a significant effect on the hydrogen permeance as will be discussed in the next sections.

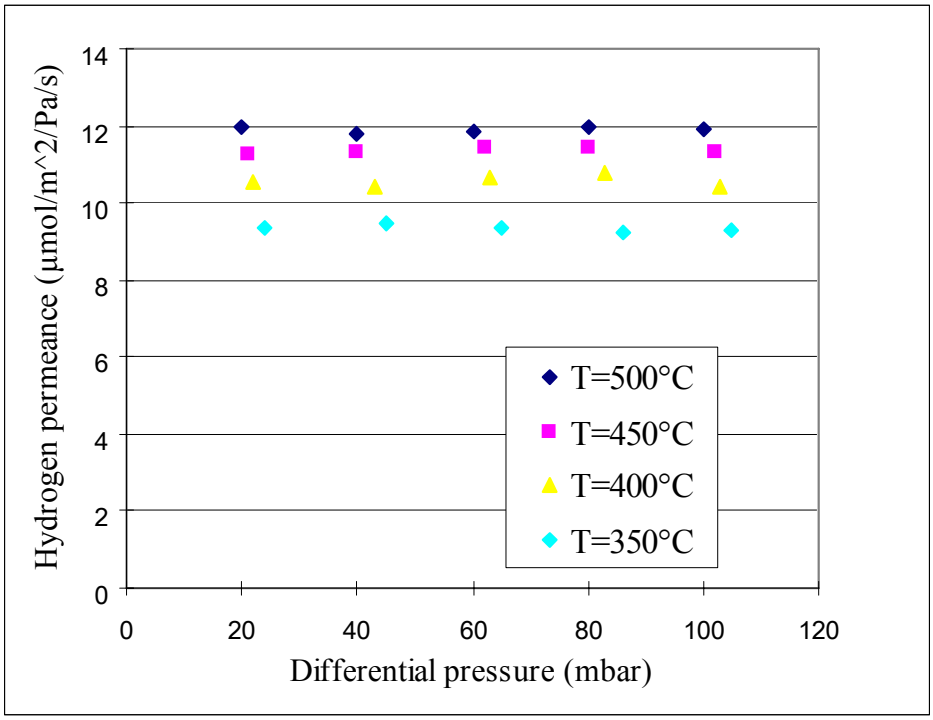


**Figure 5.4: Effect of pressure on $H_2$ permeance for a 1.79 micron Pd film (4/17)**

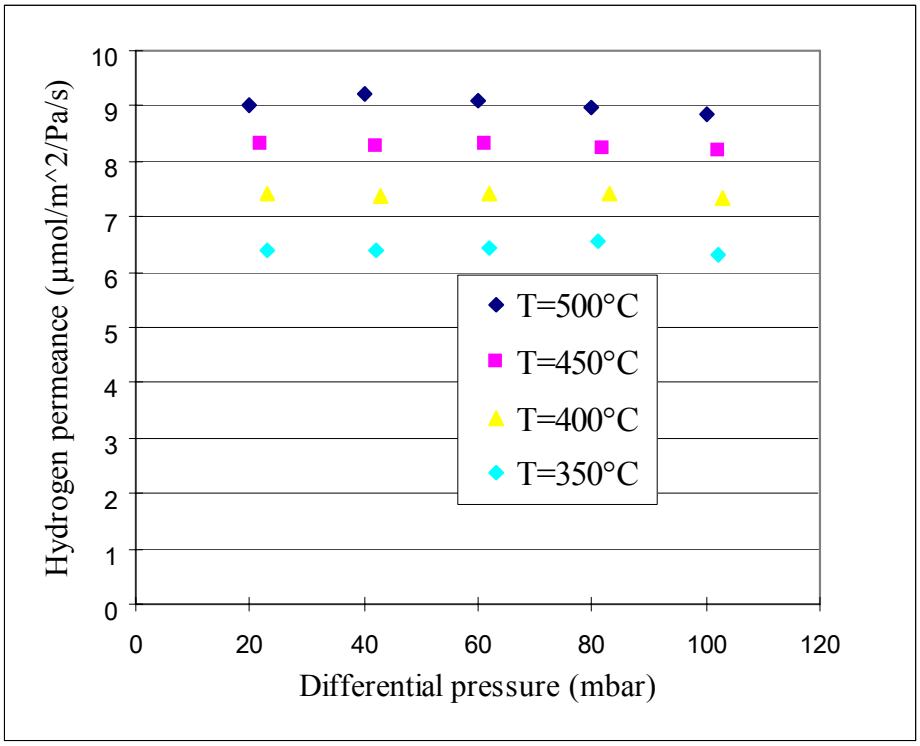


**Figure 5.5: Effect of pressure on $H_2$ permeance for a 3.96 micron Pd film (6/17)**

### 5.2.2 THE EFFECT OF TEMPERATURE ON PERMEANCE

If the flow through a membrane is Knudsen flow, the flux through the membrane must decline when the temperature increases (see Equation 2.1 in section 2.4.1).

In section (5.2.1) pressure data for nitrogen permeance suggested that Knudsen flow might have been the mechanism of nitrogen transport through the defects in the Pd film. This indicated that the defects were in the lower nanometre range. In the case of all the Pd films, the nitrogen permeance declined with an increase in temperature (see Figure 5.6 for a typical example). The temperature data confirmed that Knudsen flow dominated when nitrogen passed through the palladium film defects. The reason for the decline in permeance was that the greater vibrational energy of the $N_2$ molecules at the higher temperature resulted in more resistance to flow through tiny pores and thus a decrease in permeance.

Hydrogen temperature data was fitted to the Arrhenius equation (5.2). Arrhenius parameters for each film are listed in Appendix B. The high $R^2$-values of the Arrhenius fits indicate that the data fitted the equation well. The hydrogen permeance increased with temperature, as predicted by equation (5.2). Figure 5.7 shows higher hydrogen permeance as the temperature increases (as a function of differential pressure).

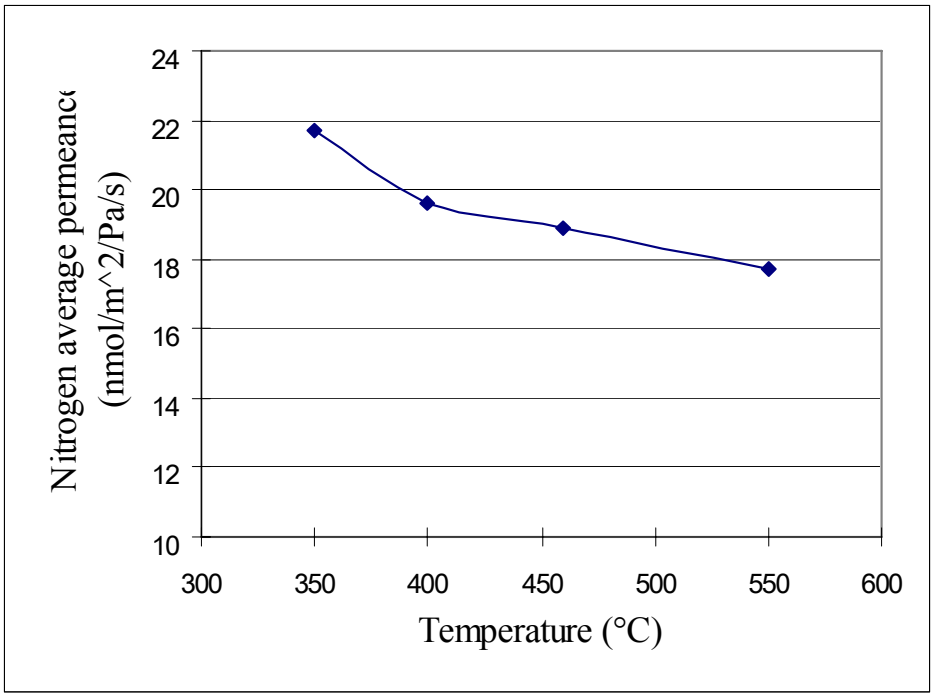


**Figure 5.6:** **Effect of temperatures on $N_2$ average permeance for a 2.92 µm Pd film (4/17)**

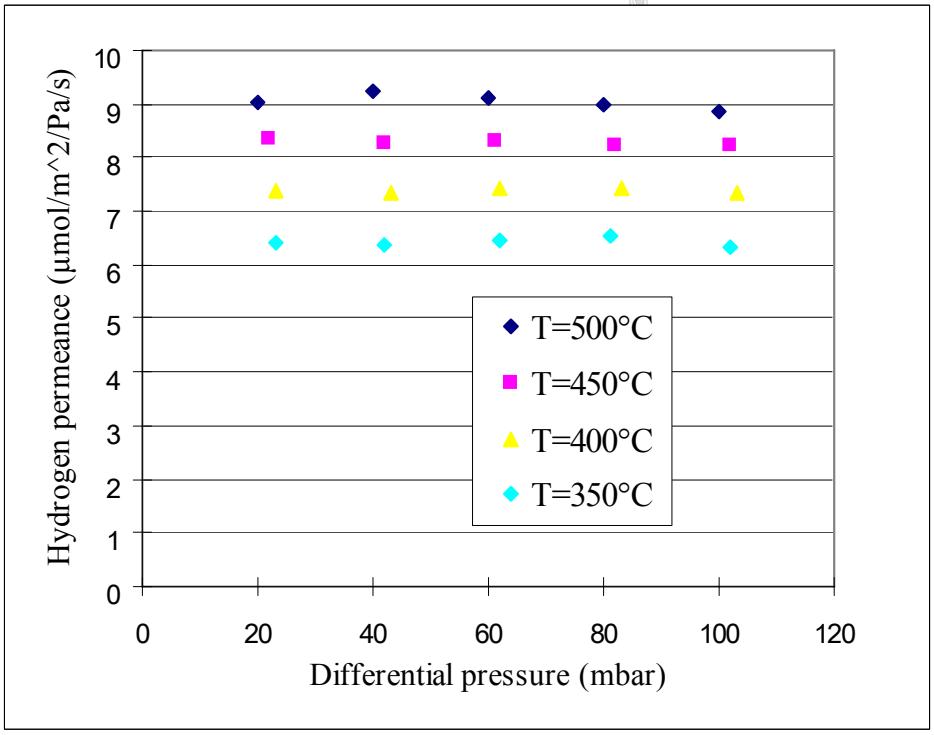


**Figure 5.7:** **Effect of temperature on $H_2$ permeance for a 3.96 µm Pd film (6/17)**

### 5.2.3 THE EFFECT OF FILM THICKNESS ON PERMEANCE

The hydrogen permeance should be inversely proportional to the Pd film thickness (see Equation 2.8 in section 2.4.5)

$$P_m = \frac{P_{er}}{l} \qquad (2.8)$$

There is a decrease in hydrogen permeance with an increase in film thickness. The decrease in permeance was not directly proportional to the inverse thickness. The reason for this is that the model equations (2.8) were formulated for thick foils exceeding the microns range. In this study, Pd films ranged from 1.72 to 3.96 μm, and it is assumed that the surface morphology and structure have more influential effects than film thickness. Therefore, this caused deviation from the model equations.

Nitrogen permeance through Pd film generally decreases with an increase in Pd film thickness, due to the fact that the thicker Pd films have fewer defects which nitrogen can flow through.

### 5.2.4 MEMBRANE SELECTIVITY

After $N_2$ and $H_2$ single gas testing, selectivities of Pd composite membranes can be calculated according to equation (5.3). The selectivity of the eleven Pd composite membranes tested at all the temperatures remained above 150, which is an indication of very good Pd composite membranes. Membrane (4/30) was prepared without performing post-cleaning after the electroless plating. It had a low selectivity of 80 (see section 4.7).

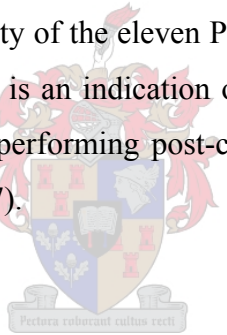


## 5.3 SUMMARY

In this study, Pd films with thicknesses from 1.7 to 4 μm were deposited on the inside layer of asymmetric α-alumina membranes (claimed pore diameter of 200 nm pore size, Pall Exekia). Hydrogen permeances of the Pd films varied between 4 and 15 μmol/($m^2$.Pa.s) at temperatures from 330 °C to 550 °C. Hydrogen to nitrogen selectivity was ≥ 150 for all membranes tested.

Hydrogen permeance fitted the flux equation well, with the permeance constant at different differential pressures. This implied a n-value of 1 in the flux equation. Temperature data fitted the Arrhenius equation very well. For the majority of the membranes, nitrogen flow through defects in the films showed signs of Knudsen flow.

Pd composite membranes were prepared on α-alumina ceramic membranes via the modified electroless plating technique in this study. The membrane hydrogen permeability of the Pd composite membranes (at a range of 4.5-12 μmol/$m^2$/Pa/s) and hydrogen/nitrogen permselectivity

(average permselectivity ≥ 150) were achieved in this study. The permselectivities of membranes (1/30), (3/30), (6/30) and (6/17), to which a modified heat treatment method was applied, were superior to Keuler's membranes, which were subjected to the previous heat treatment method (average permselectivity ≥ 100).

Pd composite membranes (1.4-4 μm thick) prepared on α-alumina ceramic membranes via the modified electroless plating technique in this study are of a superior quality of high membrane permeability and selectivity. However, the rate limiting step of the $H_2$ permeance through the Pd films thinner than 4 μm needs further investigation.

# CHAPTER 6: MEMBRANE SURFACE CHARACTERISATION

In this chapter, the results and discussion of membrane surface characterisations are presented. In section (6.1), Scanning Electron Microscopy (SEM) analysis is discussed to examine the morphology of the palladium membrane and to determine the film thickness. Additionally, Energy Dispersive Detectors (EDS) analysis is presented to investigate the composition of the palladium composite membrane. Section (6.2) presents the results of Atomic Force Microscopy (AFM) to study the surface morphology, surface roughness, and crystal size of the palladium membrane. Finally, in section (6.3), the BET (Brunauer-Emmett-Teller) analysis is presented to investigate the porosity and pore distribution of the palladium membrane. Section (6.4) focuses on results and discussions of X-Ray Diffraction (XRD) analysis concerning the composition and the crystalline of the palladium membrane.

## 6.1 SEM AND EDS

SEM (Scanning Electron Microscopy) with EDS (Energy Dispersive Detectors) was performed in the Department of Geology, University of Stellenbosch, to study the surface morphology and the impurities of the Pd composite membrane, and determine the Pd film thickness.



### 6.1.1 SEM, EDS AND PREPARATIONS OF SAMPLES

The Leo 1430VP Scanning Electron Microscope is fitted with Backscatter, Cathodoluminescence, Variable pressure, Cryo stage and Energy Dispersive detectors (EDS) and a Link EDS system and software for microanalysis and qualitative work. The system is designed to do high-resolution imaging, quantitative analyses with errors ranging from 0.5 to 0.2 wt % on the major elements and imaging of soft biological samples under variable pressure conditions. Quantitative analyses are performed with an accelerating voltage of 20 kV, beam current of 1.5 nA, spot size of 473 and a working distance of 13mm. The ZAF (Zero Alignment Feature) procedure is applied for inter-element effects. Normal SEM images and SEM images with backscatter (different elements have lighter or darker colour) were both taken.

The Energy Dispersive quantitative microanalysis of an unknown sample is based on the comparison of the unknown data (spectra) to data from standards. The sample for EDS is the same as for SEM analysis. This technique could recognise the composition of the tested samples.

Results were given in element wt % or compound (oxides/sulphides, etc) wt%. The main impurity discovered in the Pd membranes was carbon (originating from the EDTA used during Pd electroless plating) and sometimes, a little amount of Sn, (introduced during pretreatment).

To take a top view SEM image, the palladium membranes were first cut into small pieces with a surface area of 0.5 $cm^2$ using a diamond saw. The samples were mounted on aluminium stubs and then plated with gold to improve surface conductivity and prevent surface charging. For cross-section views, the membrane pieces were set into a resin disk and polished to expose the fresh cross section to a final surface roughness of 0.1 mm.

The samples were cut from five positions on the palladium composite membrane. (See Figure 6.1) This was to analyse the quality of the palladium films concerning its different positions.

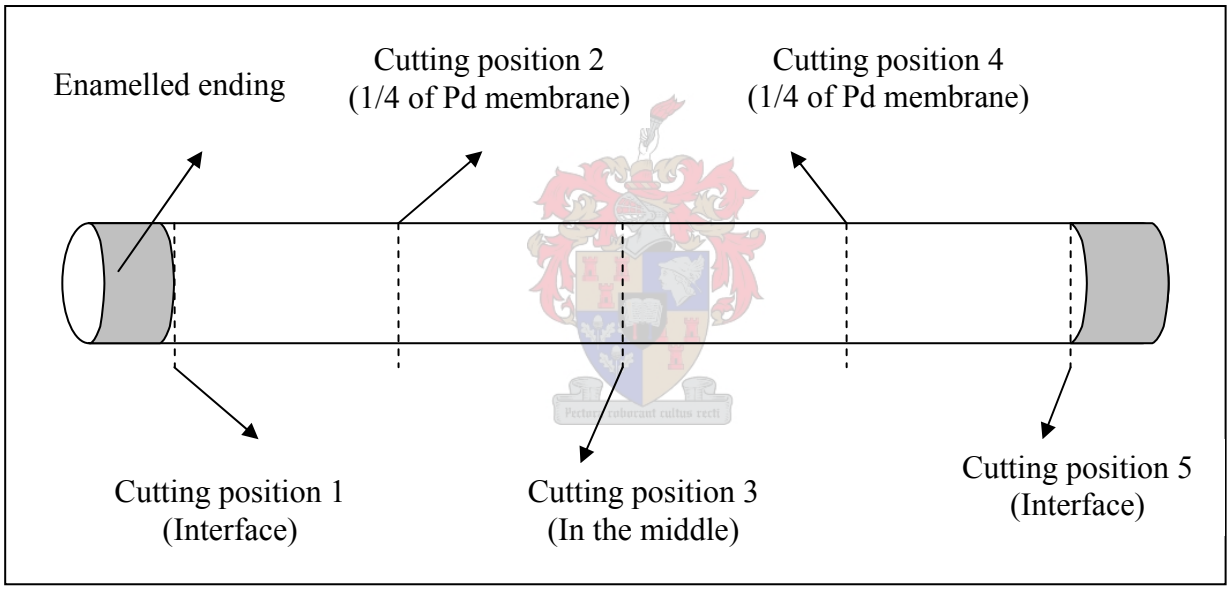


**Figure 6.1: Preparations of the palladium composite membrane samples for SEM and EDS**

The EDS analysis setup was attached to the SEM equipment; therefore, both of the two analyses were performed simultaneously.

### 6.1.2 COMPOSITIONS AND IMPURITIES

Membrane (6/17) contained four Pd layers. A heat treatment was performed after the fourth layer had been plated. Figure. 6.2 shows the SEM image (with backscatter) of Pd composite membrane (6/17) (after heat treatment). Apparently, the defects occurred during heat treatment. The holes of metal surface (dark spots) were the carbon positions. After the carbon was removed during the heat

treatment, the support membrane layer containing aluminium was exposed. This was confirmed by the EDS image in Figure 6.3 (Au was plated on the samples to improve surface conductivity and prevent surface charging before the SEM analysis). The defects decreased the permeability of the palladium membrane and caused the instability of the Pd composite membrane. Carbon was also discovered on membranes (2/17), (10/30) and (4/17). Therefore, the carbon impurity must be removed to increase the membrane permeability. Future research regarding the membrane cleaning after the electroless plating is recommended. Alternatively, another method to remove the carbon is to apply heat treatment directly after each Pd layer was plated. Each additional Pd layer, thus, can replenish the holes that carbon formed on the former Pd layer during the heat treatment.

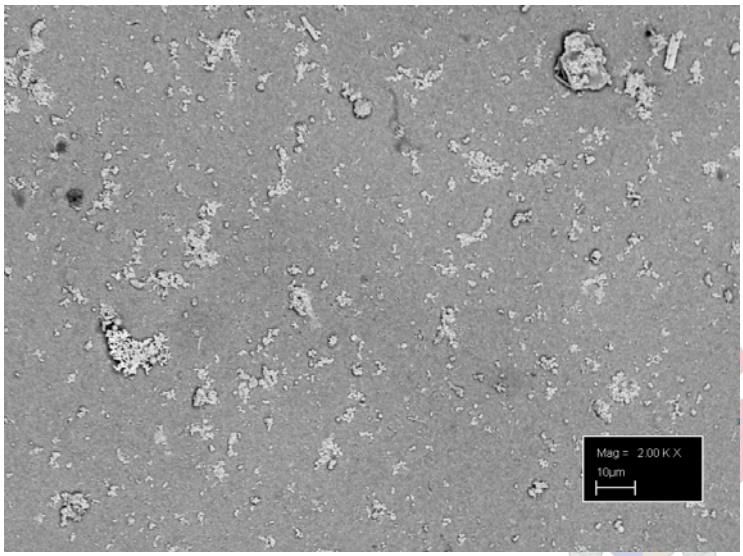


**Figure 6.2: SEM image (with Backscatter) of membrane (6/17) after annealing, 2.00 KX**

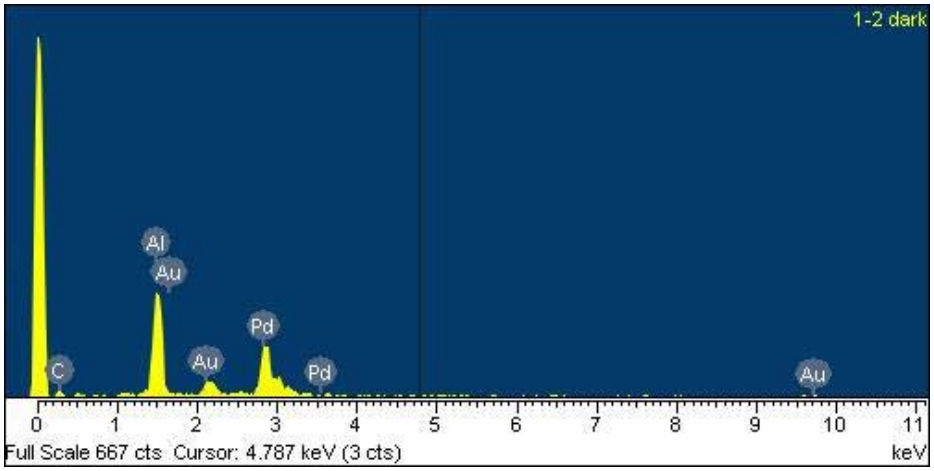


**Figure 6.3: EDS image of membrane (6/17) after annealing (black spots)**

### 6.1.3 SURFACE MORPHOLOGY

The surface morphology around the whole surface of the Pd composite membrane was examined (from position 1 to position 5). Both Figure 6.4 (taken from position 3) and Figure 6.5 (taken from position 2) are the normal SEM images of membrane (6/17) relating to Figure 6.1. Figure 6.4 shows dense, smooth and pure Pd layers confirmed by the EDS image in Figure 6.6. The membrane consisted of a smooth surface and a uniform distribution of palladium particles. However, Figure 6.5 shows dense smooth Pd layers with more impurities and defects proved by the EDS image in Figure 6.8. Several other membranes were also analysed. The results showed that the Pd composite membranes had a smoother and purer Pd film in the middle of substrate (from position 2, position 3 to position 4) than near the interface (from position 1 to position 2, as well as from position 4 to position 5). This phenomenon could be explained in two ways. One was that the support membranes had a coarse surface near the interface (see Figure 6.1, from position 1 to position 2, and from position 4 to position 5) than in the middle of the substrates (from position 2, position 3 to position 4). Therefore, more Pd should be covered near the interface. Another way was that during the electroless plating, the vacuum difference applied on the shell side of the plating reactor might not be the same along the whole length of the membrane due to the fact that the plating reactor was tilted by 45° in a beaker during the plating (see Figure 3.13). Further investigations are recommended to prove these assumptions.

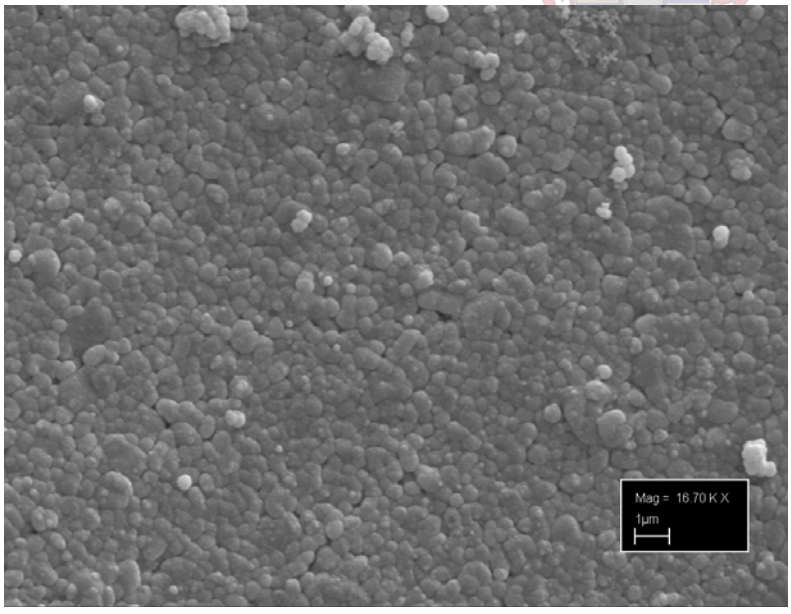


**Figure 6.4: SEM image of membrane (6/17) (position 3) after annealing, 16.70 KX**

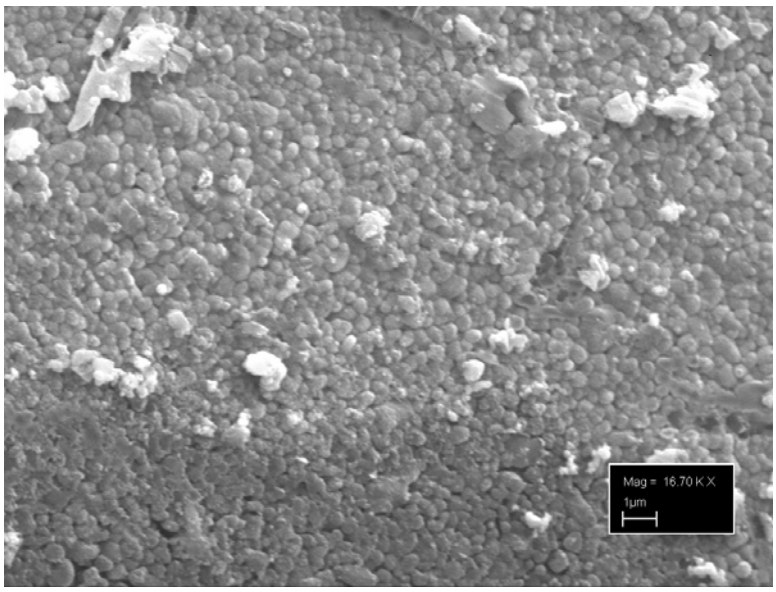


**Figure 6.5:** **SEM image of membrane (6/17) (position 2) after annealing, 16.70 KX**

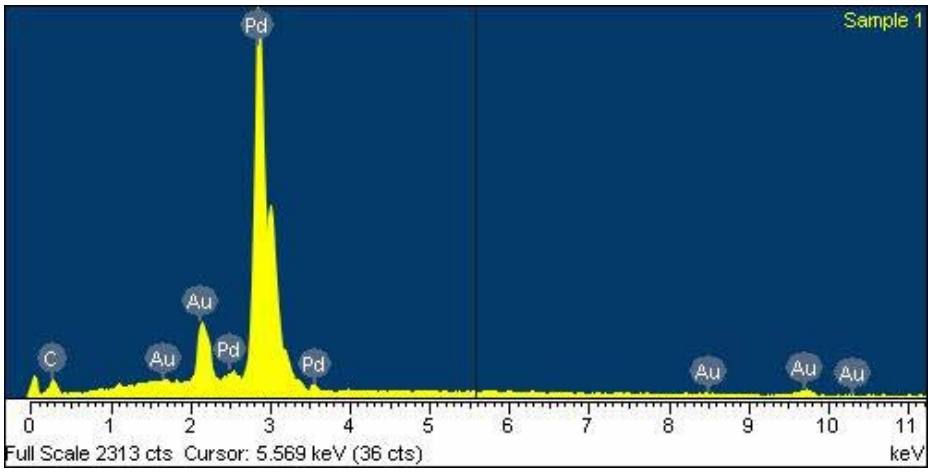


**Figure 6.6:** **EDS image of membrane (6/17) (position 3) after annealing (Pd surface)**

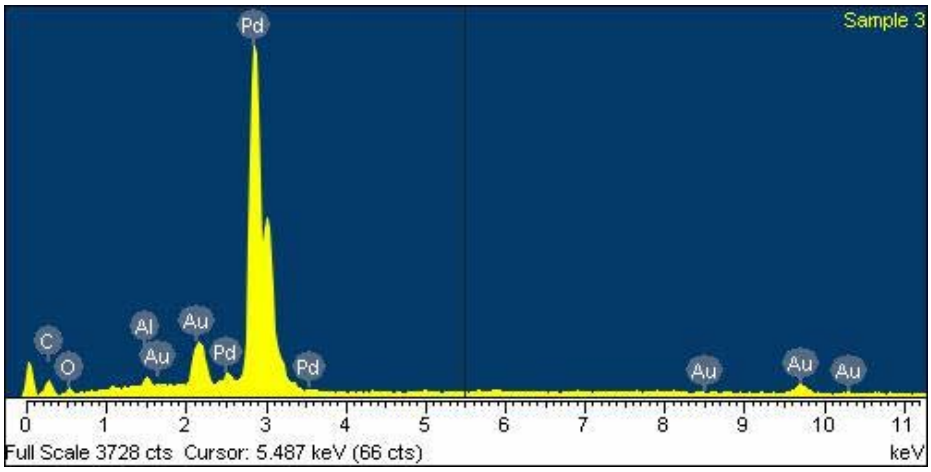


**Figure 6.7:** **EDS image of membrane (6/17) (position 2) after annealing (Pd surface)**

Figure 6.8 and Figure 6.9 show membrane (6/30) before and after heat treatment. Clearly, after the annealing, the palladium crystals agglomerate together and form into a dense and even layer. Additionally, during the annealing, the impurity of carbon was removed to form a pure Pd film.

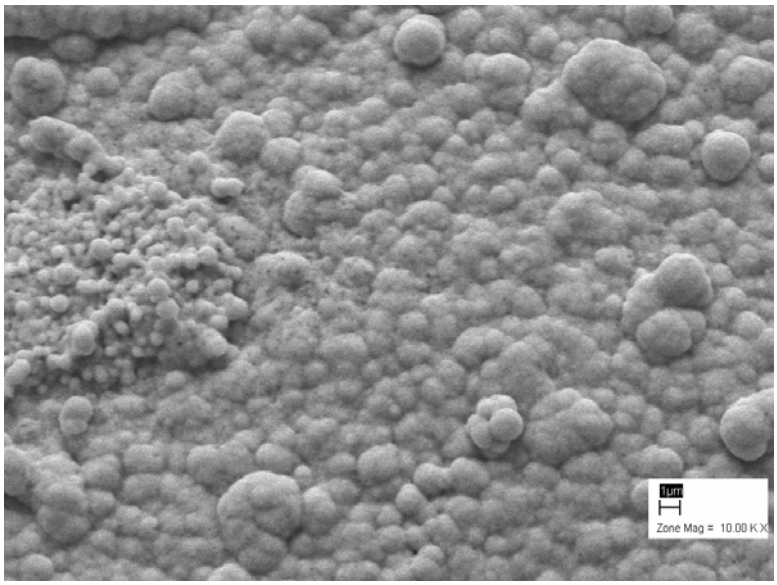


**Figure 6.8: SEM image of membrane (6/30) before annealing, 10.00 KX**

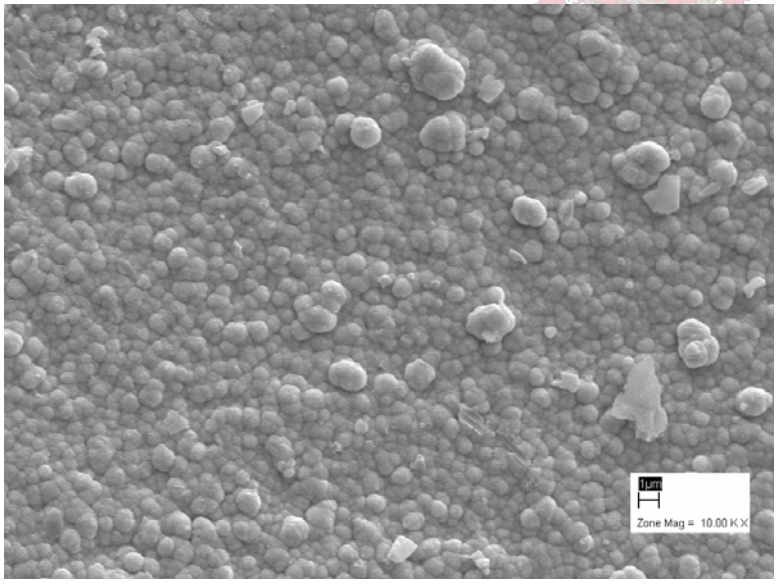


**Figure 6.9: SEM image of membrane (6/30) after annealing, 10.00 KX**

### 6.1.3 GRAIN SIZES AND COMPACTNESS

Figure 6.10 is the normal SEM image of membrane (4/17), which contained two Pd layers. Figure 6.11 is the normal SEM image of membrane (1/17), which contained three Pd layers. Apparently, the grain sizes of membrane (1/17) were much smaller than those of membrane (4/17), and the Pd

layer of membrane (1/17) was more compact. Concerning the membrane permselectivity, membrane (1/17) (average permselectivity of 276.5 from 350 °C to 550 °C) had better permselectivity than membrane (4/17) (average permselectivity of 261.75 from 350 °C to 550 °C). It could be explained that a better membrane permselectivity could be obtained when the membrane has more Pd layers and smaller Pd grain sizes and more compact Pd layers.

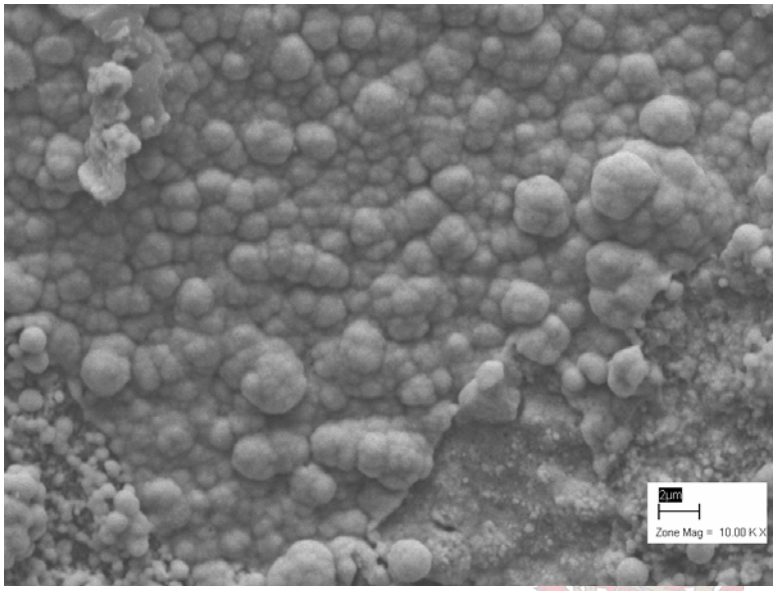


**Figure 6.10: Top view (SEM image) of membrane (4/17), 10.00 KX**

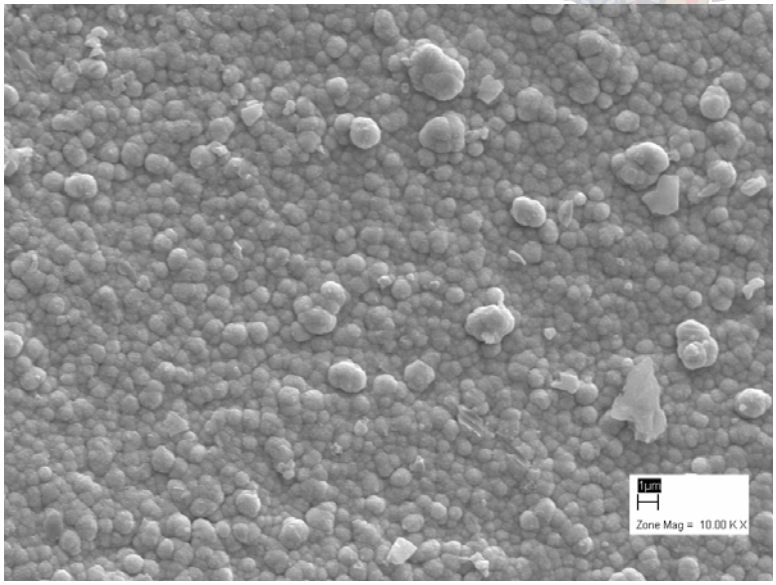


**Figure 6.11: Top view (SEM image) of membrane (1/17), 10.00 KX**

Therefore, the surface morphology and the Pd grains sizes clearly influence the quality of the Pd membrane, but the impurities, defects and Pd film thickness have a greater influence on the permselectivity of the Pd composite membrane.

### 6.1.4 PALLADIUM FILM THICKNESS

The SEM analysis was performed on twelve palladium composite membranes (except membrane 5/17) to determine the membrane thickness. Discussions concerning the theoretical thicknesses obtained by calculations, and the real thicknesses of the palladium membranes as measured by SEM are presented in this section.

#### 6.1.4.1 Theoretical thicknesses of the palladium films

Assume that the palladium film was unwrapped. Take membrane (1/17) for example. (See Figure 6.12 and Figure 6.13) Consider the palladium film as an even flat layer, thus, when it was unwrapped, it was a very thin cubic layer. Since the weight of the palladium composite membrane was recorded after the plating, the weight gain between the blank support membrane and the palladium composite membrane was equal to the mass of the palladium metal film coated on the support (i.e. the mass of the cubic palladium layer). The average theoretical thickness of the Pd film was calculated by dividing the total weight gain by the plated surface area and the density of the Pd metal.

The thicknesses of the twelve palladium films (except membrane 5/17, which was broken) are outlined in Table 6.1.

Sample calculations of the theoretical Pd film thickness for membrane (1/17) are given in the next paragraph:

$$\because \Delta m = m_2 - m_1 \tag{6.1}$$

And $$\because \Delta m = l \times \pi \times D_i \times (L - L_e) \times d_{Pd} \tag{6.2}$$

$$\therefore l = \Delta m / (\pi \times D_i \times (L - L_e) \times d_{Pd}) \tag{6.3}$$

Therefore, the palladium thickness is:

$l = 98.8mg / (3.14 \times 7mm \times 128mm \times 12023 \times 10^{-3}\, mg / mm^3 = 0.00292$ mm = 2.92 μm

| | | | |
|---|---|---|---|
| $l$ | ------- | Thickness of palladium layer | [m] |
| $d_{Pd}$ | ------- | Density of palladium (12023 kg/m$^3$) | [kg/m$^3$] |
| L | ------- | Length of support membrane | [m] |
| $L_e$ | ------- | Total length of both enamelled endings | [m] |

$D_i$ ------- Inner diameter of membrane tube [m]

m ------- Mass of Pd composite membrane [g]

**Table 6.1: Theoretical thicknesses of the palladium membranes**

| Identification of the membrane | Weight gain (mg) | Membrane layers | Calculated thickness of Pd (µm) |
|---|---|---|---|
| **Membrane Set 1** | | | |
| **1/30** | 5.4+31+30.6+40.2=107.2 | 3 | 3.37 |
| **2/30** | 4.9+13+20.9+41.8=80.6 | 3 | 2.54 |
| **3/30** | 5.4+31+30.6+40.2=107.2 | 3 | 3.37 |
| **4/30** | 4.2+30+20.5=54.7 | 2 | 1.72 |
| **5/30** | 1.1+28+35=64.1 | 2 | 1.89 |
| **6/30** | 1+29+32=62 | 2 | 1.94 |
| **10/30** | 1+41+40=82 | 2 | 2.59 |
| **12/30** | 1+32+36=69 | 2 | 2.18 |
| **Membrane Set 2** | | | |
| **1/17** | 3.8+31+34+30=98.8 | 3 | 2.92 |
| **2/17** | 1.1+31.8+23+30=85.9 | 3 | 2.54 |
| **4/17** | 1.5+31+29=60.5 | 2 | 1.79 |
| **6/17** | 6.9+32+31+34+30=133.9 | 4 | 3.96 |

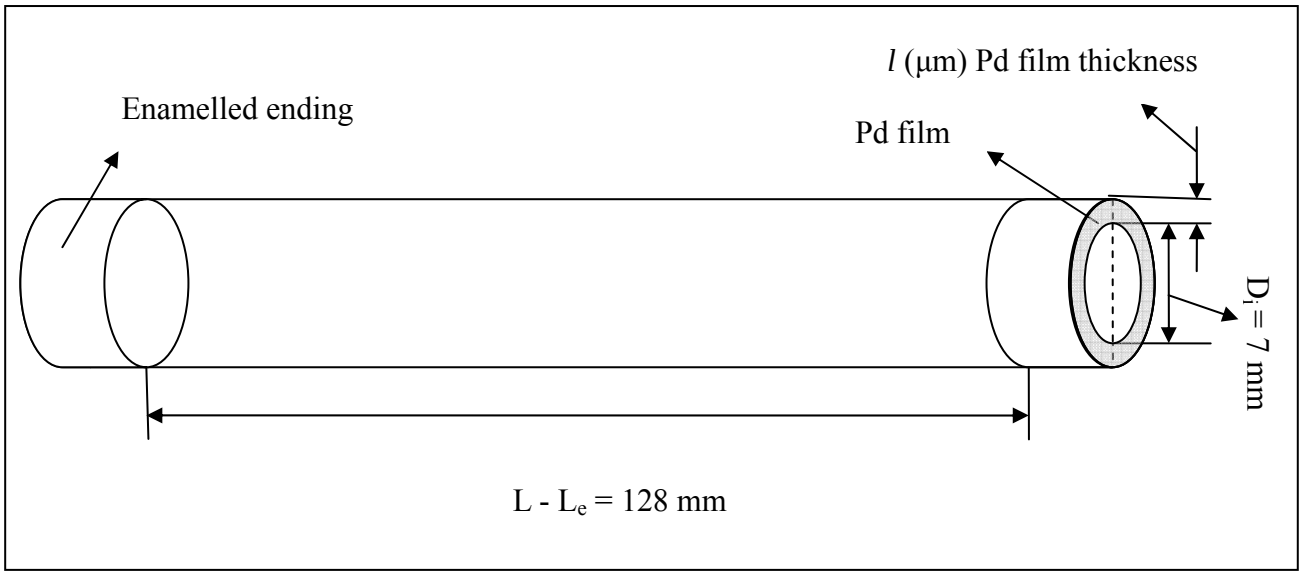


**Figure 6.12: The palladium film plated inside the support membrane (1/17)**

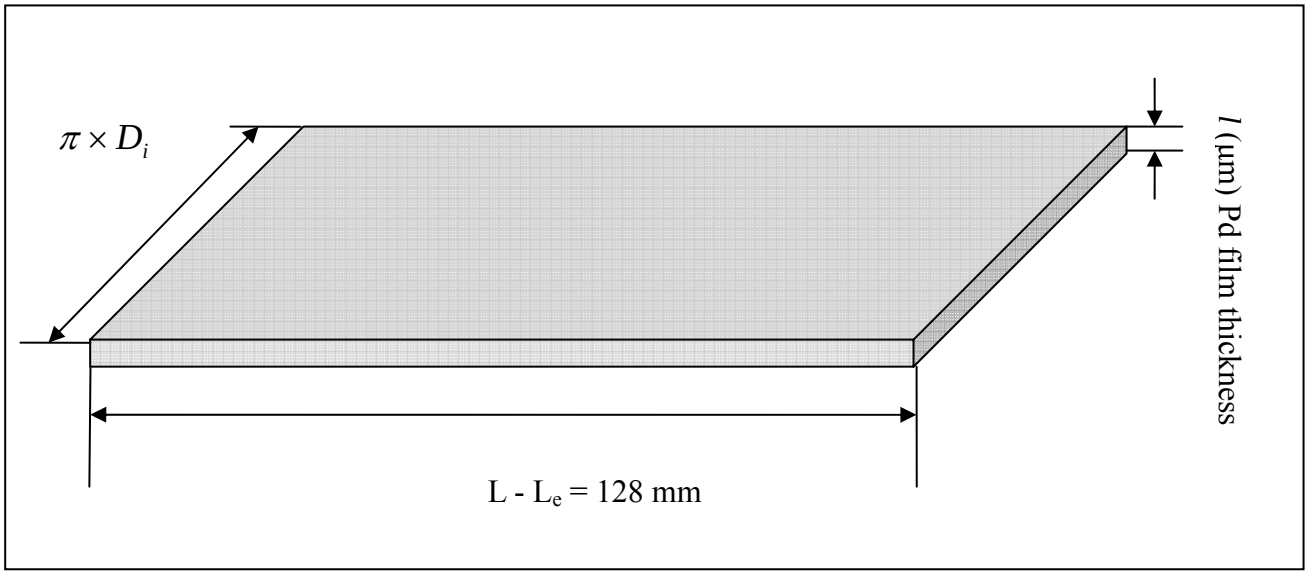


**Figure 6.13: The theoretically unwrapped palladium film of membrane (1/17)**

### 6.1.4.2 Thicknesses of the palladium membranes measured by SEM

The side view image of membrane (2/17) (Figure 6.14) clearly shows a bright Pd layer on the alumina support. Three Pd layers were applied on membrane (2/17). After application of the first layer, the membrane was tested, the second and third layers were applied and the membrane tested again. The combined thickness of the three layers should be about 2.54 microns (obtained from calculations). Figure 6.14 shows, however, a total thickness of closer to 5 microns. This was the only membrane that showed deviation between the calculated Pd thickness and the SEM determined Pd thickness. It was assumed that some impurities, such as carbon, Sn, or dust, might have increased the membrane thickness. Alternatively, it could assume that the support membrane (2/17) had a coarser surface than any other support membranes so that a poorer Pd film with uneven thickness was deposited due to the nature of electroless plating technique.

.

For all the other membranes tested by SEM, the results of the calculated thickness and the SEM determined thickness were in a good agreement. Take membrane (1/17) as an example. The calculated thickness of membrane (1/17) (2.92 microns) was in a good agreement with the SEM determined thickness (from 2.5 and 3.0 microns). (See Table 6.2). Cross view SEM image in Figure 6.15 showed a very dense Pd layer on top of the 200 nm α-alumina support membrane. The top view image of membrane (1/17) (Figure 6.16) and the good permeability and selectivity data both confirmed this (See Appendix B).

Figure 6.17 and Figure 6.18 are both cross views of the Pd film thickness of membrane (3/30). Figure 6.17 shows how the palladium nuclei penetrated into the pinholes of the support membrane. This could be due to the vacuum pulled on the shell side of the plating reactor, which assisted the Pd plating solution penetrating into the pinholes and reducing the defects of the support membrane. However, this decreased the film thickness in some area of the Pd membrane and made it thinner than the theoretical data which was calculated according equation (6.3). Figure 6.18 was also taken for the cross section of another sample from membrane (3/30), and this illustrated an even Pd layer. Thus, different parts of the Pd membrane had different Pd film thicknesses due to the different morphology of the substrates.

**Table 6.2: Theoretical thicknesses and measured thicknesses of the Pd composite membranes in this study**

| Identification of the membrane | Membrane layers | Calculated thickness of Pd (µm) | Measured thickness of Pd (µm) |
|---|---|---|---|
| **1/30** | 3 | 3.37 | 3.2 |
| **2/30** | 3 | 2.54 | 2.7 |
| **3/30** | 3 | 3.37 | 3.5 |
| **4/30** | 2 | 1.72 | 1.6 |
| **5/30** | 2 | 1.89 | 2 |
| **6/30** | 2 | 1.94 | 2 |
| **10/30** | 2 | 2.59 | 2.7 |
| **12/30** | 2 | 2.18 | 2.3 |
| **1/17** | 3 | 2.92 | 2.8 |
| **2/17** | 3 | 2.54 | 5 |
| **4/17** | 2 | 1.79 | 1.9 |
| **6/17** | 4 | 3.96 | 3.8 |

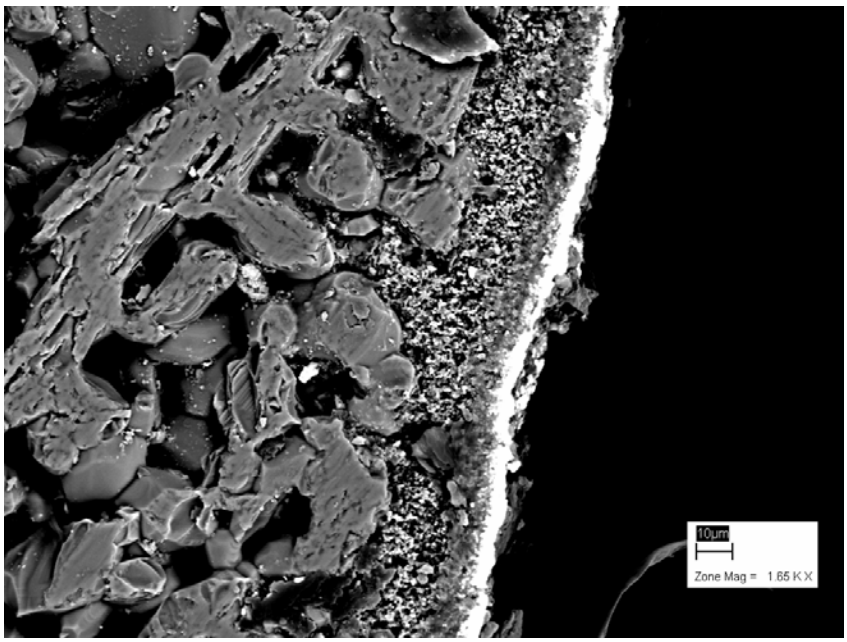


**Figure 6.14: Cross section (SEM image) of membrane (2/17) (1.65 KX)**

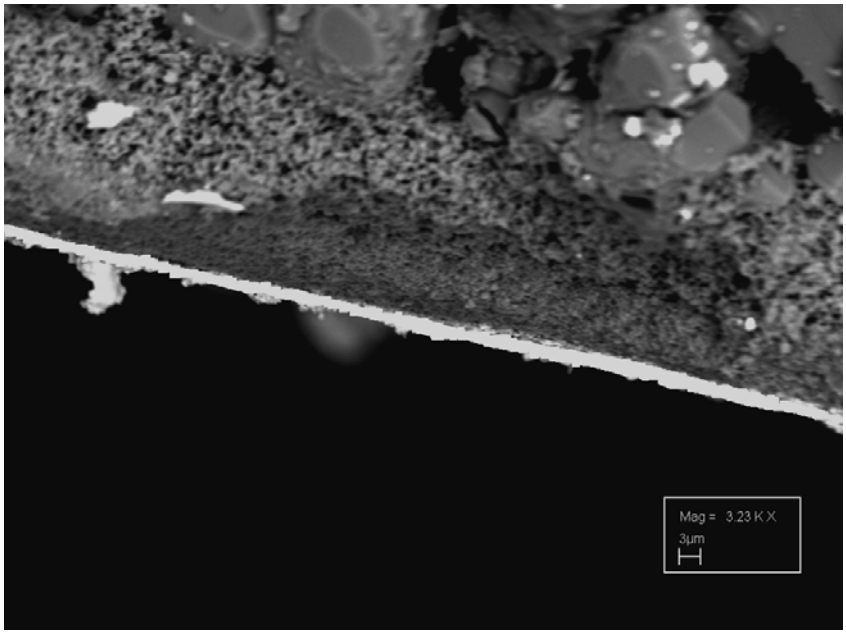


**Figure 6.15: Cross section (SEM image) of membrane (1/17) (3.23 KX)**

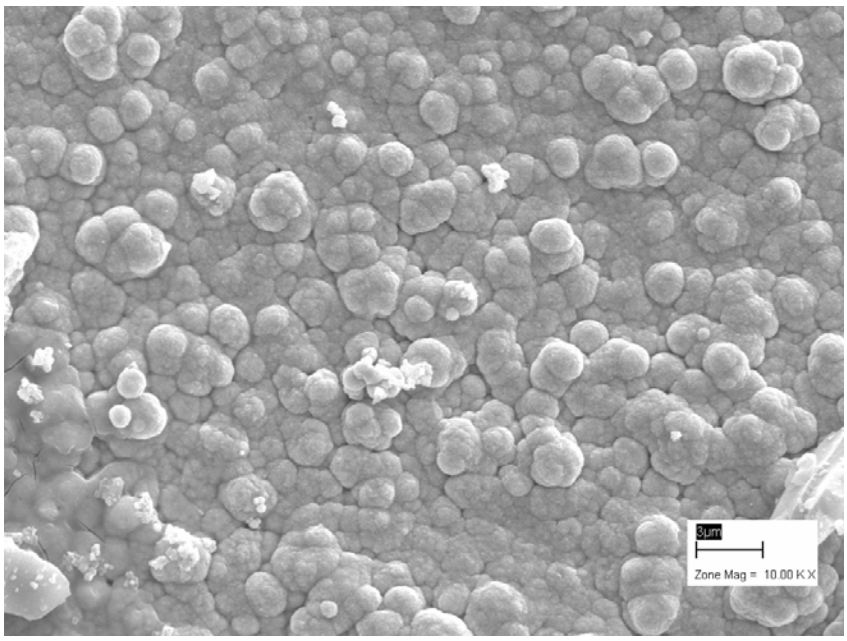


**Figure 6.16: Top view (SEM image) of membrane (1/17), (10.00 KX)**

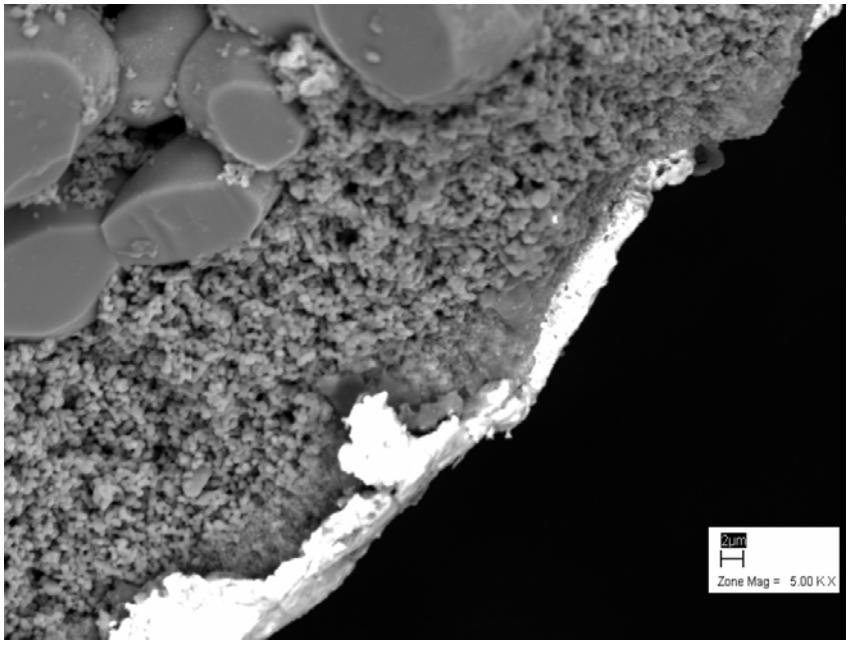


**Figure 6.17: Cross section (SEM image) of membrane (3/30), sample 1, (5.00 KX)**

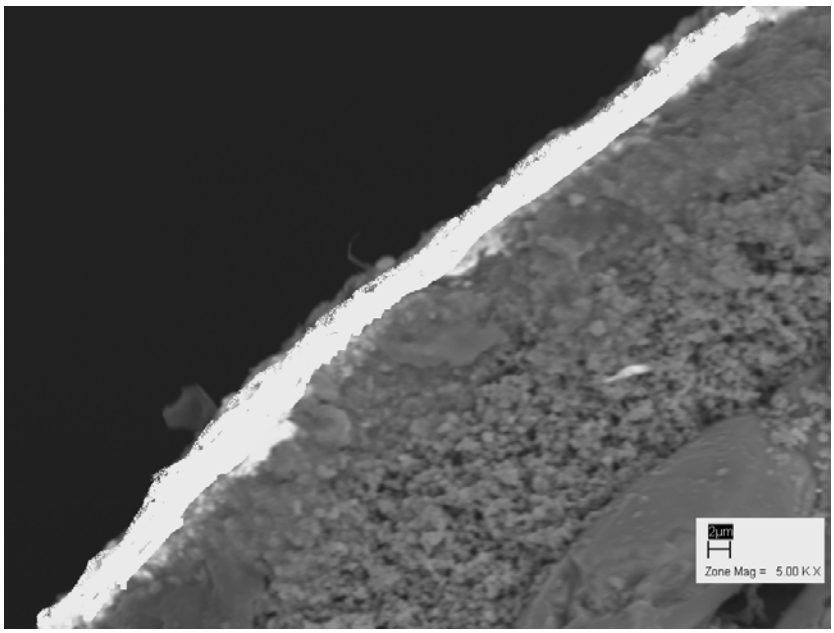


**Figure 6.18: Cross section (SEM image) of membrane (3/30), sample 2, (5.00 KX)**

Additionally, comparing Figure 6.16 and Figure 6.19, which are both under the high magnification of 10.00 KX., it is evident that there were more grain boundaries for the thinner Pd film (membrane 12/30, 2.18 µm) than the thicker Pd film (membrane 1/17, 2.92 µm). This was proved by comparing Figure 6.16 and Figure 6.19

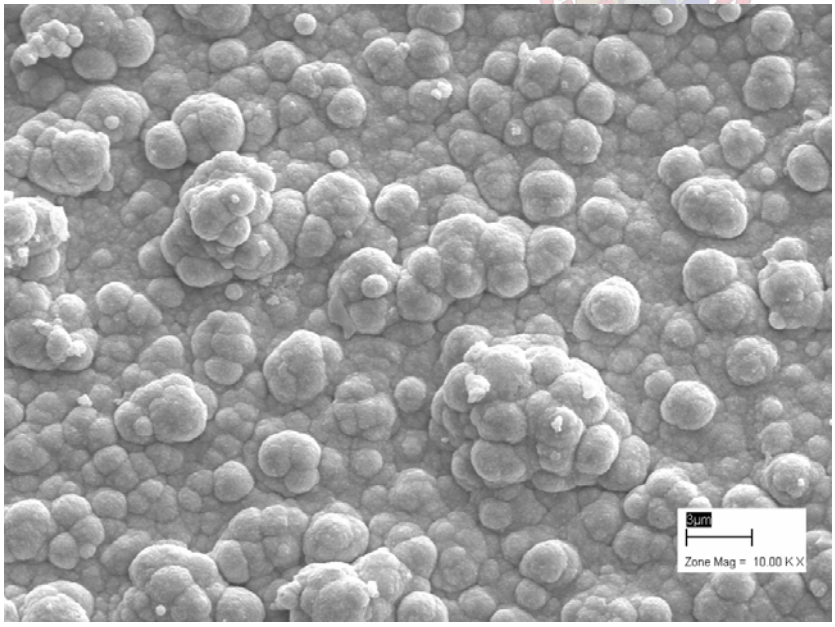


**Figure 6.19: Top view (SEM image) of membrane (12/30), (10.00 KX)**

## 6.2 AFM (Atomic Force Microscopy)

The Atomic Force Microscope (AFM) offers a method for directly observing the two- or three-dimensional structure of membranes. The materials being investigated include thin and thick film coatings, ceramics, composites, glasses, synthetic, and biological membranes, metals, polymers, and semiconductors. The AFM is being applied to studies with phenomena such as abrasion, adhesion, cleaning, corrosion, etching, friction, lubrication, plating, and polishing. By using AFM, one can not only image the surface in atomic resolution but also measure the force at nano-newton scale. The principles on which the AFM works are very simple. An atomically sharp tip is scanned over a surface with feedback mechanisms that enable the piezo-electric scanners to maintain the tip at a constant force (to obtain height information), or height (to obtain force information) above the sample surface (Li, 1997).

The AFM performed in the Department of Polymer Science for this study was a Multimode form Veeco. The analysis was done by non-contact mode without sophisticated sample preparation. The samples preparations were the same as the ones for SEM and EDS. Software was used to analyze the surface roughness. In addition, only the top view section could be analysed by AFM, since the instrument could not scan the cross section.

### 6.2.1 SURFACE ROUGHNESS AND CRYSTAL SIZE

The AFM capability to reconstruct the three-dimensional image of the membrane surface can be exploited to obtain quantitative information about the surface roughness. Figures 6.20, 6.21 and 6.22 show AFM images of the skin layer surface of the Pd composite membrane (3/30) after heat treatment. Nanoscope II software was used to perform a quantitative analysis of the surface roughness.

Figure 6.20 was taken under 10 x10 μm. The surface roughness of the whole area was about 130 nm. All the round crystals had a diameter of 1.5-2 μm. This indicated that the Pd crystals were uniform in size. In addition, the shading in the image represents different heights of the Pd surface. The lighter areas were higher, while the darker areas were lower. This illustrated that the Pd surface was not extremely smooth. The height difference between the highest area and the lowest was approximately 1000 nm.

Figure 6.21 was taken under 4 x 4 μm of the same sample. The small round crystals which grew within the large crystals had a diameter of about 0.15-0.2 μm. This indicated that the membrane had a dense Pd layer with small grain sizes. It is assumed that the small crystals were plated on the

large crystals and agglomerated into the large ones during the heat treatment.

Figure 6.22 provides a clear 3D image of the same sample. Apparently, the surface of membrane (3/30) was not smooth enough. This proved the assumptions made from SEM analysis.

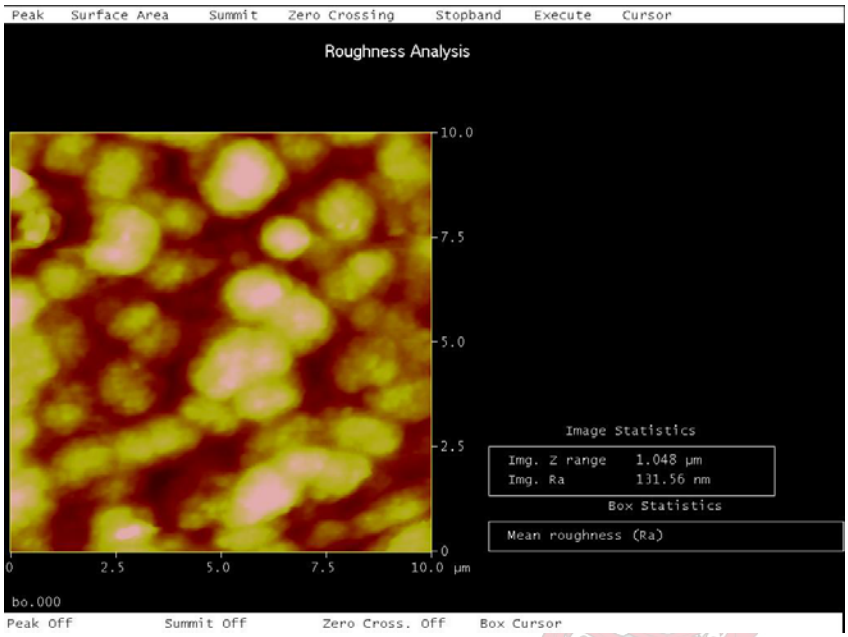


**Figure 6.20: AFM image of membrane (3/30), 10 x 10 µm**

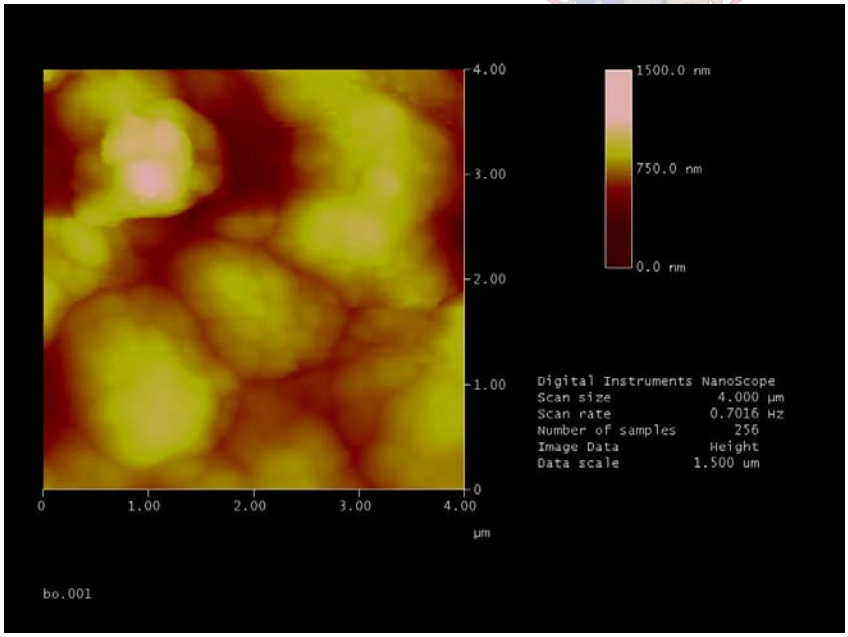


**Figure 6.21: AFM image of membrane (3/30), 4 x 4 µm**

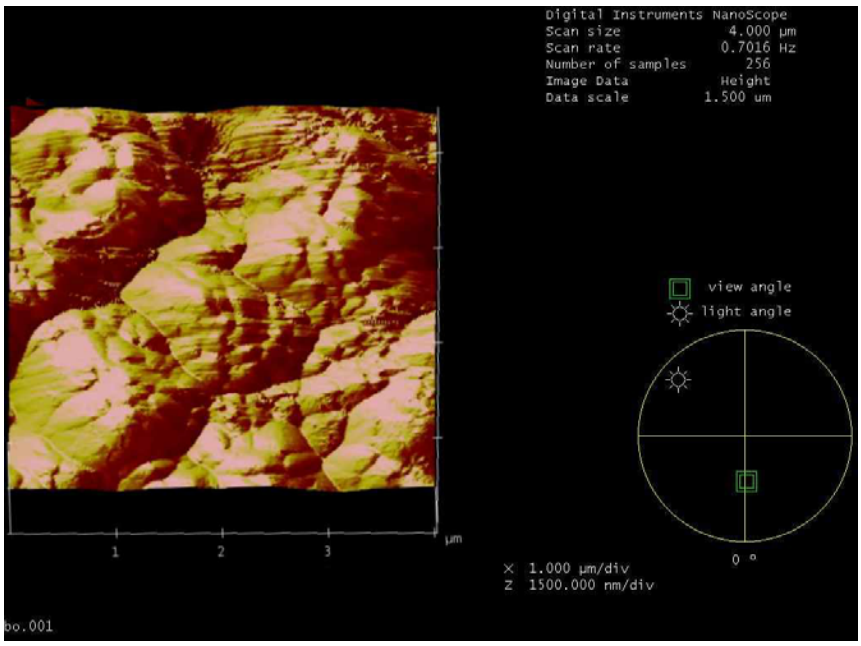


**Figure 6.22: AFM image of membrane (3/30), 3D, 4 x 4 µm**

## 6.3 BET (Brunauer-Emmett-Teller)

BET (Brunauer-Emmett-Teller) analysis for surface area and porosity was applied on membrane (3/30) (with three Pd layers). The sample was 0.8052 g. The surface areas of the samples were measured using nitrogen BET isotherms at 77.35 K on a Micromeritics Gemini 2375 volumetric analyser. Each sample was degassed for 12 h at 573 K prior to measurement. The average pore size distribution of the calcined Pd was calculated using the Barrett–Joyner–Halanda (BJH) model from a 50-point BET surface area plot.

The results of membrane (3/30) are outlined below:

- BET surface area: 0.5501 $m^2/g$
- Single point total pore volume of pores: less than 0.000437 $cm^3/g$
- Average pore diameter (4V/A by BET): 31.7876 Å

The results showed that the Pd composite membrane (3/30) had an average pore diameter of 31.7876 Å, which indicated that the membrane almost had no defects. More analysis of BET is recommended in future work.

## 6.4 XRD (X-Ray Diffraction)

X-ray diffraction (XRD) was performed to study membrane crystal structure and membrane composition.

### 6.4.1 XRD EXPERIMENTAL EQUIPMENT AND SAMPLE PREPARATIONS

A Phillips vertical X-ray diffractometer adapted using Difftech-122D digital control, with Cu Kα radiation and a graphite monochromator is used to record the spectra. A standard silicon aggregate disk is used as a reference for the accurate alignment of the goniometer. The voltage is set at 50 kV and the current at 40 mA. The X-ray powder diffraction with a modified computer-controlled Philips 1410-diffractometer is important for crystal phase identification.

The Pd films were peeled off from the ceramic substrate and ground into powders to prepare the samples for XRD analysis. 0.5 g Pd powder was required for each sample.

### 6.4.2 COMPOSITIONS AND CRYSTAL STRUCTURE

Figures 6.23 and Figure 6.24 show the X-ray diffraction patterns of palladium crystals from membrane (3/30) after heat treatment. Table 6.3 indicated the standard PDF data of palladium. (PDF data is the standard database stored in the XRD machine, referring to crystal patterns of different elements). Table 6.4 and 6.5 shows the data for the two images of membrane (3/30). The data indicated in italics was obtained from the impurity.



**Table 6.3: PDF data for palladium**

| | *hkl* | Angle (2θ) | D space (Å) | Relative Intensity |
|---|---|---|---|---|
| 1 | 111 | 40.119 | 2.2458 | 100 |
| 2 | 200 | 46.659 | 1.9451 | 60 |
| 3 | 220 | 68.121 | 1.3754 | 42 |
| 4 | 311 | 82.100 | 1.1730 | 55 |

**Table 6.4: Data for membrane (3/30), sample 1**

| No | Angle (2θ) | D space (Å) | Counts | Relative Intensity |
|---|---|---|---|---|
| 1 | 40.20 | 2.243 | 35 | 100 |
| 2 | 46.70 | 1.945 | 17 | 49 |
| ***3*** | ***52.55*** | ***1.741*** | ***13*** | ***37*** |
| 4 | 68.35 | 1.372 | 12 | 34 |

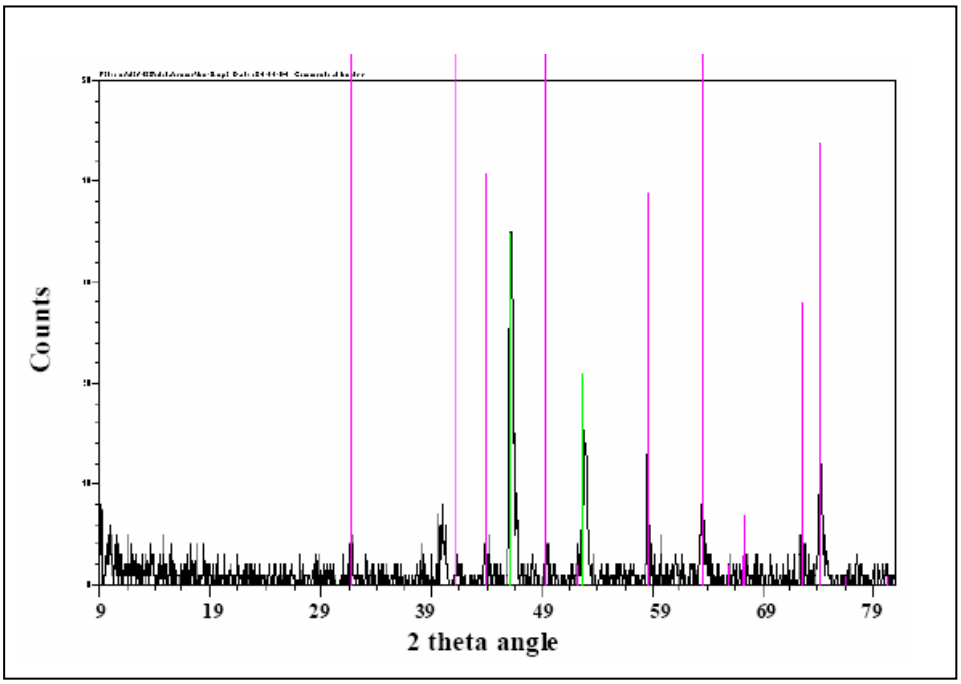


**Figure 6.23:** XRD image for membrane (3/30), sample 1

**Table 6.5:** Data for membrane (3/30), sample 2

| No | Angle | Counts | D space | Relative Intensity |
|---|---|---|---|---|
| ***1*** | ***33.90*** | ***11*** | ***2.644*** | ***28*** |
| 2 | 40.20 | 40 | 2.243 | 100 |
| 3 | 46.75 | 20 | 1.943 | 50 |
| 4 | 68.20 | 11 | 1.375 | 28 |

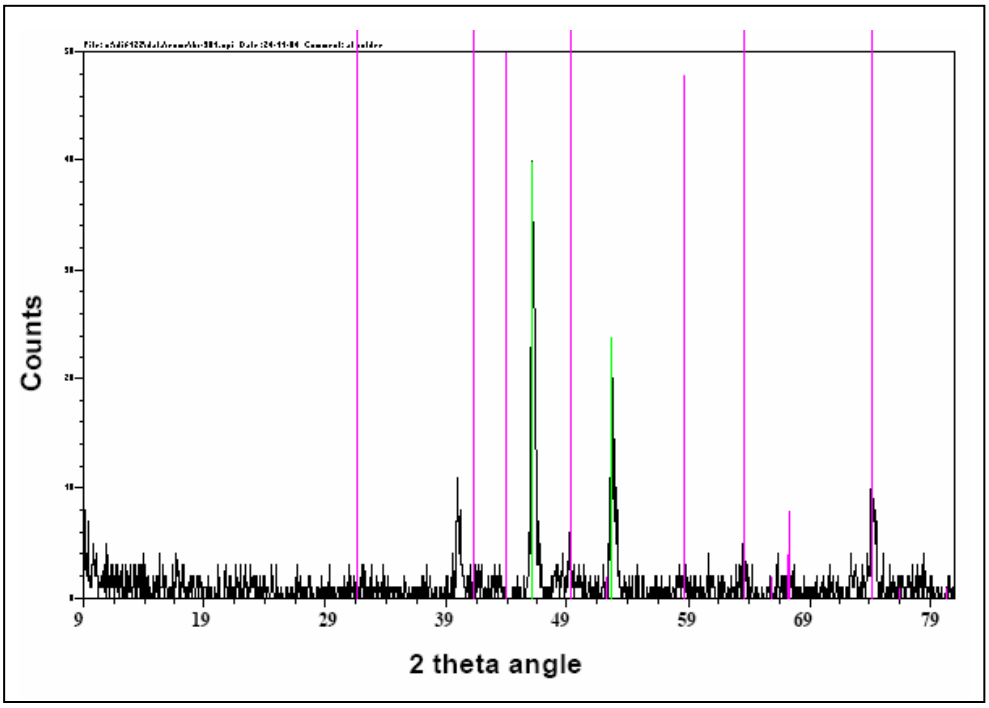


**Figure 6.24:** XRD image for membrane (3/30), sample 2

The patterns indicate that the palladium film with an fcc structure was formed after electroless plating. However, from the figures and tables above, it suggests that there was an impurity shown in Figure 6.23 and 6.24, which does not correlate with the palladium PDF data. The data of impurity did not correspond to that of Sn (impurity might be imported during pretreatment) or the carbon (impurity might be imported during Pd plating). Therefore, two possible explanations can be offered here. One was that during the additional heat treatment in air (10 hours), PdO formed and it definitely affected the crystals structure of the palladium film. Thus, the data shown in XRD images no longer only correspond with palladium, but also with PdO. Another assumption might be that there were impurities of dust trapped into the samples while preparing them. Therefore, when preparing the samples, great care should be taken to prevent an import of any impurities.

Figure 6.25 shows the XRD spectra of membrane (1/30) without additional heat treatment. The data correspond very well with palladium PDF data. Therefore, when applying the additional heat treatment, great care should be taken about the procedures so as to prevent impurities from being formed.

**Table 6.6: Data for membrane (1/30)**

| No | Angle (2θ) | D space (Å) | Relative Intensity |
|---|---|---|---|
| 1 | 40.001 | 2.2453 | 100 |
| 2 | 46.456 | 1.9456 | 60 |
| 3 | 68.234 | 1.3745 | 45 |
| 4 | 82.100 | 1.1758 | 43 |

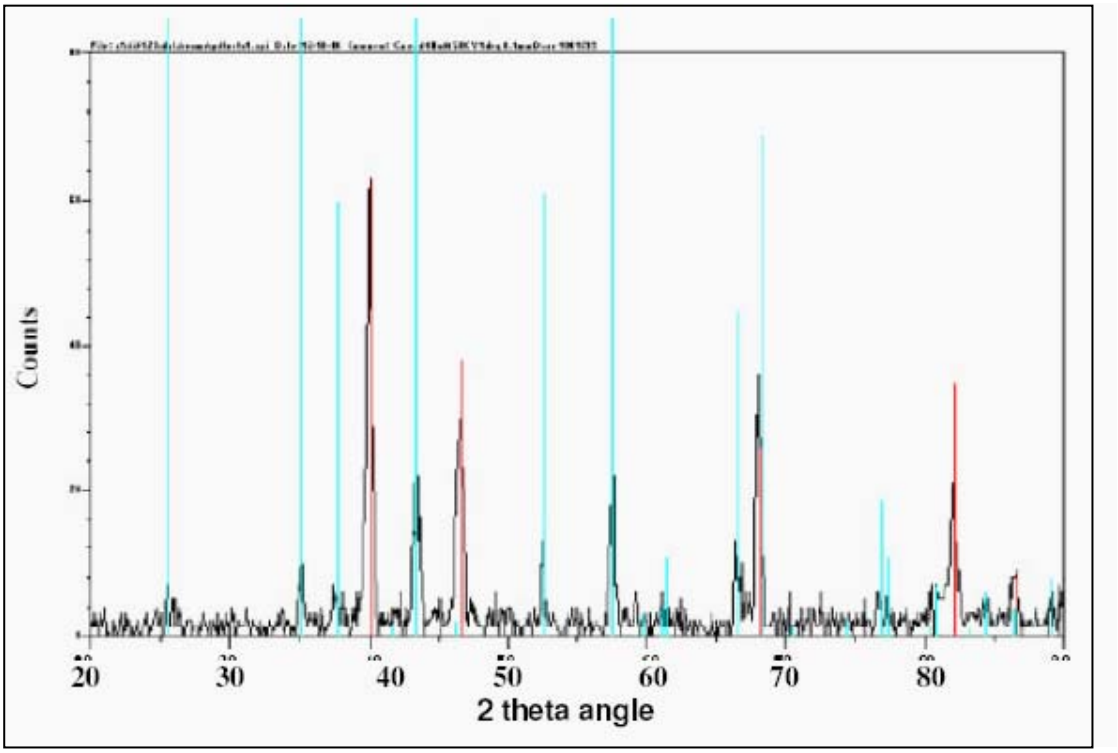


**Figure 6.25: XRD image for membrane (1/30)**

## 6.5 SUMMARY

In this Chapter the results and discussion of membrane surface characterisations were presented. Five analyses (SEM, EDS, AFM, BET, and XRD) were discussed to examine the Pd membrane morphology, film thickness, membrane composition, crystal size, crystal structure and average pore size of the palladium membrane. The relationship between the surface characteristics and the membrane permselectivity were also discussed.

From the EDS results, it was found that carbon was the main impurity in the Pd composite membranes. It caused membrane unstableness and decreased membrane selectivity. Therefore, future research regarding membrane cleaning and heat treatment after the electroless plating is recommended. Additionally, it is recommended in future work to apply heat treatment directly after each Pd layer is plated. Each additional Pd layer, thus, can replenish the holes that carbon forms on the former Pd layer during the heat treatment.

The surface morphology around the whole surface of the Pd composite membrane was examined using SEM analysis (from position 1 to position 5, Figure 6.1). The results showed that the Pd composite membranes had a smoother and purer Pd film in the middle of substrate than near the interface. Two assumptions could possibly explain this phenomenon. One was that the support membranes had a coarser surface near the interface (between the enamelled ending and the middle

of the substrate) than in the middle of the substrates. Therefore, more Pd should be covered near the interface. Another assumption was that during the electroless plating, the vacuum difference applied on the shell side of the plating reactor might not be the same along the whole length of the membrane due to the fact that the plating reactor was tilted by 45° in a beaker during plating (see Figure 3.13). Further investigations are recommended to prove/disprove these assumptions. In addition, it was found that a better membrane permselectivity could be obtained when the membrane had more Pd layers and smaller Pd grain sizes and more compact Pd layers.

The calculated theoretical thicknesses of all eleven membranes were in a good agreement with the SEM determined thicknesses. Only membrane (2/17) showed deviation between the calculated Pd thickness and the SEM determined Pd thickness. It was assumed that some impurities, such as carbon, Sn, or dusts, may have increased the actual membrane thickness. Alternatively, it could assume that the support membrane (2/17) had a coarser surface than any other support membranes so that a poorer Pd film with uneven thickness was deposited due to the nature of electroless plating technique.

The AFM analysis indicated that the Pd crystals are almost uniform in size, but not smooth enough. The results of XRD analysis show that additional heat treatment in air cause impurities in the Pd composite membranes. It was assumed that PdO formed during additional heat treatment. The XRD data of the other Pd composite membranes without additional heat treatment correspond very well with palladium PDF data. Therefore, when applying the additional heat treatment, great care should be taken about the procedures so as to prevent impurities from being imported.

The BET results showed that some Pd composite membrane, such as membrane (3/30) almost had an average pore diameter of 31.8 Å, which indicated that the membrane almost had no defects. However, more analysis by BET is recommended in future work to confirm this assumption.

# CHAPTER 7: CONCLUSIONS AND FUTURE WORK

The chief conclusions drawn from the work performed in this study can be summarised as follow:.

- A bubble point test was modified and applied in this study. The α-alumina ceramic support membranes have an average pore diameter ranging from 250 nm to 360 nm, compared with the manufacturer's claimed 200 nm pore size. The pore size of the support membrane plays an important role in Pd composite membrane permeation. Better Pd composite membranes with higher permselectivity can be prepared on a support membrane that contains smaller pore sizes and a smoother surface.

- A bubble point screening test was developed in this study. It was found that defects on the main plating surface of the support membrane have a larger negative impact than do defects on the enamelled endings, due to the fact that they cause more defects in the Pd films during electroless plating and decrease the membrane selectivity. Therefore, it is recommended that in future studies the defects on the support membranes be repaired before electroless plating..

- Proper pre-cleaning of the support membranes is important and an effective cleaning method was developed in this study. Ultrasonic cleaning (frequency of 35 kHZ) can remove the contaminants, however, it also opened the pores of the support membranes. This had an adverse effect on the membrane surface pretreatment since it provided a coarser support surface for the pretreatment. The preferable method is to rinse the support membrane with dilute sodium hydroxide solution, dilute hydrochloric acid solution, and distilled water, respectively. Alternatively, an ultrasonic cleaning with lower frequency could be investigated as a viable membrane pre-cleaning technique for future work.

- After pre-cleaning, a proper membrane surface pre-treatment step prior to electroless plating is essential to ensure good electroless plating. If the support surface is poorly activated, defects can form since palladium is not able to deposit on a non-activated surface via the autocatalytic mechanism for electroless plating. In this study, the support membrane surface turned completely black due to a uniform covering of palladium when using method 3 for pretreatment. In this method, the membrane was first stirred in $PdCl_2$ solution for 15 min, and was then dipped in distilled water 10 times (1-2 second each). Subsequently, the membrane was stirred in $SnCl_2$ solution for 15 min, and was then dipped into distilled water 10 times. This sequence was

repeated 4 times. However, $Sn^{2+}$ or $Sn^{4+}$ from the pretreatment solution or residue might form impurities if membrane cleaning after pretreatment is not performed effectively. Therefore, it is imperative that the membrane is thoroughly cleaned after pre-treatment. Alternatively, another pretreatment solution without $SnCl_2$ should be considered.

- The vacuum applied during the electroless plating on the shell side of the electroless plating reactor assisted in reducing the defects. A gauge vacuum of 20 kPa (g) proved optimum for producing good Pd coating on an α-alumina ceramic membrane (claimed pore diameter of 200 nm). Dense and smooth Pd composite membranes with high permselectivity (≥ 150 for all the Pd composite membranes) were obtained when this vacuum was applied during the electroless plating technique.

- Post-cleaning of the Pd composite membranes is important to remove carbon impurities. Membrane (4/30) was prepared without performing the post-cleaning. The characterisation results showed that the greatest concentration of impurities was found on this membrane, with the lowest selectivity of all twelve Pd composite membranes. For the other eleven composite membranes (for which identical post-cleaning methods were used) there were still some impurities, as found by EDS analysis. Due to time and material limitations, the post-cleaning has not been modified in this study. Therefore, investigation of effective methods of post-cleaning is recommended for future work.

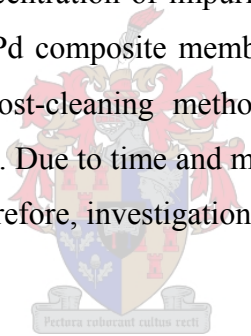


- After Pd electroless plating, heat treatment of the Pd composite membranes was essential to remove carbon and other impurities. Better adhesion between Pd and the support surface was obtained during the heat treatment. Moreover, the Pd nuclei agglomerated to form a more compact Pd surface. In addition, by using a new method of assessment for heat treatment (i.e. cutting the Pd composite membranes into two pieces and then exposing them to two different heating methods) the most effective heat treatment method could be identified without the influences of the substrates or the plating technique. The preferable procedure was to anneal the Pd composite membrane in $N_2$ for 5 h from room temperature to 320°C, and then oxidize it in air for 2 h at 320°C, followed by annealing it in $N_2$ for 130 min from 320°C to 450°C and then in $H_2$ for 3 h at 450°C. Finally the membrane was cooled down in $N_2$ to 350°C and held at this temperature for 30 min. Additional annealing in $H_2$ for 10 hours caused cracking of the Pd composite membranes and decreased the permselectivity of the Pd composite membranes. Extra oxidation in air for more than 10 hours changed the structure of the Pd films. PdO then forms and decreases the $H_2$ permeation through the Pd composite membranes.

- Bubble point screening tests of the Pd composite membranes showed that the defects were mainly located at the interface between the enamelled endings and the plating surface, or close to the interface. To reduce such defects, applying a gauge vacuum on the shell side of the plating reactor coated more Pd layers. Finally, when the Pd layer was more than 3 μm thick, no defects were found when the bubble point screening tests were performed.

- As could be expected, the $N_2$ permeance through the Pd composite membranes increased with increasing defects. However, the $N_2$ permeance through the Pd composite membranes decreased with an increasing Pd film thickness and an increasing temperature, at which the permeation tests were performed. Additionally, the $N_2$ permeance did not vary significantly with an increase in average pressure, indicating that the $N_2$ flow through the Pd composite membrane is Knudsen flow.

- The $H_2$ permeance through the Pd composite membranes decreased with increasing Pd film thickness and increased with an increasing temperature. This study confirmed that Sievert's law, where n = ½ (n refers to equation 5.1), is not applicable to the thin films synthesised in this study. Diffusion did not appear to be the rate-limiting step for the membranes prepared in this study.

- The permselectivities of the eleven Pd composite membranes prepared in this study remained above 150 at all the temperatures, indicating good quality Pd membranes. Only membrane (4/30), which was prepared without post-cleaning, had a low selectivity of 80.

- EDS analysis proved very useful for identifying the type and amount of impurities on the Pd films. AFM analysis assists with three-dimensional assessment of the surface morphology of the Pd composite membranes (including determining the roughness of the Pd films and the Pd crystal sizes). The samples should be less than 0.5 $cm^2$ and approximately flat to allow the beam to penetrate.

- Pd composite membranes were prepared on α-alumina ceramic membranes via the modified electroless plating technique in this study. The membrane hydrogen permeability of the Pd composite membranes (at a range of 4.5-12 $\mu mol/m^2/Pa/s$) and hydrogen/nitrogen permselectivity (average permselectivity ≥ 150) were achieved in this study. The permselectivities of membranes (1/30), (3/30), (6/30) and (6/17), to which a modified heat treatment method was applied, were superior to Keuler's membranes, which were subjected to

the previous heat treatment method (average permselectivity ≥ 100). AFM and BET analysis showed that dense and smooth Pd films with smaller Pd crystals sizes and compact Pd layers were obtained.

- The procedures of Pd electroless plating technique for preparation of Pd composite membranes were successfully modified in this study. The following steps are suggested for future investigations:

    - Bubble point screening tests on support membranes
    - Nitrogen permeation tests on support membranes
    - Bubble point tests on support membranes
    - Support membrane pre-cleaning
    - Support membrane surface pretreatment
    - Preparation of initial 1 μm Pd layer via electroless plating
    - Prepration of 2nd, 3rd or more Pd layers via electroless plating with a gauge vacuum of 20 kPa (g)
    - Post-cleaning after electroless plating
    - Heat treatment after post-cleaning

- The characterisation procedures for Pd composite membranes have been improved in this study. The following procedures are suggested for future investigations:

    - Bubble point screening tests on Pd composite membranes
    - Pd composite membrane permeability and permselectivity tests (from 350°C to 550 °C) via nitrogen or hydrogen respectively (from 100 kPa to 150 kPa)
    - Analytical characterisations for Pd composite membrane morphology and structure using via scanning electron microscopy (SEM), energy dispersive detectors (EDS), atomic force microscopy (AFM), Brunauer-Emmett-Teller (BET) and X-ray diffraction (XRD) analysis

- Some factors, however, which affect preparation of Pd composite membranes, need further clarification, viz. better surface pretreatment procedures without tin in the pretreatment solution (to avoid tin impurities), the method of membrane post-cleaning after electroless plating (to remove impurities), determination of why PdO forms during heat treatment and how it affects the permselectivity of the Pd composite membranes, as well as the relationship between Pd film

morphology structure and the procedures of electroless plating with vacuum. In addition, further investigations into the rate limiting step of the $H_2$ permeance through the Pd films thinner than 4 μm, are recommended.

# REFERENCE


Armor JN, *Applied Catalysis*, **49** (1989), 1-25

Armor JN, *Catalysis Today*, **25** (1995) 199-207

Athavale SN and Totlani MK, *Metal Finishing*, **87** (1989) 23-27

Antoniazzi AB, Haasz AA and Strangeby PC, *Journal of Nuclear Materials*, **162-164** (1989) 1065

Aoki K, Yokoyama S, Kusakabe K et al., *Korean Journal of Chemical Engineering*, **13** (1996) 530-537

Brinker CJ and Scherer GW, *Sol-gel Science*, Academic Press, New York (1990) 1-40

Buxbaum RE and Kinney AB, *Industrial and Engineering Chemistry Research*, **35** (1996), 530-537

Buxbaum RE and Marker TL, *Journal of Membrane Science*, **89** (1993), 29-38

Boudart M and Hwang HS, *Journal of Catalysis*, **39** (1975) 44-52

Cao Y, Li HL, Szpunar JA, Shmayda W, *Materials Science and Engineering,* **A 379** (2004) 173–180

Cannon KC and Hacskaylo JJ, *Journal of Membrane Science*, **65** (1992) 259-268

Cheng YS, Yeung KL, *Journal of Membrane Science,* **158** (1999), 127-141

Cohen RL, D'Amico JF et al., *Journal Electrochemical Society: Electrochemical Science and Technology*, **118** (1971) 2042

Collins JP and Way JD, *Industrial and Engineering Chemistry Research*, **32** (1993) 3006-3013

De Ninno A, Violante V and La Barbera A, *Physical Review B*, **56** (1997) 2417-2420

Dittmeyer, RV et al, *Journal of Molecular Catalysis A*: *Chemical,* **173** (2001) 135-184.

Van Dyk LD, *The evaluation of different uses of an extractor Catalytic Membrane Reactor,* PhD thesis, University of Stellenbosch, Stellenbosch, South Africa, (2005)

Edlund DJ, *US Patent* 5,393,325 (1995) 1-14

Feldstein N, *Journal Electrochemical Society: Electrochemical Science and Technology*, **121** (1974) 738-744

Gavalas GR, Megiris CE and Nam SW, *Chemical Engineering Science*, **44** (1989) 1829-1835

Glazunov GP, *Journal of Hydrogen Energy*, **22**, (1997), 263-268

Gryaznov VM, Serebryannikova OS and Serov YM, *Applied Catalysis A: General*, **96** (1993) 15-23

Hou Kaihu, Hughes Ronald, *Journal of Membrane Science,* **214** (2003), 43-55

Hsieh HP, *Inorganic Membranes for Separation and Reaction*, Elsevier Science Publishing Company, New York, USA (1996), 1-591

Hsiung TH, Christman DD, Hunter EJ et al., *AIChE Journal*, **45** (1999) 204-208

Iojoiu EE, Walmsley JC, Raeder H, Miachon S, Dalmon JA, research report,

Itoh N, *Studies in Surface Science and Catalysis*, **54** (1990), 268-269

Itoh N and Govind R, *AIChE Symposium Series*, **85** (1989) 10-17

Jakobs E, Koros WJ, *Journal of Membrane Science*, **124** (1997) 149-159

Jayaraman V, Lin YS, Pakala M et al., *Journal of Membrane Science*, **99** (1995a) 89-100

Jayaraman V and Lin YS, *Journal of Membrane Science*, **104** (1995b) 251-262

Jansen JC, Koegler JH, Van Bekkum H, et al., *Microporous and Mesoporous Materials*, **21** (1998) 213-226

Jung SH, Kusakabe K, Morooka S et al., *Journal of Membrane Science*, **170** (2000) 53-60

Keuler JN, *Preparation and Characterisation of Palladium Composite Membranes*, M.Eng Thesis, University of Stellenbosch, Stellenbosch, South Africa, (1997) 1-203

Keuler JN, *Optimising Catalyst and Membrane Performance and Performing A Fundamental Analysis On The Dehydrogenation of Ethanol and 2-Butanol In A Catalytic Membrane Reactor,* PhD thesis, University of Stellenbosch, Stellenbosch, South Africa, (2000)

Keuler JN, *Separation Science and Technology*, **37(2)** (2002)

Kikuchi, E and Uemiya, S, *Gas Separation and Purification*, **5** (1991) 261

Li AW, Xiong GX, Gu JH, and Zheng, LB, *Journal of Membrane Science,* **110** (1996), 257-260

Li AW, Liang W and Hughes R, Workshop: *'Applications and future possibilities of catalytic membrane reactors'*, Turnhout (16-17 Oct 1997) 106-109

Li AW, Liang W and Hughes R, *Separation and Purification Technology*, **15** (1999) 113-128

Li AW, Liang W, Hughes R, *Catalysis Today,* **56** (2000), 45–51

Li HongQiang, *www.chembio.uoguelph.ca*, (1997)

Li ZY, Maeda H, Kusakabe K et al., *Journal of Membrane Science*, **78** (1993) 247-254

Loweheim FA, *Modern Electroplating*, John Wiley & Sons, New York, (1974) 342-357, 739-747

Ma YH *at el*, Challenges in Composite Pd and Pd/Alloy Membrane for High Temperature Hydrogen Separation, Conferences, (2004)

McBride RB and McKinley DL, *Chemical Engineering Progress*, **61** (1965) 81

Morooka S, Yan S, Yokoyama S et al., *Separation Science and Technology*, **30** (1995) 2877-2889

Mouton DW, *The Development of a Membrane Reactor for the Dehydrogenation of Isopropanol,* Master thesis, University of Stellenbosch, Stellenbosch, South Africa, (2003)

Nam SE, Lee KH, *Journal of Membrane Science,* **192** (2001), 177–185

Nam S, Lee S and Lee K, *Journal of Membrane Science*, **153** (1999), 163-173

Noble RD and Stern SA, *Membrane Separation Technology Principles and Applications*, published by Elsevier Science B. V., Amsterdam, The Netherlands, (1995), 556

Ohno I, Wakabayashi O and Haruyama S, *Journal Electrochemical Society: Electrochemical Science and Technology*, **132** (1985) 2323-2330

Osaka T and Takematsu H, *Journal Electrochemical Society: Electrochemical Science and Technology*, **127** (1980) 1021-1029

Paglieri SN, Foo KY, Way JD et al., *Industrial and Engineering Chemistry Research*, **38** (1999) 1925-1936

Rhoda RN, 1959, Electroless palladium plating, *Transaction Institution of Metal Finishing*, **36**

Roa F, Way JD, *Applied Surface Science,* **240** (2005), 85–104

Razima S. Souleimanova, Alexander S. Mukasyan, Arvind Varma, *Separation and Purification Technology,* **25** (2001), 79–86

Sakamoto Y, Chen FL, Kinari Y et al., *International Journal of Hydrogen Energy*, **210** (1996) 1017-1024

Scott K and Hughes R, *Industrial Membrane Separation Technology*, published by Blackie Academic & Professional, Glasgow, UK, (1996), 1-300

Shu J, Grandjean BPA, Van Neste A et al., *Canadian Journal of Chemical Engineering*, **69** (1991) 1036-1060

Shu J, Grandjean BPA, Ghali E et al., *Journal of Membrane Science*, **77** (1993) 181-195

Shipley CR, *Plating and Surface Finishing*, **71** (1984) 92-99

Soria R, *Catalysis Today*, **25** (1995) 285-290

Souleimanova RS, Mukasyan AS, *Chemical Engineering Science,* **54** (1999), 3369-3377

Suzuki H, *US Patent,* 4,699,892 (1987) 1

Tanaka DA, Tanco MA, *Journal of Membrane Science,* 247 (2005) 21–27

Tong JH, Suda H, Haraya K, Matsumura Y, *Journal of Membrane Science,* **xxx** (2005), **xxx–xxx**

Uemichi Y, Shouji K, Sugioka M et al., *Bulletin Chemical Society Japan*, **68** (1995) 385-387

Van den Meerakker JEAM, *Applied Electrochemistry*, **11** (1981) 395

Uemiya S, Sato N, Ando H et al., *Journal of Membrane Science*, **56** (1991) 303-313

Uzio D, Peureux J and Giroir-Fendler A, *Applied Catalysis A: General*, **96** (1993) 83-97

Vitulli G, Pitzalis E, Salvadori P et al., *Catalysis Today*, **25** (1995) 249-253

Ward TL and Dao T, *Journal of Membrane Science*, **153** (1999) 211-231

Wu LQ, Xu NP, and Shi J, *Ind. Eng. Chem. Res.,* **39**, (2000), 342-348

Xomeritakis G and Lin YS, *Journal of Membrane Science*, **120** (1996) 261-272

Xomerirakis, G and Lin, YS, *AIChE Journal,* 44 (l) (1998) 174-183.

Xiong, GX, et al., *Catalysis Today,* 25 (1995) 237-240

Yang Li *at el, Journal of Membrane Science,* **xxx** (2005), xxx–xxx,

Yeung KL, Sebastian JM and Varma A, *Catalysis Today*, **25** (1995a) 231-236

Yeung KL and Varma A, *AIChE Journal*, **41** (1995b) 2131-2139

Yoshida H, Konishi S and Naruse Y, *Journal Less-Common Metals*, **89** (1983) 429

Zhao HB, Pflanz K, Gu JH et al., Journal of Membrane Science, **142** (1998) 147-157

Zheng WJ, Wu, LY *Materials Science and Engineering*, **A283** (2000) 122–125

# APPENDIX A

## List of chemicals used

| **Name** | **Purity** | **Supplier** |
|---|---|---|
| Ammonia solution | 28 wt % | Fluka |
| Ethanol | 99.8 wt % (0.02 % $H_2O$) | Merck |
| HCl | 37 wt % | Merck |
| Hydrazine | 35 wt % solution | Aldrich |
| EDTA ($Na_2EDTA.2H_2O$) | 99 wt % | Aldrich |
| NaOH | 97 wt % | Merck |
| $(NH_3)_4PdCl_2.H_2O$ | 99.99 wt % | Aldrich |
| $PdCl_2$ | 99.99 wt % | Fluka |
| $SnCl_2.2H_2O$ | 99.99 wt % | Aldrich |

# APPENDIX B

## Hydrogen and nitrogen permeance data through Pd composite membranes

| Membrane | Theoretical Thickness (micron) | T (°C) | Avg. $H_2$ permeance ($\mu mol/m^2.Pa.s$) | Avg. $N_2$ permeance ($nmol/m^2.Pa.s$) | Permelectivity | | Arrhenius parameters for hydrogen permeance | | $R^2$ value for n=1 in permeance equation |
|---|---|---|---|---|---|---|---|---|---|
| 1/30 | 3.37 | 550 | 6.54 | 22.71 | 287 | | $P_0$ = | 4.3234E-10 | 0.9989 |
| | | 450 | 5.34 | 23.63 | 200 | | $E_D$ = | 17876 | 0.9991 |
| | | 400 | 4.46 | 24.45 | 182 | | $R^2$ = | 0.9934 | 0.9999 |
| | | 350 | 3.88 | 25.77 | 155 | | | | 0.9853 |
| | | | | | | | | | |
| 2/30 | 2.54 | 550 | 7.89 | 10.23 | 771 | | $P_0$ = | 1.756E-10 | 0.9956 |
| | | 450 | 6.76 | 11.29 | 598 | | $E_D$ = | 15736 | 0.9976 |
| | | 400 | 5.68 | 12.89 | 440 | | $R^2$ = | 0.9921 | 0.9959 |
| | | 350 | 4.79 | 13.67 | 350 | | | | 0.9987 |
| | | | | | | | | | |
| 3/30 | 3.37 | 550 | 7.76 | 22.22 | 349 | | $P_0$ = | 4.878E-10 | 0.9976 |
| | | 450 | 6.57 | 23.56 | 279 | | $E_D$ = | 16285 | 0.9998 |
| | | 400 | 5.49 | 24.79 | 221 | | $R^2$ = | 0.9823 | 0.9987 |
| | | 350 | 4.73 | 25.43 | 186 | | | | 0.9997 |
| | | | | | | | | | |
| 4/30 | 1.72 | 550 | 5.68 | 51.34 | 110 | | $P_0$ = | 8.237E-10 | 0.9987 |
| | | 450 | 4.58 | 51.67 | 88 | | $E_D$ = | 21356 | 0.9986 |
| | | 400 | 4.78 | 52.22 | 91 | | $R^2$ = | 0.9543 | 0.9992 |
| | | 350 | 3.98 | 53.89 | 73 | | | | 0.9984 |
| | | | | | | | | | |
| 5/30 | 1.89 | 550 | 9.7 | 10.67 | 909 | | $P_0$ = | 5.543E-10 | 0.9965 |
| | | 450 | 8.89 | 11.23 | 791 | | $E_D$ = | 10231 | 0.9945 |
| | | 400 | 7.76 | 12.67 | 612 | | $R^2$ = | 0.9731 | 0.9987 |
| | | 350 | 6.87 | 13.76 | 499 | | | | 0.9969 |
| | | | | | | | | | |
| 6/30 | 1.94 | 550 | 8.76 | 26.38 | 332 | | $P_0$ = | 2.168E-10 | 0.9923 |
| | | 450 | 7.86 | 27.44 | 286 | | $E_D$ = | 98211 | 0.9929 |
| | | 400 | 6.75 | 28.49 | 236 | | $R^2$ = | 0.94563 | 0.9943 |
| | | 350 | 5.72 | 29.65 | 193 | | | | 0.9956 |

| Membrane | Theoretical Thickness (micron) | T (°C) | Avg. $H_2$ permeance ($\mu mol/m^2.Pa.s$) | Avg. $N_2$ permeance ($nmol/m^2.Pa.s$) | Permselectivity | | Arrhenius parameters for hydrogen permeance | | $R^2$ value for n=1 in permeance equation |
|---|---|---|---|---|---|---|---|---|---|
| 10/30 | 2.59 | 550 | 9.87 | 18.23 | 541 | | $P_0$ = | 1.893E-10 | 0.997 |
| | | 450 | 8.57 | 19.27 | 444 | | $E_D$ = | 10202 | 0.99894 |
| | | 400 | 7.69 | 20.32 | 378 | | $R^2$ = | 0.9483 | 0.9999 |
| | | 350 | 6.48 | 21.43 | 302 | | | | 0.9918 |
| | | | | | | | | | |
| 12/30 | 2.18 | 550 | 8.56 | 22.34 | 383 | | $P_0$ = | 1.4386E-10 | 0.9923 |
| | | 450 | 7.58 | 23.65 | 320 | | $E_D$ = | 11267 | 0.9987 |
| | | 400 | 6.03 | 24.37 | 247 | | $R^2$ = | 0.9232 | 0.9992 |
| | | 350 | 5.63 | 25.69 | 219 | | | | 0.9995 |
| | | | | | | | | | |
| 1/17 | 2.92 | 550 | 7.37 | 20.12 | 366 | | $P_0$ = | 1.962E-10 | 0.9994 |
| | | 450 | 5.88 | 20.56 | 285 | | $E_D$ = | 12833 | 0.9945 |
| | | 400 | 4.97 | 20.98 | 236 | | $R^2$ = | 0.9478 | 0.9969 |
| | | 350 | 4.76 | 21.67 | 219 | | | | 0.9959 |
| | | | | | | | | | |
| 2/17 | 2.54 | 550 | 10.78 | 40.34 | 267 | | $P_0$ = | 1.986E-10 | 0.9949 |
| | | 450 | 9.12 | 41.23 | 221 | | $E_D$ = | 9917 | 0.9994 |
| | | 400 | 8.45 | 42.87 | 197 | | $R^2$ = | 0.9582 | 0.9997 |
| | | 350 | 7.12 | 42.38 | 168 | | | | 0.9999 |
| | | | | | | | | | |
| 4/17 | 1.79 | 550 | 11.9 | 40.24 | 296 | | $P_0$ = | 3.467E-10 | 0.9978 |
| | | 450 | 11.35 | 40.87 | 277 | | $E_D$ = | 8718 | 0.9989 |
| | | 400 | 10.5 | 41.65 | 252 | | $R^2$ = | 0.9692 | 0.9981 |
| | | 350 | 9.34 | 41.98 | 222 | | | | 0.9998 |
| | | | | | | | | | |
| 6/17 | 3.96 | 550 | 9.04 | 8.34 | 1083 | | $P_0$ = | 1.765E-10 | 0.9999 |
| | | 450 | 8.28 | 9.39 | 882 | | $E_D$ = | 9762 | 0.9983 |
| | | 400 | 7.38 | 10.65 | 692 | | $R^2$ = | 0.9319 | 1 |
| | | 350 | 6.42 | 11.87 | 540 | | | | 0.9910 |

# APPENDIX C

## List of symbols

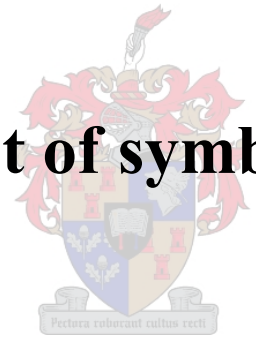

| | | | |
|---|---|---|---|
| $A_p$ | = | Surface area of support membrane for plating | [$m^2$] |
| C | = | hydrogen surface concentration | [$mol/m^3$] |
| $C_{Pd}$ | = | concentration of palladium in plating solution | [g/l] |
| D | = | coefficient for diffusion through a membrane film, diffusivity | [$m^2/s$] |
| $D_e$ | = | effective diffusivity | [$m^2/s$] |
| $D_i$ | = | Inner diameter of membrane tube | [m] |
| $d_p$ | = | membrane pore diameter | [m] |
| $E_D$ | = | diffusion activation energy | [J/mol] |
| $G_f$ | = | geometric factor accounting for porosity and tortuosity | |
| H | = | mean curvature of the meniscus | |
| J | = | permeation flux | [$mol/m^2.s$] |
| *l* | = | film thickness | [m] |
| L | = | Length of support membrane | [m] |
| $L_e$ | = | Total length of both enamelled endings | [m] |
| M | = | molecular mass | [g/mol] |
| m | = | mass of Pd composite membrane | [g] |
| $m_{Pd}$ | = | Mass of plated palladium film | [g] |
| n | = | pressure exponent | |
| P | = | pressure | [Pa] |
| $P_0$ | = | pre-exponential factor of permeability coefficient | [$mol.m/m^2.Pa.s$] |
| $P_{er}$ | = | permeability coefficient | [$mol.m/m^2.Pa.s$] |
| $P_{H_2}$ | = | hydrogen pressure | [Pa] |
| $P_h$ | = | hydrogen partial pressures on the high pressure pressure side | [Pa] |
| $P_l$ | = | hydrogen partial pressures on the low pressure side | [Pa] |
| $P_m$ | = | permeance | [$mol/m^2.Pa.s$] |
| r | = | membrane pore radius | [m] |
| $R_0$ | = | Universal constant | [8.314 J/mol.K] |
| $S_c$ | = | Sievert's constant | |
| T | = | temperature | [K] |
| $V_m$ | = | Volume of support membrane | [$m^3$] |
| $V_s$ | = | Volume of plating solution | [$m^3$] |

**Greek symbols**

| | | |
|---|---|---|
| α | = | separation factor |
| σ | = | the interfacial tension |

# APPENDIX D

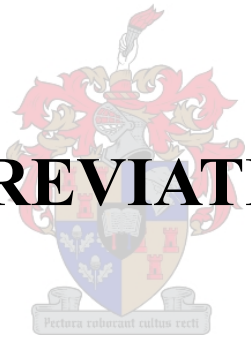


## ABBREVIATIONS

| | |
|---|---|
| AFM | atomic force microscopy |
| BET | Brunauer-Emmett-Teller |
| CNRS | Centre National de la Recherche Scientifique |
| CVD | chemical vapour deposition |
| EDS | energy dispersive detectors |
| MOCVD | metal organic chemical vapour deposition |
| MPSS | macroporous stainless steel |
| SCT | Societé des Céramiques Techniques |
| SEM | scanning electron microscopy |
| SUS | Shape stainless steel |
| XRD | X-ray diffraction |